Superiority Enhancement of Geo-Jute by Chemical Modification Through Gamma Radiation

A Thesis Submitted in Partial Fulfillment of the Requirements for the Degree

of

DOCTOR OF PHILOSOPHY

in

Applied Chemistry and Chemical Engineering,

University of Dhaka

By Nasrin Akter

(Reg No: 78/2021-2022)

Department of Applied Chemistry and Chemical Engineering

Faculty of Engineering and Technology

University of Dhaka

Dhaka 1000, Bangladesh

March, 2026

DECLARATION

I certify that the work contained in the thesis is original and was completed by me under the supervision of my supervisors. I also declare that this work has not been submitted to any other institution for any degree.

Signature of the Candidate

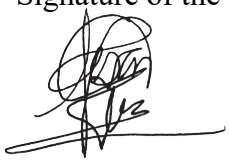

30. 03. 2026

Nasrin Akter

Reg No: 78/2021-2022

Session-2021-2022

CERTIFICATE

This is to certify that the work contained in the thesis entitled "Superiority Enhancement of Geo-Jute by Chemical Modification Through Gamma Radiation" submitted by Nasrin Akter, Registration No.: 78/2021-2022, Session: 2021-2022 for the award of the degree of Doctor of Philosophy (Ph.D.) to the Department of Applied Chemistry and Chemical Engineering, Faculty of Engineering and Technology, University of Dhaka, Bangladesh, is a record of authentic research works carried out by her under our joint supervisions and steerage. We considered that the thesis had met the standards and fulfilled the requirements of the rules and regulations governing the nature of the degree. The contents embodied in the thesis have not been submitted for the award of any other degree or diploma in this or any other university.

Supervisors:

1. 30.03.2026

Dr. Sayed Mohammed Shamsuddin

Professor
Dept of Applied Chemistry and Chemical Engineering
University of Dhaka
Dhaka-1000, Bangladesh

2. 30.03.2026

Md Ashaduzzaman, PhD

Professor
Dept of Applied Chemistry and Chemical Engineering
University of Dhaka
Dhaka-1000, Bangladesh

3.

Dr. Mubarak Ahmad Khan

Former Scientific Advisor
Bangladesh Jute Mills Corporation
Former Director General
Atomic Energy Research Establishment
Ganakbari savar baipayl,
Dhaka-1349

Dedicated

To

My family members and all teachers

ACKNOWLEDGEMENTS

The author extends heartfelt gratitude to the Most Merciful and Almighty Allah for His infinite blessings and guidance throughout the entire journey of this research.

The author wishes to express sincere appreciation to Professor Dr. Sayed Mohammed Shamsuddin, Professor Md. Ashaduzzaman, Ph.D., Department of Applied Chemistry and Chemical Engineering, University of Dhaka, and Dr. Mubarak Ahmad Khan, former Scientific Advisor, Bangladesh Jute Mills Corporation, and former Director General, Atomic Energy Research Establishment, Ganakbari, Savar, for their unwavering support, encouragement, and valuable advice. Their constructive criticism, motivation, and profound scientific insight have been instrumental in shaping the author's growth as a researcher. Their wisdom has not only inspired but also significantly enriched the entire research process.

The author also gratefully acknowledges Dr. Salma Sultana, Chief Scientific Officer, Bangladesh Atomic Energy Commission, Nuclear and Radiation Chemistry Division, Institute of Nuclear Science and Technology, for her kind cooperation and guidance.

Special thanks are due to Dr. Md. Firoz Mortuza, Principal Scientific Officer, and Mr. Khalid Hossain, Senior Technician, Bangladesh Atomic Energy Commission, Gamma Source Division, Institute of Food and Radiation Biology, for providing the opportunity and support for research work in IFRD.

The author expresses profound gratitude to Professor Dr. Lal Mohan Baral, Head, Department of Textile Engineering, Ahsanullah University of Science and Technology, Tejgaon Industrial Area, Dhaka, for granting access to laboratory facilities and for his kind cooperation.

The author is deeply thankful to Dr. Sharmin Zaman Emon, Ph.D., Center for Advanced Research in Sciences (CARS), University of Dhaka, for invaluable support, and to Mrs. Dipa Islam, Senior Scientific Officer, Biomedical and Toxicological Research Institute, Bangladesh Council of Scientific and Industrial Research (BCSIR), for her generous assistance and valuable time.

The author also extends sincere appreciation to Ms. Tania Akter, Senior Scientific Officer, and Mr. Khairul Islam, Assistant Scientific Officer, Latif Bawany Jute Mills Ltd., for their valuable suggestions, help, and encouragement throughout the research work.

The author gratefully acknowledges the Bangladesh Council of Scientific and Industrial Research (BCSIR) for its support in facilitating this degree.

Thanks, are also due to all the teachers of the Department of Applied Chemistry and Chemical Engineering, University of Dhaka, for their cordial support, as well as to the technical and administrative staff for their cooperation and assistance in providing necessary facilities.

Finally, the author expresses heartfelt gratitude to his family members for their unwavering love, patience, and support, which have been a constant source of strength throughout his life and research journey.

(Nasrin Akter)

Nasrinakter.luna@gmail.com

ABSTRACT

Natural fiber jute inherently possesses greater tensile strength (TS) than other natural fibers and offers numerous applications in geotechnical applications as a replacement for synthetic fibers. This research aims to enhance the physio-mechanical properties of jute fabric by improving its environmental durability. The study improves durability by chemically modifying materials using gamma radiation. Bitumen emulsion and unsaturated polyester resin were used for chemical modification. First, the jute fabric is treated with a chemical (polymer mixture), and a suitable formulation (30% BE + 10% UPR) is chosen based on durability tests. Then, the chemically treated jute fabric is irradiated with gamma radiation, selecting an appropriate dose (5 kGy) through durability testing. Finally, the pre-treated jute fabric is subjected to chemical treatment and gamma radiation, and its durability is assessed using an accelerated weathering tester. Pre-treatment was performed in two ways: (i) HEMA pre-treated, and (ii) benzoyl peroxide pre-treated. The HEMA-treated jute fabric showed better durability than the other treated sample. The tensile strength of HEMA-pre-treated samples was 50% higher than that of the raw jute fabric. At each step, samples were characterized by FT-IR, XRD, and TGA analyses, and their physico-mechanical properties were measured through tensile strength and water absorption tests. After chemical modification, the OH groups in the jute fabrics are reduced, decreasing hydrophilicity and increasing hydrophobicity, thereby enhancing the physico-mechanical properties. This research aims to strengthen these properties without making the fabric entirely plastic by breaking additional OH bonds. Pre-treatment generates free radicals from jute cellulose, and gamma radiation promotes their formation and cross-linking within the cellulose-polymer matrix. Cross-linking improves the fabric's physico-mechanical properties. Durability and physical tests show improvements in these properties. FTIR, XRD, and TGA analyses confirm the formation of free radicals and the cross-linking of jute cellulose with the polymer mixture. This research partially enhances the hydrophobicity of jute fabric. Gamma radiation not only boosts cross-linking but also reduces excess chemicals on the fabric surface, increasing porosity between yarns and making the fabric more biodegradable and eco-friendlier. An accelerated weathering test compares durability under artificial and outdoor conditions. In the lab, an accelerated weathering tester provides quicker results than outdoor exposure by controlling temperature, light, and water spray. Overall, durability testing using this method yields faster results than natural outdoor testing. Significant improvements in TS and durability testing were observed in the treated jute fabric compared to the

raw jute fabric. Whereas raw jute fabric deteriorates after 45 days, treated jute fabric showed enough tensile strength after 90 days. On the other hand, in the accelerated weathering durability test, after 28 days, the treated jute fabric showed significantly higher tensile strength and weight than the raw jute fabric.

TABLE OF CONTENTS

Chapter 1: Introduction 16
1.1 Introduction 17
1.2 Background of the Study 18
1.3 Aims and Objectives of the Study 21
1.4 Outline of the Research 22
Chapter 1: Introduction 22
Chapter 2: Literature Review 22
Chapter 3: Materials and Methods 22
Chapter 4: Results and Discussions 22
Chapter 5: Conclusion 22
Chapter 2: Literature Review 23
2.1 Geo-Textiles 24
2.2. Basic Functions of Geo-Textile 24
2.2.1 Separation 25
2.2.2 Reinforcement 26
2.2.3. Filtration 27
2.2.4 Drainage (or fluid transmission) 28
2.2.5 Fluid Barrier 28
2.3 Major Applications of Geo-Textiles 29
2.4 Geo-Jute 29
2.5 Advantages of Geo-Jute 30
2.6 Application of Geo-Jute 30
2.7 About Jute Fibre 30
2.8 Biochemical Constituents of Jute Fibre 31
2.9 Physical Properties of Jute Fibre 31
2.10 Eco-friendly Jute Processing 32
2.11 Disadvantages of Jute Fibre 33
2.12 Chemical Modification of Jute Fibre 34
2.13 Surface Modification 35
2.13.1 Methods of Surface Modification 36
2.13.1.1 Chemical Method 36
2.13.1.2 Physical Modification 37

2.14 Cross-linking 37
2.15 Gamma Radiation (γ-Irradiation) 38
2.16 Effect of γ-Irradiation on Surface Modification/ Cross-Linking 38
2.17 Bitumen Emulsion 39
2.18 Unsaturated Polyester Resin (UPR) 41
2.19 Accelerated Weathering Test 42
Chapter 3: Materials and Methods 44
3.1 Research Work Flow and Experimental Design 45
3.1.2 Holistic Research Workflow 47
3.2 Raw Materials Used 47
3.3 Chemical Used 48
3.3.1 Bitumen Emulsion 48
3.3.2 Unsaturated Polyester Resin (UPR) 49
3.3.3 Auxiliary Chemicals Used 49
3.4 Machinery Used 50
3.4.1 GSM Cutter 50
3.4.1.1 Determination of GSM 51
3.4.2 Titan Universal Strength Tester 51
3.4.2.1 Determination of Tensile Strength 52
3.4.3 Padding Machine 52
3.4.4 Gamma Radiation Chamber 53
3.4.5 Measurement of Moisture Content and Moisture Regain 53
3.4.6 Water Absorption and Hydrophilicity Study of Jute Fibre 54
3.4.7 Measurement of Fabric Thickness 55
3.4.8 Scanning Electron Microscopy (SEM) 56
3.4.9 Fourier Transform Infrared Analysis 56
3.4.10 X-ray Diffractometer 57
3.4.11 TGA Analysis 58
3.4.12 Antibacterial Activity Assessment 59
3.4.13 Accelerated Weathering Test: 60
3.5. Biodegradability and Durability Considerations 63
Chapter 4: Results and Discussion 64

4.1 Selection of Optimum Polymer Mixture Formula by Soil Burial Test 66
4.1.1 Working Procedure 67
4.1.2 Sample Preparation 67
4.1.3 Analysis of Tensile Resistance 68
4.1.4 Analysis of Fabric Weight 69
4.1.5 Analysis of Water Absorbency by Measuring Moisture Regain%, Content%, and Water Uptake% 70
4.1.6 Analysis of Surface Morphology by SEM Images 71
4.1.7 Analysis of Infrared Spectral (FT-IR) Analysis 71
4.1.8 Analysis of X-ray diffraction curve 74
4.1.9 Determination of Thermal Degradation by Thermogravimetric (TGA) Analysis 76
4.1.10 Analysis of Weight Loss at Different Time Durations after Soil Burial 77
4.1.11 Analysis of Tensile Strength (TS) in Different Time Durations after Soil Burial 79
4.1.12: Key Findings 80
4.1.13: Comments 80
4.2 Selection of Optimum Radiation Dose 81
4.2.1 Working Procedure 82
4.2.2 Sample Preparation 82
4.2.3 The γ-Radiation Effect on Cellulose of Jute Fabric 83
4.2.4 Analysis of the TS Between TJF and UJF After Applying Gamma(γ) Radiation 84
4.2.5 Analysis of Moisture Content, Moisture Regain, and Water Uptake% After Applying γ-Radiation 85
4.2.6 SEM Analysis of Chemically Treated, and Chemically Treated with Gamma - Irradiated Jute Fabric 86
4.2.7 Analysis of FT-IR of Raw Jute Fabric, Chemically Treated Jute Fabric, and Chemical Treatment with Gamma-Irradiated Jute Fabric. 88
4.2.8 XRD Analysis of Raw, Chemically Treated, and Chemical Treated with Gamma-Irradiated Jute Fabric 89
4.2.9 TGA Analysis of Raw, Chemically Treated, and Chemical Treated with Gamma-Irradiated Jute Fabric 90
4.2.10 Analysis of Durability by TS (Tensile Strength) Loss 91
4.2.11 Key Findings 92
4.3 Pre-Treatment of Jute Fabric, Then Chemical Modification 93
4.3.1 Work Flow Diagram 94

4.3.2 Preparation of the Research Sample 94
4.3.3 Pre-Treatment Process-1: Benzoyl Peroxide Treatment 95
4.3.3.1 (a) Selection of Benzoyl Peroxide (%) by the change of tensile strength 96
4.3.3.1(b) Reaction involved in pre-treatment process-1 97
4.3.3.2 Proposed Cross-Sectional View of Benzoyl Peroxide Pre-Treated Jute Fabric 100
4.3.3.3 FTIR Analysis of Benzoyl Peroxide Pre-Treated Jute Fabric with Raw Jute Fabric 100
4.3.3.4 Analysis of X-Ray Diffraction (XRD) of Benzoyl Peroxide Pre-Treated Grey Jute 102
4.3.4 (a) Pretreatment Process-2 (Pre-Treatment of Jute by HEMA (2-Hydroxyethyl Methacrylate) 104
4.3.4.1 Reaction Involved in Pre-Treatment Process-2 105
4.3.4.2 Possible Cross-Sectional View of HEMA Pre-Treated Jute Fabric 107
4.3.4.3 FTIR Analysis HEMA Pre-Treated Jute Fabric 107
4.3.4.4 XRD Analysis of HEMA Pre-Treated Jute Fabric 109
4.3.5 Key Findings 110
4.4 Measurement of Durability Properties by Weathering Test 111
4.4.1 Comparative Analysis of Physio-Mechanical Properties 112
4.4.2 Analysis of Tensile Strength 112
4.4.3 Analysis of Fabric Weight 113
4.4.4 Analysis of Fabric Thickness 113
4.4.5 Analysis of Moisture Regain, Moisture Content, and Water Uptake% 114
4.4.6 Analysis of Surface Morphology 115
4.4.7 TGA Analysis 117
4.4.8 Antimicrobial Activity Assessment 119
4.4.9. Analysis of Tensile Strength After Accelerated Weathering Test 120
4.4.10 Comparison of Weight After Accelerated Weathering Test 122
4.4.11 Comparison of Thickness After Accelerated Weathering Test 123
4.4.12 Comparison of Cellulose Degradation from the FTIR Graph Before and After Accelerated Weathering Exposure 124
4.4.13 XRD-Analysis Before and After Weathering Exposure 125
4.4.15 Some Photographs of this Research Work 126
4.5 Cost Analysis 128

Chapter 5: Conclusion..... 129
5.1 Conclusion..... 130
5.2 Key Findings of the Study..... 132
5.3 Research Contribution..... 132
5.4 Practical Implications for Geo-Textile Applications 132
5.5 Limitations of the Study..... 133
5.6 Recommendations for Future Research 133
References..... 135

LIST OF FIGURES

Figure 2. 1 Separation function of geotextiles between two soil layers: (a) without geotextile, showing mixing of subgrade and aggregate; (b) with geotextile, maintaining layer stability and preventing soil intermixing [33]. 26
Figure 2. 2 The reinforcement mechanism of geotextiles in soil structures, where tensile resistance of the fabric improves load distribution and increases the overall stability of the soil mass [34]. 26
Figure 2. 3 Filtration mechanism of geotextiles allowing water to pass through while preventing soil particle migration, thereby maintaining hydraulic stability within the soil system [33]. 27
Figure 2. 4 Drainage function of geotextiles facilitating in-plane flow of water through the fabric while retaining surrounding soil particles [33]. 28
Figure 2. 5 Fluid Barrier Application of Geosynthetic Materials Used to Prevent Downward Seepage of Liquid Contaminants into Underlying Soil Layers [36]..... 29
Figure 2. 6 Picture of a jute plant and its Structure. 33
Figure 2. 7 Schematic illustration of property enhancement in fibre material after surface modification [55]. 36
Figure 2. 8 A cross-linked polymer [61]..... 38

Figure 3. 1 A GSM cutter is used for determining the mass per unit area of jute fabric samples. 50
Figure 3. 2 Titan Universal Strength Tester used for measuring the tensile strength and elongation properties of jute fabric samples. 51
Figure 3. 3 Laboratory Padding Mangle Used For Applying Chemical Treatment Uniformly To Jute Fabric Samples. 52
Figure 3. 4 Gamma radiation chamber used for irradiating chemically treated jute fabric samples [79]. 53
Figure 3. 5 Electronic balance used for accurate measurement of fabric and chemical sample weights. 54
Figure 3. 6 Oven dryer used for drying treated jute fabric samples under controlled temperature conditions. 55
Figure 3. 7 Thickness gauge used to measure the thickness of jute fabric samples. 55
Figure 3. 8 Scanning Electron Microscope (SEM) used to observe the surface morphology of untreated and treated jute fibres. 56
Figure 3. 9 Spectrophotometer used for analyzing optical and chemical properties of treated jute samples. 57
Figure 3. 10 X-ray diffractometer used to analyze the crystalline structure of jute fibres. 58
Figure 3. 11 A thermogravimetric analyzer (TGA) was used to evaluate the thermal stability of jute fibre samples. 58
Figure 3. 12 Laboratory incubator used during biological or soil burial durability testing of jute fabric samples. 60
Figure 3. 13 QUV accelerated weathering tester used to simulate environmental weathering conditions for durability analysis. 61

Figure 3. 14 (a) Weathering cycle and (b) Sample in the specimen holder of the weathering machine. 62

Figure 4.1. 1 Working Procedure of the Selection of Polymer Mixture. 67
Figure 4.1. 2 Comparison of tensile strength. 68
Figure 4.1. 3 (a) Weight increasing in g/m^2, (b) Weight gain % chemically treated jute fabric. 69
Figure 4.1. 4 Comparison of water absorbency of untreated and chemically treated jute fabrics showing (a) MR%, (b) MC%, and (c) WU%. The gradual decrease in MR%, MC%, and WU% indicates reduced hydrophilicity due to polymer impregnation and crosslinking within the jute structure. 70
Figure 4.1. 5 SEM images showing the surface morphology of (a)Raw jute fabric and (b) polymer-treated jute fabric. 71
Figure 4.1. 6 FTIR spectra of raw jute fabric, bitumen emulsion, unsaturated polyester resin (UPR), and polymer-treated jute fabric. The untreated jute shows a strong O–H stretching band (~3400 cm^{-1}) and characteristic cellulose peaks, indicating its hydrophilic nature. In the treated fabric, the reduced O–H intensity and the appearance of strong C=O (~1725 cm^{-1}) and C–O–C (1250–1050 cm^{-1}) bands confirm ester formation and crosslinking between the jute cellulose and the polymer components, indicating successful polymer impregnation and increased hydrophobicity. 73
Figure 4.1. 7 XRD patterns of raw jute fabric (lower) and chemically treated jute fabric (upper). The raw jute shows characteristic diffraction peaks at 2θ ≈ 16.1°, 22.8°, and 34.8°, corresponding to the semi-crystalline Cellulose I structure. In the treated fabric, the broadened and reduced peak around 2θ ≈ 22° indicates decreased crystallinity due to crosslinking between cellulose hydroxyl groups and the polymer matrix (bitumen emulsion and unsaturated polyester resin), confirming the structural modification of the jute fibers. 74
Figure 4.1. 8 Thermogravimetric analysis (TGA) curves of raw jute fabric and chemically treated jute fabric. The treated sample exhibits reduced initial moisture loss and improved thermal stability compared with raw jute, indicating that the polymer coating and crosslinking affect the thermal degradation behavior of the fibers. 76
Figure 4.1. 9 Comparison of weight loss (g/m²) of untreated jute fabric (UJF) and chemically treated jute fabrics (TJF1–TJF4) during soil burial tests at 0, 15, 45, and 90 days. The treated samples exhibit reduced weight loss compared to raw jute, with increasing resistance to biodegradation observed at higher resin content due to polymer crosslinking and protective coating effects. 78
Figure 4.1. 10 Variation of tensile strength (kPa) of untreated jute fabric (UJF) and chemically treated jute fabrics (TJF1–TJF4) during soil burial tests at 0, 15, 45, and 90 days. The treated samples exhibit improved tensile strength retention compared to raw jute, with higher polymer content resulting in enhanced durability due to crosslinking and reduced biodegradation. 79

Figure 4.2. 1 Working procedure of radiation dose selection. 82
Figure 4.2. 2 (a) Abstraction of H and OH (b) Open the cellulose cycle (c) Chain scission after γ-irradiation. (Reused from [9]) 83

Figure 4.2. 3 Variation of tensile strength (kPa) of untreated jute fabric (UJF) and treated jute fabric (TJF) under different γ-radiation doses (2.5–10 kGy). The tensile strength increases to an optimum dose (5 kGy) due to radiation-induced crosslinking, followed by a decrease at higher doses due to chain scission and degradation. 84
Figure 4.2. 4 Single bar diagram showing the comparison of Moisture Regain (MR), Moisture Content (MC), and Water Uptake (WU) of untreated and chemically treated jute fabrics under different γ-irradiation doses. 85
Figure 4.2. 5 Morphological view of (a) Chemically treated and (b) Chemically treated with γ-radiated jute fabric. 86
Figure 4.2. 6 FTIR graph of raw, chemical-treated, and γ-radiated jute fabric. 88
Figure 4.2. 7 XRD graph of raw, chemical-treated, and γ-radiated jute fabric. 89
Figure 4.2. 8 TGA analysis of raw, chemically treated, and chemical treated with gamma-irradiated jute fabric. 90
Figure 4.2. 9 Analysis of loss of tensile resistance after soil burial. 91

Figure 4.3. 1 Workflow diagram of pre-treatment and chemical modification. 94
Figure 4.3. 2 Working procedure of the diagram of the pre-treatment process-1. 95
The optimum concentration of benzoyl peroxide was determined experimentally by evaluating the tensile strength of treated jute fabrics at different BP concentrations, as represented in Figure 4.3.3 96
Figure 4.3. 3 Tensile strength v/s benzoyl peroxide % of mercerized jute fabric. 96
Figure 4.3. 4 Possible cross-sectional view of benzoyl peroxide pre-treated with chemically treated jute fabric. 100
Figure 4.3. 5 FTIR spectral comparison of raw and benzoyl peroxide pre-treated jute fabric showing esterification and polymer–cellulose crosslinking. 101
Figure 4.3. 6 X-ray diffraction (XRD) patterns of raw jute, bitumen/PR/γ-radiation treated jute, and benzoyl peroxide (BP) pre-treated jute composites, illustrating variations in cellulose I crystallinity and structural modification induced by chemical treatment and irradiation. 103
Figure 4.3. 7 Workflow diagram of the Pre-treatment process-2. 104
Figure 4.3. 8 Possible cross-sectional view of HEMA pre-treated jute fabric. 107
Figure 4.3. 9 FTIR spectra of raw and HEMA pre-treated jute fabric composites, showing the change of functional groups, including reduction of hydroxyl (–OH) intensity and formation of ester (C=O) and ether (C–O–C) linkages, confirming successful graft polymerization and crosslinking with HEMA, UPR, and bitumen. 108
Figure 4.3. 10 Comparative X-ray diffraction (XRD) patterns of raw, bitumen–polyester resin treated, and HEMA-modified jute fabrics under γ-irradiation indicating structural transformation and crystallinity variation. 109

Figure 4.4. 1 Comparative evaluation of (i) tensile strength and (ii) percentage elongation of raw and chemically modified jute fabrics (Bitumen + PR, Bitumen + PR + γ-irradiation, HEMA + Bitumen + PR + γ-irradiation, and BP + Bitumen + PR + γ-irradiation systems). 112
Figure 4.4. 2 (a) Weight gain and (b) Weight Extension (%). 113

Figure 4.4. 3 Comparison of thickness. 114
Figure 4.4. 4 Changes of (i) MR (moisture regain) %, (ii) MC (moisture content) %, and (iii) WU (water uptake) %. 114
Figure 4.4. 5 (ia.), (ib.) Raw jute fabric, (ii) bitumen +PR treated, (iii) bitumen + PR + γ irradiation (iv)HEMA+ Bitumen+ PR+ γ-radiation, (v) BP+ Bitumen+ PR+ γ-radiation. 116
Figure 4.4. 6 Comparative thermogravimetric analysis (TGA) of untreated and chemically modified jute fabrics indicating thermal degradation behavior and stability. 118
Figure 4.4. 7 (i) raw jute fabric(A) (ii) Raw Jute+Bitumen+PR+ γ-radiation(B), Raw jute+HEMA+Bitumen +PR+ γ-radiation (C), Raw jute+ BP+Bitumen+PR+ γ-radiation (D)... 119
Figure 4.4. 8 (i) raw jute fabric (A) (ii) Raw Jute+Bitumen+PR+ γ-radiation (B), Raw jute+HEMA+Bitumen +PR+ γ-radiation (C) Raw jute+ BP+Bitumen+PR+ γ-radiation (D).... 119
Figure 4.4. 9 (a) Loss of Tensile Strength (b)Strength Loss (%) after accelerated weathering exposure. 121
Figure 4.4. 10 Graphical analysis of fabric weight loss before and after weathering exposure. 122
Figure 4.4. 11 Comparison of thickness before and after weathering exposure. 123
Figure 4.4. 12 (a) FTIR graph of before weathering exposure, (b) FTIR graph of after weathering exposure. 124
Figure 4.4. 13 (a)XRD graph before weathering exposure (b) XRD graph after weathering exposure. 125

LIST OF TABLES

Table 2. 1 Chemical treatment of jute fabric [23]. 34
Table 2. 2 Chemical composition of Bitumen emulsion [65] 40
Table 2. 3 Assessment of Laboratory and Natural Weathering Exposure [75]. 42

Table 3. 1 Specification of plain-woven jute fabric used in the experimental work 48
Table 3. 2 Chemical composition of the bitumen emulsion used for surface treatment of jute fabric is given below: 48
Table 3. 3 List of auxiliary chemicals used in the experimental treatment process. 50
Table 3. 4 Weathering cycle [75]. 62

Table 4.1. 1Formulation of the chemical % used to treat the jute samples 68
Table 4.1. 2 Value of XRD graph for raw jute fabric 75
Table 4.1. 3 Value of XRD graph for chemically treated jute fabric 75
Table 4.1. 4 Summary of thermogravimetric analysis of raw jute (UJF) and treated jute (TJF) .. 77

Table 4.2. 1 Comparative data from the FTIR graph 89

Table 4.3. 1 Peak intensity analysis from the FTIR graph 102
Table 4.3. 2 Analysis of peak intensity from FTIR graph 108

Table 4.4. 1 Data table for comparison of tensile strength: 112
Table 4.4. 2 Statistical analysis of data from correlation 115
Table 4.4. 3 Pearson correlation 115

Table 4.5. 1 The cost of raw materials and different chemicals individually 128

LIST OF ABBREVIATIONS

AWE	Accelerated weathering exposure
ASTM	American Society for Testing and Materials
AOS	Apparent opening size
BE	Bitumen emulsion
BS	British standard
CRE	Constant rate of elongation
GSM	Grams/square meter
HEMA	2-Hydroxyethyl methacrylate
ISO	International organization for standardization
JGT	Jute geo-textiles
MR	Moisture Regain
MC	Moisture Content
TJF	Treated jute fabric
TS	Tensile strength
UPR	Unsaturated polyester resin
WU	Water uptake

Chapter 1: Introduction

1.1 Introduction

Geotextiles are mainly used for geotechnical engineering. The primary uses of geotextiles include soil erosion control, providing permeable properties, and supporting various types of rock and civil engineering construction. The key requirements of geotextiles are resistance to environmental stresses, such as air and UV radiation, and protection against bacterial and fungal attacks [1]. Synthetic fibres are the primary components of geotextiles, which are neither biodegradable nor eco-friendly [2]Generally, polypropylene, polyester, polyamide, and polyethylene are used to manufacture geotextiles [3]. Whereas jute fibre has more potential mechanical strength than other natural fibres, such as hemp, kenaf, cotton, and pineapple, for the use of geotextiles[4]. But not comparable with synthetic fibre. For the use of jute fibre in place of synthetic fibre, the modification of the jute fibre is necessary [5]. In this study, the mechanical strength and durability of jute fabric are improved through gamma radiation-induced polymer coating. This is a new concept in the research era. Natural fibre jute is biodegradable, eco-friendly, and cheaper than other fibres. Natural polymer jute is composed of cellulose, hemicellulose, and lignin [6]. Cross-linking and graft copolymerization of natural polymers with synthetic polymers enhance their mechanical strength and durability [7]. The potential method of chemical modification of natural fibers is the coupling method, in which coupling agents react with both the chemical and natural components of the fibers [8]. In recent years, the world has sought to utilize natural products to protect the environment from pollution and maintain a safe environment by reducing the release of unhygienic gases, carbon emissions, and greenhouse gases [9]. The main drawbacks of jute are its chemical components, specifically cellulose, which contain an -OH group. This -OH creates intramolecular and intermolecular bonds inside the fibre and also creates an extramolecular bond with moist air. The tendency to form extramolecular bonds with the outside environment makes jute fabric hydrophilic in nature; as a result, the degradation of jute fabric occurs very quickly [10]. Only a polymer coating or chemical/surface modification of jute fibre can reduce the bond formation of outside air and make jute fabric more durable by lowering the -OH group content in cellulose. Gamma irradiation generates free radicals in cellulose, whereas lignin is less affected. This free radical facilitates the formation of cross-links with the polymer mixture and the cellulose in the jute fabric [11].

In this research, bitumen emulsion and polyester resin were used to chemically modify jute fabric. In contrast, bitumen emulsion creates a coating on the jute fabric, and the polyester resin bonds

with the jute fabric cellulose via gamma radiation and other peroxide treatments. This treatment reduces the number of OH groups on the cellulose in jute fabric, thereby increasing its durability and mechanical strength.

The most important properties of bitumen emulsion are viscosity, consistency, and adhesion. The bitumen emulsion is a hydrocarbon with no reaction groups. It is used locally for road construction and for coating cellulosic materials, such as wooden products and bamboo fibre materials [12] On the other hand, polyester resin is soluble in styrene monomer. When this solution is mixed with peroxide, it generates a free radical, but when combined with bitumen emulsion, it does not undergo a reaction; instead, the bitumen forms only a coating on the jute fabric [13]. The coating of jute fibre makes jute fabric more durable than raw jute fabric, and crosslinking with jute fabric cellulose and a polyester resin improves its mechanical strength by reducing -OH groups and hydrophilicity.

1.2 Background of the Study

Generally, geosynthetics are used for soil erosion control and slope stabilization. Another use of geosynthetics is for hill slope stabilization and drainage. Soil erosion-induced slope failure is a critical environmental and geotechnical problem in tropical and monsoon-prone regions, where intense rainfall accelerates surface runoff and land degradation. The primary objective of this research is to develop an eco-friendly, biodegradable, and mechanically durable alternative material capable of preventing soil erosion and stabilizing slopes during the critical vegetation establishment period. Many researchers have tried to use jute Geotextiles in place of geosynthetics. But jute geo textiles are limited by their poor durability and low mechanical strength. Geosynthetics are made from PE, PP, PET, and PVC, but these synthetic fibres are not eco-friendly or biodegradable [14] [15] . The excessive reliance on petroleum-based geosynthetics contributes to long-term environmental persistence and microplastic pollution. While synthetic fibres play a vital role in all spheres of Geotextiles, increasing the use of natural fibres for geo-textile applications is necessary to reduce environmental pollution and carbon emissions, and to promote the use of sustainable products. Many researchers have attempted to enhance the mechanical properties of jute fabric in various ways. Only mercerization and peroxide treatment [16]. Increase the strength of cellulosic fibre, but do not make jute fabric suitable for geo-technical purposes. Only bitumen emulsion-coated without polyester resin, gamma radiation does not ideally use the jute fabric for geo-technical purposes [17] .Therefore, improving the durability and mechanical

performance of jute for short-to-medium-term geotechnical use remains a key research challenge. On the other hand, natural fibre composites are considered sustainable products; however, jute fibre composites are technically challenging and not commonly used for geotechnical purposes. A graphene-based nano-engineered jute composite exhibits higher tensile strength, making it a potential replacement for glass fiber composites [18]. Natural fibre jute has tensile strength comparable to that of glass and carbon fibres, and it is suitable for natural rubber-reinforced composites. These composite materials are used as an alternative to glass and carbon fibre composites, which are costly for use in geo-technical applications [19].

Jute fibre-reinforced low-density polyethylene composite materials are produced by compression molding, which enhances the composite's tensile, bending, and modulus of elasticity. This research work utilized HEMA- and benzoyl peroxide-treated jute fibre as a replacement for polyethylene composite or synthetic fibre composite [20] [21]. Most researchers work to develop jute fibre-reinforced composites to replace synthetic fibre composites, but their geotechnical applications are rare [22-24]. Jute geotextiles have already demonstrated strong performance in filtration, separation, drainage, and soil erosion control, accounting for over half of all geo-textile uses. Their effectiveness in preventing soil erosion lies in their ability to enhance surface drainage while keeping soil particles in place and supporting re-vegetation. Jute geotextiles also show promising potential for use in many other application areas [25]. Only bitumen emulsion-treated jute fabric with a natural fly ash, soil, and cow dung manure mixture increases the strength of jute fabric, and buried samples for up to 21 days. BE-treated jute fabric loses 17.03% and 14.49% of its strength compared to the non-biodegradable sample [26]. Jute fabric needs a minimum durability of 6 months for geotechnical use. Therefore, extending functional durability while retaining biodegradability is essential for field-scale erosion control applications.

A jute fabric matrix composite with polypropylene/polyethylene improved mechanical properties sufficiently. Peroxide-treated jute fabric was used for this research purpose. However, this composite is used as an alternative to composite materials rather than as a synthetic fibre composite, not for geotechnical purposes. Improving the adhesion between the fibre-matrix composite, pre-treatment of the jute fabric played a vital role [31]. A jute fibre-reinforced polypropylene composite is an alternative to synthetic fibre-reinforced composites; the strength of synthetic fibres like carbon, aramid, and coir is not comparable to that of natural fibres like jute and hemp. However, the jute fibre composite is comparable to the synthetic fibre composite and

is used for composite material. Benzoyl peroxide is used as a photo-initiator chemical for jute fabric reinforcement and polypropylene composites, helping increase tensile and bending strength [27] . Conventionally, jute fibre is used for carpet backings, sacking, ropes, and canvas. However, the increase in jute fabric-reinforcement composites is vital, and jute fabric reinforcement with a urethane acrylate-based composite is a new area of research. It is a low-cost, readily available thermoset composite, though it is not suitable for geotechnical purposes [5].Radiation has a significant impact on the composite of jute fabric. UV and gamma radiation improve the mechanical properties and also the adhesion between the fabric and the matrix in the composite materials. Chemical treatment with high-energy radiation (gamma) and nonionizing radiation (UV) improves the physical and chemical properties of jute fabric. Radiation ionizes cellulose, creating free radicals that reduce hydroxyl groups (OH) and form additional free radicals, which then create covalent bonds [28] . Reducing the (OH) group content decreases moisture regains and moisture content, thereby improving the physicochemical properties of jute fabric. When high-energy gamma radiation interacts with solid cellulose, it undergoes Compton scattering, and the energy trapped in the cellulose is nucleated into macro-cellulosic radicals. These free radicals are responsible for altering the biological and physicochemical properties of the cellulosic fibre (Jute fibre) [28]. The main drawbacks of geosynthetics are that they are not biodegradable and not eco-friendly. Geosynthetics effectively control soil erosion and road embankments, but their longevity is high, posing a threat to environmental pollution. Natural fibre geotextiles have limited longevity, but they control soil erosion and perform other geotechnical applications, and degrade gradually, which is environmentally safe. Thus, biodegradable geotextiles are particularly suitable for temporary erosion control, slope protection, and re-vegetation support in environmentally sensitive areas.

Nowadays, concerns about environmental safety, interest in sustainable products, and the recycling of waste, as well as the use of natural fibre, are increasing day by day due to their limited longevity and biodegradability [29] . Accordingly, this research aims to develop a chemically and radiation-modified jute geotextile with enhanced short-term durability and mechanical strength suitable for soil erosion control and slope stabilization.

An alternative to replacing geosynthetics is treating natural fibres to increase durability for a specific period [21].

1.3 Aims and Objectives of the Study

The main purpose of this research is to use jute geotextile for soil erosion control and slope stabilization in place of geosynthetics [15]. But the low durability and poor mechanical strength are the principal barriers to the use of jute fabric for geo-technical purposes. The natural fibre jute is composed of various chemical components, including cellulose, hemicellulose, and lignin. In contrast, cellulose is formed by the residue of glucose, which is joined through an acetal linkage. This linkage is formed by hydroxyl and carbonyl groups [30]. The hydroxyl (-OH) groups in cellulose make jute hydrophilic, causing moisture absorption that weakens inter-fibre bonding and reduces mechanical strength. Thus, reducing jute's hydrophilicity through chemical treatment can enhance its tensile strength, durability, and suitability for geotechnical applications.

This research aims to develop a biodegradable jute-based geotextile with controlled porosity and hydrophobicity, combining mechanical robustness with environmental sustainability. The intended applications include soil erosion control, slope stabilization, surface drainage management, and temporary geotechnical protection in environmentally sensitive areas. The broad objective of the research plan is designed based on the above argument.

1. To emphasize the durability of jute fabric by reducing the hydrophilicity.
2. To modify the physicochemical characteristics of jute fabric.
3. To analyze the physicochemical properties by FTIR, XRD, TGA, TS, and water absorbency results.
4. To optimize the durability properties of jute fabric by decreasing the microbial attack, which ensures the antimicrobial test.
5. To examine the biodegradability of jute fabric by burying it in soil for varying periods and conducting an accelerated weathering test.

1.4 Outline of the Research

In this research work, the inspiration for the research, the collection of raw materials, the working procedure, and the analysis of the treated samples are discussed in separate chapters, each elaborated. Each chapter summary or content is given below:

Chapter 1: Introduction

This chapter presents the general discussion, background study, and aims and objectives of the research work.

Chapter 2: Literature Review

This chapter provides theoretical background on geotextiles, including a literature survey and a review of relevant literature for the research.

Chapter 3: Materials and Methods

Details of different raw materials, Sample preparation, and different testing routes of the research work are described in this chapter.

Chapter 4: Results and Discussions

Data collection and Data analysis of the different tests in this research work. Appropriate discussion of the research works, the results, and the discussion was divided into four (4) different segments:

4.1. Selection of optimum polymer mixture formula for chemical modification.
4.2. Selection of optimum radiation dose.
4.3. Pre-treatment of jute fabric, then chemical modification.
4.4. Measurement of durability by weathering test.

Chapter 5: Conclusion

Finally, the conclusion is described in this chapter. This is the end chapter of this research work, which also discusses Key Findings of the Study, Research Contribution, Limitations of the Study, Recommendations for Future Research, and provides a List of References for the thesis.

Chapter 2: Literature Review

2.1 Geo-Textiles

The term “Geo” originates from the Greek word “Earth,” meaning that any textile material applied within soil for a technical function is known as a geo-textile. According to the Textile Institute, geotextiles are permeable textile materials used for filtration, drainage, separation, reinforcement, and stabilization in civil engineering works involving earth, rock, or other construction materials. An alternative definition of geotextiles states that geotextiles are permeable fabrics used in conjunction with soil or rock as a functional component of human-made structures [2], [3]. Synthetic fibers are widely used as the primary raw materials for manufacturing geotextiles. However, several natural plant fibers are also utilized in geotextile production. Since geotextiles made from natural fibers are biodegradable, they are particularly suitable for applications requiring temporary performance. Current soil erosion prevention practices employ hard engineering methods (retaining walls, riprap, gabions) and soft engineering approaches (vegetative cover, mulching, erosion control blankets, and rolled erosion control products). Geotextiles are widely used as rolled erosion control products to minimize splash erosion, reduce runoff velocity, retain soil particles, and promote vegetation establishment on exposed slopes and embankments.

The application of geotextiles for soil erosion control is well established and not novel; however, improving their environmental compatibility and hydraulic performance remains an active research area.

Additionally, natural fiber–based geotextiles offer key advantages, including low cost, greater strength and durability, easy availability, good flexibility, and environmental friendliness [3] . Jute geotextile (JGT) is a technical textile and represents a natural alternative to synthetic geotextiles. Various woven and nonwoven forms of JGT have been created for numerous geotechnical purposes, including enhancing pavement performance, preventing soil erosion, supporting embankments, and improving drainage systems. However, existing JGT products often fail to meet required mechanical and hydraulic performance criteria under sustained field loading, highlighting the need for material modification and structural optimization [4], [31] .

2.2. Basic Functions of Geo-Textile

The primary functions of geo-textiles are given below:

a. Separation

b. Reinforcement

c. Filtration

d. Drainage (or fluid transmission)

e. Fluid Barrier. [32]

For soil erosion control, filtration and drainage functions are critical. The geotextile must permit water flow while preventing soil particle migration, ensuring slope stability, and minimizing surface washout.

2.2.1 Separation

The separation function is a crucial application of geotextiles as illustrated in Figure 2.1, which creates a stable interface between two layers of soil, such as coarse aggregates and fine-grained subsoil. When geotextiles are placed between the soil layers, they prevent the intermixing of the soil layers under applied loads, thereby preventing the intrusion of large particles, such as pebbles, into the subgrade. This separation ensures that each layer maintains its structural integrity and intended engineering performance throughout the construction's lifespan. In essence, separation involves positioning a flexible, porous geotextile between dissimilar materials, allowing each layer to retain its functional properties without contamination or displacement [32].

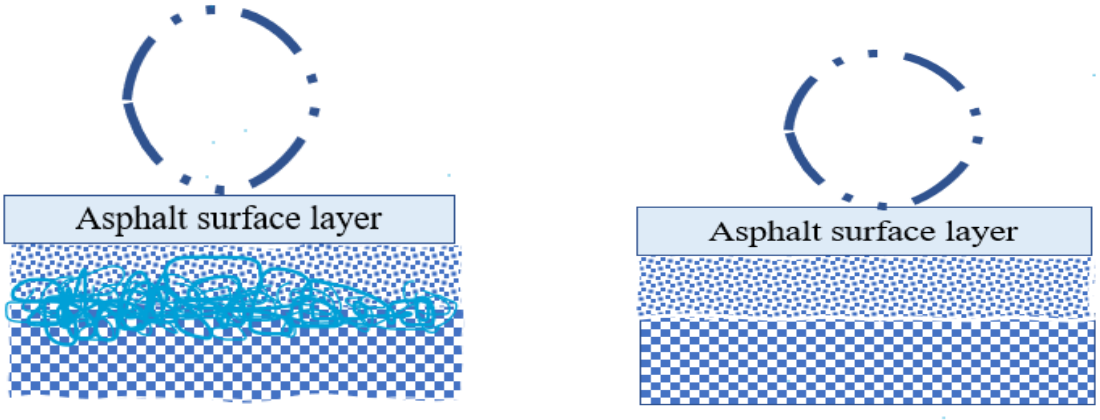

(a) Without geo-textile (b) With geo-textile

Figure 2. 1 Separation function of geotextiles between two soil layers: (a) without geotextile, showing mixing of subgrade and aggregate; (b) with geotextile, maintaining layer stability and preventing soil intermixing [33].

2.2.2 Reinforcement

Figure 2.2 depicting the reinforcement techniques using geotextiles are employed when the subgrade exhibits inadequate strength or stability, and high-tensile-strength geotextiles are use. Their inclusion within the soil mass improves interparticle friction and bonding, thereby improving load distribution throughout the composite structure. As external loads act on the system, the geotextile mobilizes these forces into tensile stresses, enabling the reinforced soil to sustain higher loads and improving key mechanical properties, including puncture resistance and overall structural performance [32].

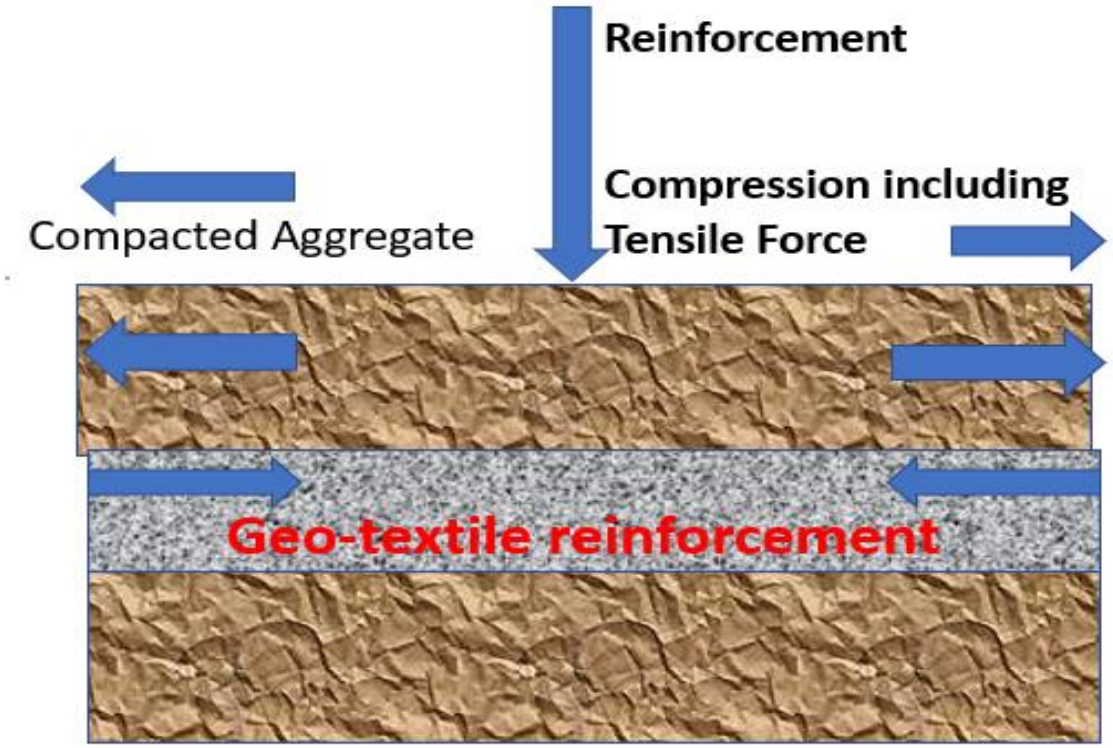

Figure 2. 2 The reinforcement mechanism of geotextiles in soil structures, where tensile resistance of the fabric improves load distribution and increases the overall stability of the soil mass [34].

2.2.3. Filtration

Figure 2.3 illustrate the filtration techniques for geotextiles work through the stabilized interaction between a geotextile and the surrounding soil, which permits adequate water passage while restricting soil loss throughout the intended service life. A standard illustration of this role is the placement of geotextiles in pavement trench drains. Effective filtration requires the geotextile-soil system to be in hydraulic equilibrium, which supports perpendicular (cross-plane) liquid flow. This function is characterized by the geotextile's permittivity or cross-plane hydraulic conductivity. An essential parameter in this context is the Apparent Opening Size (AOS), which is a pore-size parameter; 95% of openings are smaller and are evaluated against the particle-size distribution of the soil. During operation, coarse particles accumulate at the geotextiles interface to form a stable bridge, which subsequently retains finer particles and ensures long-term filtration performance [32].

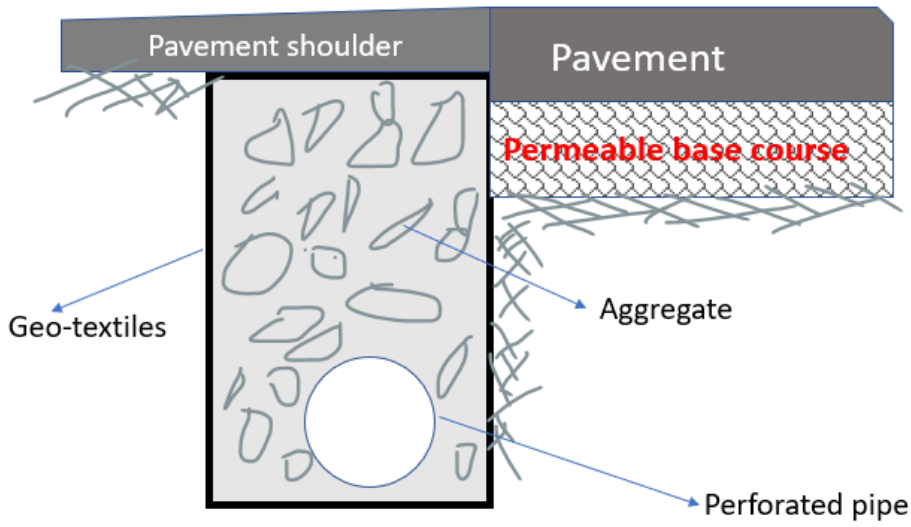

Figure 2. 3 Filtration mechanism of geotextiles allowing water to pass through while preventing soil particle migration, thereby maintaining hydraulic stability within the soil system [33].

2.2.4 Drainage (or fluid transmission)

For various environmental or structural reasons, liquids and gases may accumulate within a soil mass over time. Geotextiles can be employed as depicted in Figure 2.4 to collect and channel these fluids toward designated drainage or vent pathways, enabling in-plane flow through the fabric without displacing soil particles. In drainage applications, geotextiles with adequate filtration capacity and high permeability can effectively facilitate lateral fluid movement while preventing soil loss [32].

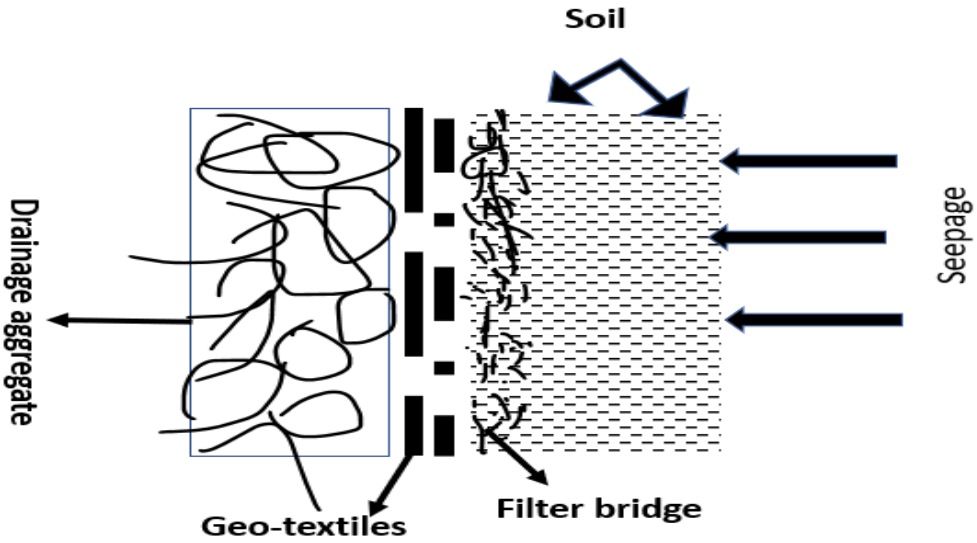

Figure 2. 4 Drainage function of geotextiles facilitating in-plane flow of water through the fabric while retaining surrounding soil particles [33].

2.2.5 Fluid Barrier

Another function of geosynthetics is acting as a nearly impermeable barrier to fluid movement. As illustrated in Figure 2.5, when a geosynthetic layer is placed at the base of a pond or containment structure, it effectively blocks the downward seepage of liquid waste, thereby preventing contamination of the underlying natural soil [35].

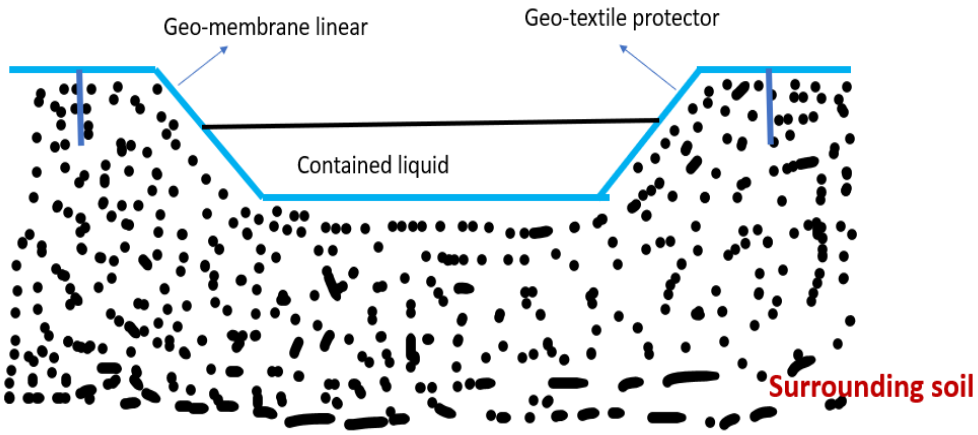

Figure 2. 5 Fluid Barrier Application of Geosynthetic Materials Used to Prevent Downward Seepage of Liquid Contaminants into Underlying Soil Layers [36].

2.3 Major Applications of Geo-Textiles

1. Soil erosion control by the protection of riverbanks
2. Stabilization of seabeds
3. Safeguarding coastal zones
4. Construction of coastal defense systems
5. Drainage and dewatering works
6. Systems requiring either cross-plane or in-plane water movement
7. Lining and protection of reservoirs and lakes
8. Use in concrete mattress structures
9. Installation of vertical filtration or separation screens
10. Fabrication of geo-bags and similar containment units [2].

2.4 Geo-Jute

Jute geotextiles (JGT) have gained importance due to their favorable physical, mechanical, and hydrological characteristics [37]. Environmental studies of jute geotextiles indicate that their biodegradation contributes organic matter to soil, supports vegetation growth, and avoids long-term microplastic accumulation associated with synthetic geotextiles. However, rapid

biodegradation under microbial attack and moisture limits their service life in erosion control applications, necessitating controlled durability enhancement.

2.5 Advantages of Geo-Jute

1. Jute geotextiles have high water absorption capability.
2. Excellent drapability.
3. Initial strength is high.
4. Biodegradable
5. Easy availability.

2.6 Application of Geo-Jute

Geo-textiles are widely used for soil erosion control through soil reinforcement in various applications, such as slopes and river banks, roads, and infrastructure [15] . The attributes of Geo-jute have made it an appropriate fabric for many civil engineering applications where soil poses a challenge. Geo-jute has been applied successfully in the following areas:

1. Slope management
2. Erosion control & soil conservation
3. Stabilization of earthen embankments
4. Protection of river canal banks
5. Strengthening of road pavements
6. Consolidation of soft soil
7. Landscaping.
8. Mulching, etc [38].

2.7 About Jute Fibre

Jute is a naturally occurring, biodegradable fibre due to its hydrophilic nature and complex polymeric structure [39] . Commonly known as the “golden fibre”, it plays a vital role as a significant cash crop in Bangladesh. The long-term sustainability and competitiveness of jute, especially compared with synthetic fibers, heavily depend on enhancing its performance characteristics to further strengthen the country's agro-based economy. Jute possesses several advantageous features, including its low density, non-abrasive nature, biodegradability, and renewability, which make it an attractive substitute for traditional glass and synthetic textile fibers [40]**.** Owing to its abundance and eco-friendly nature, jute stands as the second most widely

produced cellulosic fibre in the world. The hydrophilic nature of jute leads to moisture absorption, swelling, fibre weakening, and accelerated microbial degradation, directly reducing mechanical strength under field conditions. Therefore, reducing hydrophilicity is essential to improving the durability of jute geotextiles in erosion control applications.

2.8 Biochemical Constituents of Jute Fibre

The approximate biochemical composition of jute fibre is summarized below:

- Cellulose → approximately 60–65 %
- Hemicellulose → approximately 20–24 %
- Lignin → approximately 12–13 %
- Water-soluble components → approximately 1–2 %
- Fats and waxes (oily materials) → approximately 0.5–1 %

These values are consistent with those reported in fibre science and natural fibre composite literature [41-44]. The relatively high cellulose content contributes to the good tensile strength of jute fibres, whereas the presence of hemicellulose and hydroxyl (–OH) groups makes the fibre highly hydrophilic, which affects durability in moist environments.

2.9 Physical Properties of Jute Fibre

Typical physical characteristics of jute fibres reported in the literature are summarized below:

1. Ultimate Length-2'5mm

2. Diameter-18 microns

3. Single fibres Length-0.2- 30 inch.

4. Single fibres Tex-1·9-2·2

5. Single fibres Tenacity-40-70 g/tex

6. Single fibres Extension at break-2·0 percent

7. Moisture regains at 65% Relative humidity

I. Absorption -12·8 percent

II. Desorption -14·6 percent

8. Specific gravity-1·48

These physical properties make jute one of the strongest natural fibres and suitable for applications such as ropes, sacks, carpets, and geotextiles. However, the relatively low elongation and high moisture absorption can limit its durability when exposed to humid or soil environments [23], [44-45].

2.10 Eco-friendly Jute Processing

Jute is regarded as the first adaptable biodegradable fibres, ranking second only to cotton in worldwide annual production. Classified as a bast fibre, its structural composition is primarily based on cellulose, hemicellulose, and lignin. The plant grows most effectively in warm, humid, and rain-fed subtropical environments- conditions typical of the eastern part of the Indian subcontinent. Bangladesh, in particular, possesses an ideal climate for jute cultivation, which has allowed it to become the world's chief producer and exporter of raw jute and jute-based goods. During the 2007-2008 period, Bangladesh produced nearly 990,000 tons of raw jute, of which approximately 477,000 tons were exported. Consequently, the country accounted for approximately 63.26% of global jute exports during those years [46].

A distinguishing characteristic of jute is its hygroscopic nature, primarily influenced by its substantial hemicellulose content. Moisture plays a crucial role in determining fibre properties during harvesting, storage, and processing. If the moisture content is too low, jute fibre becomes stiff and brittle, resulting in breakage and significant fibre loss during mechanical handling. Conversely, excessive moisture creates conditions favorable to microbial growth, leading to rapid deterioration and a reduction in the quality of processed jute. Under standard atmospheric conditions (65±5 % relative humidity), jute typically contains around 12-14% moisture by weight, and this value increases proportionally with rising humidity [47].

A flow chart illustrating the significant steps is presented below:

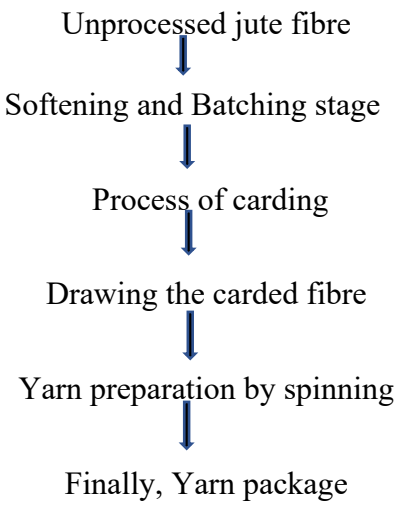

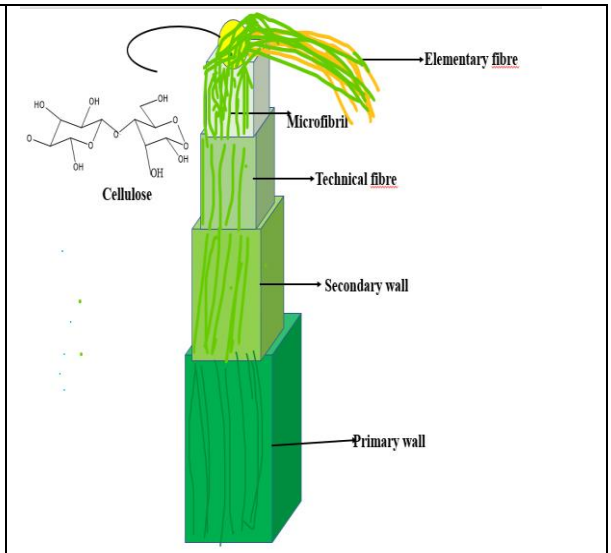

Jute Plant	Structure of the jute plant

Figure 2. 6 Picture of a jute plant and its Structure.

2.11 Disadvantages of Jute Fibre

Though jute fibre has more fibre length and tensile strength than other natural fibre, it has some major disadvantages. Some important disadvantages are given below:

a. Jute fibres have 65.2% cellulose, and cellulose has -OH group, which loses jute fibre durability properties in moist air.

b. Hemicellulose also has OH, which makes a covalent bond outside the environment and is affected by microorganisms very quickly.

c. The water absorbency is higher for its hydrophilicity. The moisture content of jute fibre is (5-13) % [48-50].

d. Thermal degradation of jute fibre is done in two steps: first, degradation of hemicellulose(220-280^{o}C), and then lignin degradation at (280-300^{o}C). As a result, above 250 °C, jute fibre is unsafe.

e. On the other hand, jute fibre is hydrophilic, and polymer is hydrophobic, and poor interfacial adhesion has been found in fibre matrix composite[51].

2.12 Chemical Modification of Jute Fibre

Table 2. 1 Chemical treatment of jute fabric [23].

Process	**Agent/Chemical**	**Result**
Alkali treatment	NaOH	It increases fibre surface roughness by disrupting hydrogen bonds and reducing lignin, wax, and oil, and also increases fibre diameter.
Acetylation	Acetyl reactive group (CH3CO) compound	The reaction between the acetyl group and the hydrophilic hydroxyl groups (OH) of the fibre, which removes moisture, hence decreases the hydrophilic nature of the fibre. The dimensional stability of composites increases.
Silane treatment	SiH4	It is used as a coupling agent. A silane coupling agent may reduce the hydroxyl groups on cellulose at the fibre-matrix interface.
Benzoylation treatment	Benzoyl chloride	Benzoyl (C6H5C=0) in benzoyl chloride decreases the hydrophilic nature of the treated fibre, causing improvement in interfacial adhesion and thermal stability of the fibre.
Permanganate treatment	MnO̅4 group	Graft copolymerization is initiated by highly reactive (Mn3+) generated in the treatment of fibre by potassium permanganate (KMnO4) in acetone solution.

Peroxide Treatment	Benzoyl peroxide (BP, ((C6H5CO)2O2) and dicumyl peroxide (DCP, (C6H5C(CH3)2O)2)	Peroxide helps generate free radicals from jute fabric cellulose and also activates cellulose for further reactions, such as cross-linking, thereby improving jute fabric durability and reducing hydrophilicity.
Coupling agent (maleated)	PP grafted with maleic anhydride (PP-g-MA) and acrylic acid	This improves the fibre's wettability and interfacial adhesion.

2.13 Surface Modification

Surface modification with different materials/polymers is a modern technique. Dettre and Johnson, in 1964, first coated a lotus leaf to increase its superhydrophilicity [52].In recent years, as the use of polymers has increased for various purposes, surface modification has become necessary. Surface modification of a polymer alters its physical and chemical properties. Surface modification of a polymer involves treating its outermost surface with a different functional group, thereby enhancing its wettability, dye absorbance, and other properties. It increases mechanical strength, among other benefits, making surface treatment a primary focus in Polymers for biomaterial applications. Surface modification methods have attracted greater attention in the global scientific literature when applied to polymers. Traditionally, surface modification methods are of two types: (a) chemical methods, and (b) physical methods [53-54].

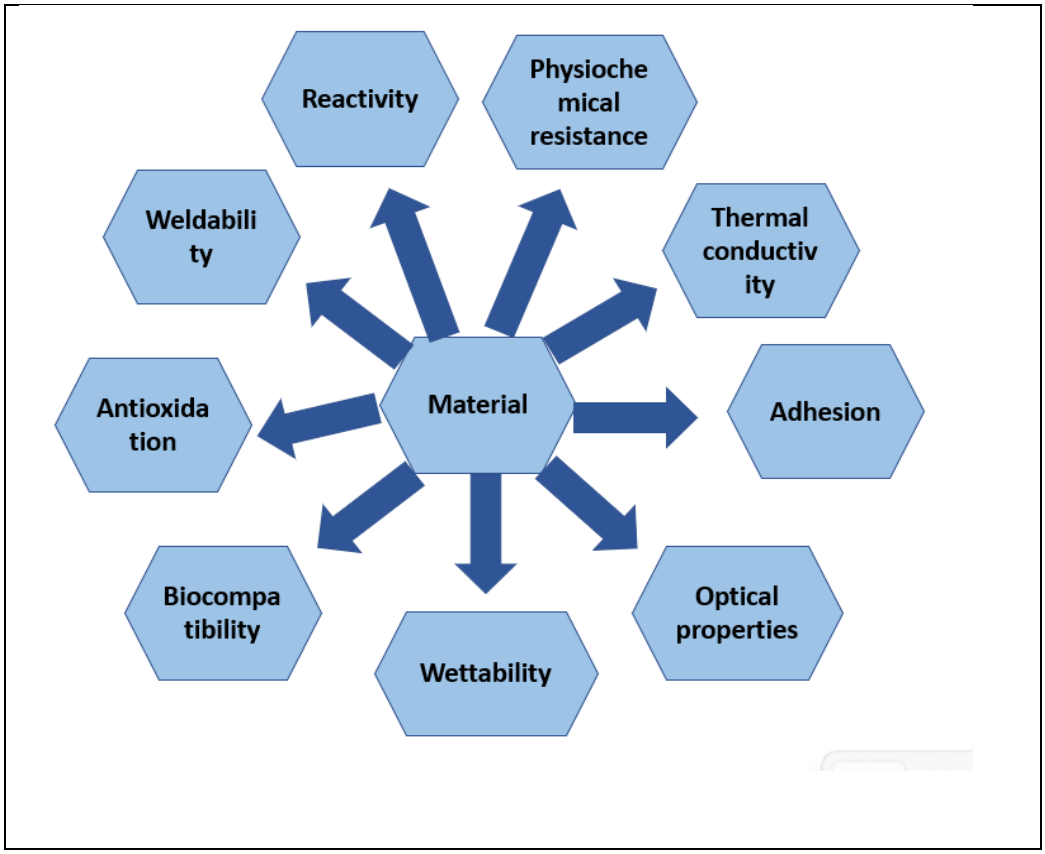

Figure 2. 7 Schematic illustration of property enhancement in fibre material after surface modification [55].

2.13.1 Methods of Surface Modification

1. Chemical Method
2. Physical method

2.13.1.1 Chemical Method

Chemical modification is a process that uses different chemicals to alter the structure or functional groups through chemical reactions. A notable example of chemical modification is coating in wet chemistry. The coating of a material must meet various requirements, including adhesion to the substrate and the expected mechanical and functional properties. Some improved properties of a material are given below:

a. Scratch

b. Wear resistance

c. Hydrophobicity

d. Antibacterial

e. Antistatic

f. Chemical resistance, etc.

The most important condition for coating a material is low temperature, because the plastic material cannot be deformed, undergoes no physical change, and experiences no chemical degradation[56].

2.13.1.2 Physical Modification

When surface modification cannot change a polymer or material's inherent chemical properties but can improve physical properties, such as strength, by imparting a hydrophobic nature, it is called physical surface modification [57]. Various processes can physically modify a material; heat and gas treatments are the most common methods—flame and corona treatments are also used mainly for industrial purposes. A key benefit of physical surface modification compared with other techniques for producing a superhydrophobic surface is that it eliminates the need for environmentally hazardous fluorinated polymer [58]. Moreover, polymers treated physically tend to be durable, showing minimal ageing or degradation, since the induced surface roughness does not significantly alter the underlying surface chemistry [53].

2.14 Cross-linking

Cross-linking is a polymerization technique that connects two or more polymer chains by a covalent bond. Cross-linking makes a polymer harder, stronger, stiffer, and more durable. When cross-linking is extensive, it creates a random three-dimensional interconnection of polymer chains. Today, many composite materials are made from a combination of cross-linking techniques. Cross-linking makes the polymer more hydrophobic and rigid. Various hard plastic materials are used for electrical purposes, and melamine and hard plastic crockery are made using these techniques. Recently, surface modification of materials has been achieved using various coating materials, such as bitumen emulsion and resin. In a coating process, coating materials are cross-linked to the polymer surface via covalent bonds. Formation of a covalent bond in cross-linking requires the creation of a free radical. The creation of free radicals involves various. The cross-linking or curing of coating compositions can occur through several fundamental pathways or mechanisms. The first is through free radical or oxidizing reactions, assisted by elevated temperature and the presence of air. Various radiation sources, such as UV light and gamma radiation, can also initiate cross-linking. Another major pathway involves a chemical reaction,

such as the condensation reaction between an alcohol or an amine and a carboxylic acid. The epoxy group, in particular, undergoes ring-opening. While specific two-component systems can be cured at ambient temperature, others require elevated heat to complete the process [59] [60].

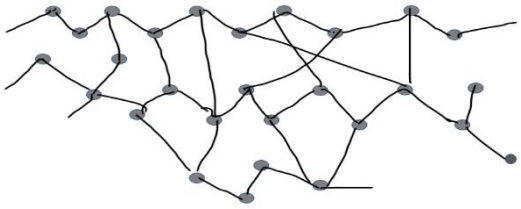

Figure 2. 8 A cross-linked polymer [61].

2.15 Gamma Radiation (γ-Irradiation)

Numerous types of radiation, such as gamma radiation, are high-energy electromagnetic radiation. A photon has no rest mass, electric charge, or magnetic moment. Gamma radiation is generated from an individual photon. The energy of gamma radiation is calculated by the following formula, where frequency is denoted by ν, and the wavelength is denoted by λ[62] : -

$$E = h\nu = hc/\lambda \quad \text{eq (1)}$$

Gamma rays are released from the transition of an electron from a higher energy state to a lower energy state, typically generated from alpha or beta decay or through various nuclear reactions. The energy spectrum of gamma (γ) rays is inherently discrete, and the transitions of gamma(γ) are governed by specific rules, similar to those that apply in optical spectroscopy[62].

2.16 Effect of γ-Irradiation on Surface Modification/ Cross-Linking

High-energy, short-wavelength gamma(γ) rays can be used to alter surfaces in several ways. When these interact with a substrate, they produce free radicals and free molecules from their surfaces. Free radicals can damage or alter plant cells, affecting morphology, physiology, biochemistry, and plant anatomy, depending on the intensity of irradiation doses. On the other hand, free radicals may continue to react or cease activity through processes such as molecular recombination. Gamma (γ) radiation plays a vital role in the production of free radicals without any chemical

composition, reactive group, or chemical reaction. In cross-linking polymerization, sufficient free-radical formation is required to form covalent bonds between polymer chains. For this reason, γ-irradiation is commonly used for post-crosslinking of polymers, providing a clean method that does not require additional reactive groups or chemical additives [28]. As a result, gamma rays change the morphology of natural polymer (plant cell). Gamma irradiation was applied to modify the permeable membranes of a polymer prepared by blending poly(hydroxyurethane) with poly (vinyl alcohol) (PVA) in varying proportions. The resulting polymer membranes were designed to exhibit different levels of hydrophilicity, flexibility, initial elastic moduli, and surface energy, depending on their alloy composition, higher gamma radiation doses, enhanced porosity, and increased hydrophilic properties, because limited research has been conducted on gamma irradiation for surface modification. Evaluating the advantages of a broad range of polymers remains challenging [49-51][11], [53].

2.17 Bitumen Emulsion

Bitumen emulsions (BE) were first developed in the early twentieth century using anionic surfactants as emulsifying agents, which initially offered certain benefits but also present several limitations. Over time, many countries abandoned anionic surfactants as cationic emulsions became the norm in the late 1950s. Not only are cationic bitumen emulsions driven by their superior ability to bond with mineral aggregates, but also by challenging environmental conditions. This improved adhesion results from the differing mechanisms of anionic and cationic types of emulsions [65] Polarity and breaking behavior are the main properties for the selection of bitumen emulsion [66]. Typically, anionic types of bitumen emulsions break down upon contact, mainly through water evaporation. In contrast, cationic bitumen emulsions break down when the positively charged emulsifiers chemically bond to the surface and to water, which is then released. France is the only leader in the production and application of bituminous emulsions, producing 97% of cationic type bitumen emulsions, with a small quantity of anionic type emulsions, and storing them for different uses, especially for coating purposes [12], [50-54]. In this research, bitumen emulsion was used for coating.

Table 2. 2 Chemical composition of Bitumen emulsion [65]

Component name	**Content, % wt.**	**Note**
Raw bitumen	30-80%	Bitumen used for road construction and modified formulations can be employed when improved performance is required.
Water	15-70%	Usually, soft water is used for making bitumen emulsion. The hardness of used water should not exceed 6 mEq/l.
Emulsifier	.15-.30%	Both types of emulsifiers are used, namely anionic and cationic, yielding three classes of emulsions: EBC-1, 2, and 3.
Acid	0,1–1,0%	As an acid, 25–37% hydrochloric acid is used to maintain the pH of the aqueous phase at 1.5–3.5. It converts the emulsifier into an ionic form, allowing adjustment of the pH of both the aqueous phase and the emulsion.
Растворитель	0,5–3,0%	For increasing stickiness, solvents are used, which are emitted during the decay of the bitumen emulsion (as the film-forming agent), and to facilitate its dispersion in water.
Modifier of a disperse phase	2,0–10,0	To produce bitumen emulsion, some polymers may act as a modifier of the dispersed phase. They serve as polymers used for the extended-temperature-range performance of viscous bitumen, with simultaneous increases in heat resistance, crack resistance, and flexibility.

Stabilizer	0,05–0,5	Calcium chloride is used as a stabilizer at 30–35% in aqueous solution.
Thinner (if necessary)	5–30	It is used to increase bitumen penetration to the desired value. Vacuum gas oils, oil fractions, and other similar products are used.

2.18 Unsaturated Polyester Resin (UPR)

Unsaturated polyesters (UPR) are widely used synthetic copolymers for a range of applications, including fibers, plastics, composites, and coatings. A wide range of product varieties with different chemical and mechanical properties can be produced by selecting monomers, initiators, curing agents, additives, and modifiers. They are appealing because their production costs are low. In the composite industry, their application is as matrices. Among composites, fiberglass-reinforced composites are the most significant [13].

Unsaturated polyester resin (UPR) serves as the basic framework for producing crosslinked polyester materials. UPR is produced by a step-growth polymerization process, in which the polyester monomer is used to cross-link the polymer. The polyesters typically come from ethylene glycol (commonly known as antifreeze), which contains hydroxyl groups at both ends. Unsaturated polyester resin is an antifreeze chemical, and in its production, an organic acid acts as an organic (vinyl diacyl chloride), driving the reaction under acid catalysis. This reaction proceeds via condensation polymerization, releasing hydrogen chloride (HCl) as hydroxyl groups form, thereby promoting free-radical formation and cross-linking [72].

Unsaturated polyester resins (UPR) play a vital role in the manufacture of composite materials. They are often referred to as the backbone of the composites industry, accounting for approximately 75% of total resins used. This resin incorporated some unsaturated components, typically maleic anhydride or fumaric acid, within the dicarboxylic acid portion of its structure. After synthesis, the polymer is mixed with a reactive monomer, such as styrene, to produce a low-viscosity resin. After curing, styrene monomer reacts with the polymer's unsaturated side groups, forming a solid thermoset [73].The use of UPR has beneficial properties and applications.

However, it is a thermoset used in various polymer matrix composites and natural cellulose reinforcement composites [74].

2.19 Accelerated Weathering Test

Durability testing of a material is conducted using two methods: natural outdoor exposure and accelerated weathering tests. Natural outdoor exposure uses natural light sources (Sunlight) and water (Rainwater), which are uncontrollable and entirely dependent on nature; as a result, they require sufficient time for durability testing. On the other hand, an accelerated weathering tester machine used an artificial light source (UV) and an artificial water spray, which is controllable and needs less time for the durability test. An accelerated weathering tester machine; all parameters are set up as per requirements. Now, accelerated laboratory weathering testing machines are widely favored for predicting long-term outdoor performance. In many modern applications, outdoor exposure trials are no longer conducted and are even considered unnecessary. However, the accelerated weathering tester cannot fully replicate all types of natural conditions, though the laboratory chamber is more commonly used today. In addition, several test variables may produce inaccurate results, leading to misleading outcomes. Different manual settings of the accelerated weathering chamber, like time, sequence, and weathering cycles, differ significantly from outdoor conditions. Consequently, depending too heavily on accelerated testing alone results in incorrect or incomplete conclusions [75].

Table 2. 3 Assessment of Laboratory and Natural Weathering Exposure [75].

Accelerated Tests	**Outdoor Tests**
Testing compartment	Racks in open fields
Controlled weathering conditions	Conditions not-controlled
Non-natural light source	Natural light (Sunlight)
Controlled weather conditions	Natural weather conditions

Synthetic geotextiles provide long service life but contribute to long-term environmental persistence and microplastic pollution. In contrast, jute geotextiles provide temporary

reinforcement and degrade naturally, making them environmentally preferable for erosion control during vegetation establishment stages.

Chapter 3: Materials and Methods

3.1 Research Work Flow and Experimental Design

This research work followed a systematic approach to prepare an end product from raw jute fabric through chemical modification for use in geotechnical applications, such as soil erosion control. The work follow diagram given below:

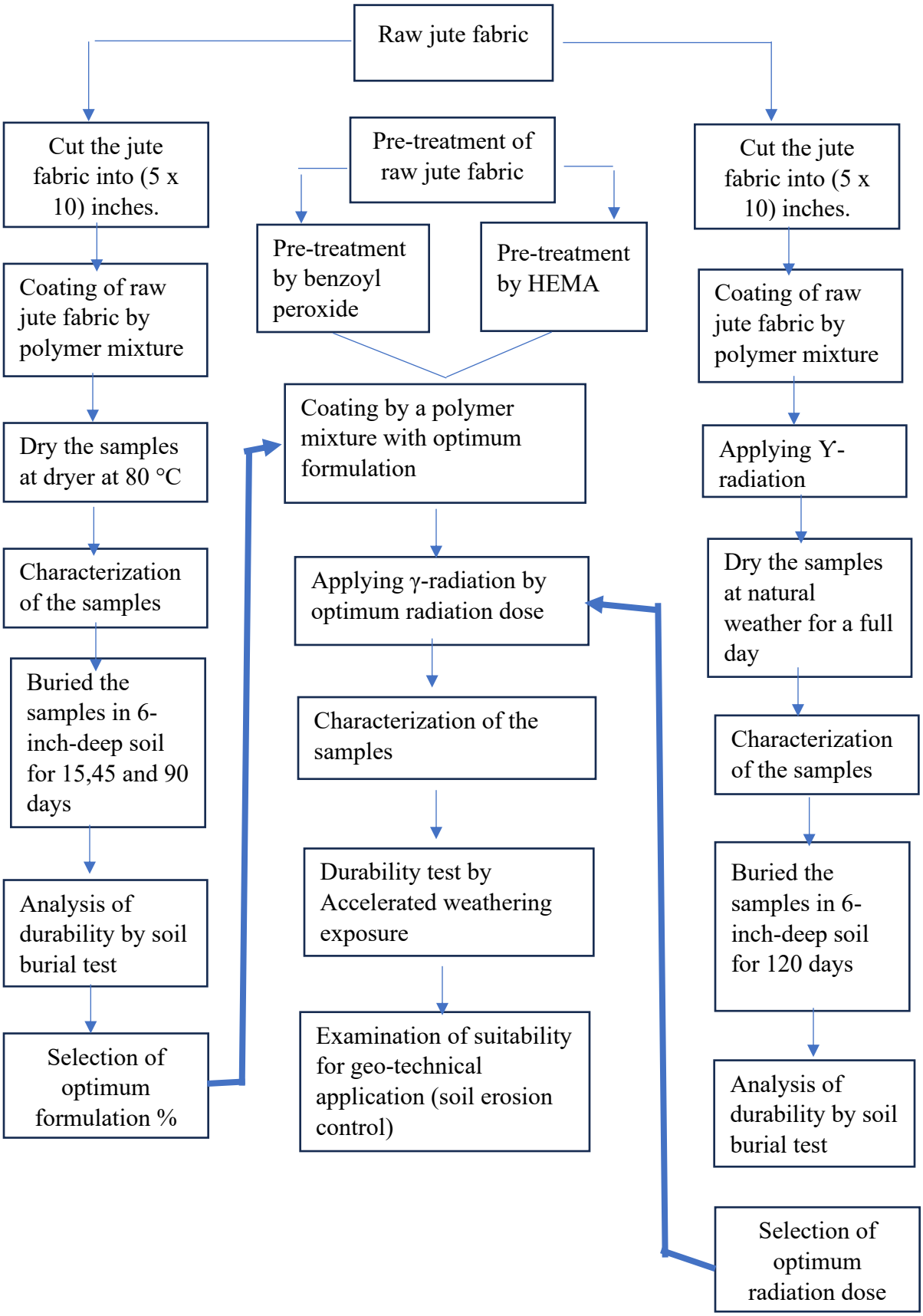
Raw jute fabric
Cut the jute fabric into (5 x 10) inches.
Coating of raw jute fabric by polymer mixture
Dry the samples at dryer at 80 °C
Characterization of the samples
Buried the samples in 6-inch-deep soil for 15,45 and 90 days
Analysis of durability by soil burial test
Selection of optimum formulation %
Pre-treatment of raw jute fabric
Pre-treatment by benzoyl peroxide
Pre-treatment by HEMA
Coating by a polymer mixture with optimum formulation
Applying γ-radiation by optimum radiation dose
Characterization of the samples
Durability test by Accelerated weathering exposure
Examination of suitability for geo-technical application (soil erosion control)
Cut the jute fabric into (5 x 10) inches.
Coating of raw jute fabric by polymer mixture
Applying Y-radiation
Dry the samples at natural weather for a full day
Characterization of the samples
Buried the samples in 6-inch-deep soil for 120 days
Analysis of durability by soil burial test
Selection of optimum radiation dose

The rationale for this workflow is to compare untreated jute geotextiles with treated and coated jute composites to understand how surface modification influences durability, hydraulic behavior, and biodegradation in soil erosion control applications. Many previous studies of natural jute fibre suggest that baseline mechanical properties of jute fabric can be improved by chemical or surface treatment of jute fabric [74], [76]. Therefore, untreated jute was first investigated to establish a reference performance benchmark.

3.1.2 Holistic Research Workflow

The summarized research process is given below:

1. Collection of jute yarn
2. Fabric preparation
3. Sample preparation for chemical treatment
4. Pre-treatment of jute fabric
5. Coating of pre-treated sample by bitumen emulsion and unsaturated polyester resin
6. Apply gamma radiation
7. Characterization of the samples
8. Identify biodegradation by soil burial test and accelerated weathering exposure.
9. Analysis of appropriateness for the use of soil erosion control

This structured workflow ensures logical progression from material selection to performance evaluation for geotechnical applications.

3.2 Raw Materials Used

12 lbs/spyndle jute yarn were used for producing jute fabric in this research work. These jute fabrics were collected from Akij Jute Mills Ltd., Muksudpur.

The selection of 12 lbs/spyndle yarn was based on its common use in the production of jute geotextiles due to its balanced tensile strength, flexibility, and availability in industrial-scale weaving operations. According to previous studies on natural fiber geotextiles, medium-count yarns such as 10–14 lbs/spyndle provide suitable fabric density and mechanical stability required for erosion control applications.

Using significantly finer yarn could reduce mechanical strength, whereas coarser yarn could increase fabric stiffness and reduce soil retention efficiency. Therefore, 12 lbs/spyndle yarn was selected as an optimal compromise between structural strength and permeability.

Table 3. 1 Specification of plain-woven jute fabric used in the experimental work

Fabric Type	EPI	PPI
Plain weave	12	12

The plain weave structure was selected because it provides a uniform pore distribution and sufficient permeability, both essential characteristics for geotextile materials used in soil stabilization and erosion control.

3.3 Chemical Used

3.3.1 Bitumen Emulsion

In this study, bitumen emulsion was used as a coating material to enhance the moisture resistance and durability of jute geotextiles. Bitumen coating helps reduce rapid biodegradation of natural fibers when exposed to soil moisture and microbial activity.

Bitumen emulsion is a long-chain hydrocarbon with no functional groups for reaction.

To prepare a bitumen emulsion, different proportions of bitumen, water, and a surfactant are required. Generally, 50–75% bitumen is mixed with water and an emulsifying agent to make a bitumen emulsion.

During bitumen emulsion production, emulsion stability is an important factor because it directly influences coating uniformity and durability of the composite material. Bitumen emulsions have various applications, including road infrastructure, pavement construction, surface treatment, and coating [21] [68].

Table 3. 2 Chemical composition of the bitumen emulsion used for surface treatment of jute fabric is given below:

Bitumen	Water	Emulsifiers	
65%	34.5%	0.5%	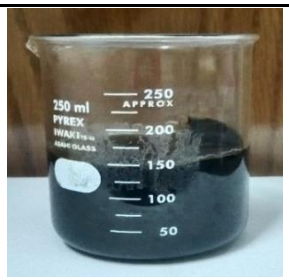 Bitumen emulsion

Bitumen Emulsion purchased from Abdullah al Hasib Hardware, 35 Kaptan Bazar, Dhaka-1203, Bangladesh.

The bitumen emulsion used in this research was purchased from Abdullah Al Hasib Hardware, 35 Kaptan Bazar, Dhaka-1203, Bangladesh.

3.3.2 Unsaturated Polyester Resin (UPR)

Unsaturated polyester resin is a popular synthetic thermosetting polymer used to produce composite materials. Natural fibre reinforcement in composite materials is made from unsaturated polyester resin to reduce environmental impact. Unsaturated polyester resin is most popular for its availability and low cost. Day by day, the use of natural fibre-reinforced biocomposites made from unsaturated polyester resin (UPR) is increasing rapidly, used in construction, automotive interior parts, and various electrical components [77] . In this research, polyester resin was used as a coating material that cross-links with the jute fabric's cellulose [21].

3.3.3 Auxiliary Chemicals Used

Various auxiliary chemicals were used in this research. These were purchased from Nasem Plastic Industries, but only HEMA was collected from the IRPT research lab, which is manufactured in Germany. The names of these auxiliaries, their chemical formula, and functions are given below:

Table 3. 3 List of auxiliary chemicals used in the experimental treatment process

SL.	Name of Chemical	Chemical Formula	Functions
1.	Methyl ethyl ketone peroxide (MEKP)	$[(CH_3)(C_2H_5)C(O_2H)]_2O_2$	Cross-linking agent
2.	Cobalt Naphthenate	$C_{22}H_{14}CoO_4$	Used as a curing agent
3.	Styrene monomer	$C_6H_5CH{=}CH_2$	Used as a solvent
4.	HEMA (2-hydroxyethyl methacrylate)	$C_6H_{10}O_3$	Used as an adhesive material
5.	Benzoyl Peroxide	$(C_6H_5{-}C(=O)\ O{-})_2$	Used as a bleaching agent to increase antimicrobial properties
6.	Methanol	CH_3OH	As a solvent
7.	Aceton	C_3H_6O	As a solvent
8.	Caustic Soda	NaOH	Used for causticization of jute fabric
9.	Acetic Acid	CH_3COOH	Used to neutralize jute fabric after causticization.

All of the chemicals were used in a laboratory form.

3.4 Machinery Used

3.4.1 GSM Cutter

GSM Cutter **Area: 100 cm²** **Country of Origin**: England **Manufacturer Name:** James H. Heal	

Figure 3. 1 A GSM cutter is used for determining the mass per unit area of jute fabric samples.

3.4.1.1 Determination of GSM

Test Method: ASTM-D3776

Procedure:

i) Cut the samples by a GSM cutter, and the area of the GSM cutter is100cm^2.

ii) After that, condition the samples in a standard atmosphere.

iii) Then weigh the samples.

iv) The sample weight was taken at least 5 times, and the average result was taken.

v) The average result was multiplied by 100, and GSM was found [71].

3.4.2 Titan Universal Strength Tester

Titan universal Tensile strength tester **Model No:** 510/01/1087 **Country of origin:** England **Manufacturer Name**: James H. Heal and Co. Ltd **Functions:** Determine the tensile strength	

Figure 3. 2 Titan Universal Strength Tester used for measuring the tensile strength and elongation properties of jute fabric samples.

3.4.2.1 Determination of Tensile Strength

Test method: ASTM standard D-5035

Procedure:

- Cut the samples into (16 cm x 5 cm).
- Set the samples by a clamped which have top and bottom jaws. The pressure of clamping was optimal; as a result, it did not slip or break at the backside of the jaws.
- The optimum pretension was maintained throughout the machine's start-up time.
- The machine operated under constant rate of extension (CRE), and it broke down after a specific time.
- A similar procedure was repeated five times for every sample in only the warp direction, and then mean value was calculated[71].

3.4.3 Padding Machine

Padding Mangle **Manufacturer**: Mathis **Model:** P-8L **Country of Origin:** China	

Figure 3. 3 Laboratory padding mangle used for applying chemical treatment uniformly to jute fabric samples.

The pressure on the padding mangle was set to 0.2 MPa to achieve a uniform pickup percentage, and the machine was run at 20 RPM. A 200 mL polymer mixture was taken in a padder according to the following formula. To achieve a uniform absorption rate during the time of the padding process. All samples were undergoing five rounds through the padder, and each time, the amount

of polymer mixture was controlled. Moreover, after the completion of the padding process, pick-up % were measured. After padding, dry the samples in an oven dryer at 80 °C and then subject them to a curing process [78].

3.4.4 Gamma Radiation Chamber

The gamma radiation dose was measured using a Frickle dosimeter, which consists of an aerated solution of ferrous sulfate (FeSO4) in sulfuric acid (H2SO4). The solution was instantaneously irradiated with the samples. The colorless original ferrous sulfate turned into colored ferric sulfate after irradiation. By measuring the optical density of the irradiated solution with a spectrophotometer, the total number of dosages was assessed [79].

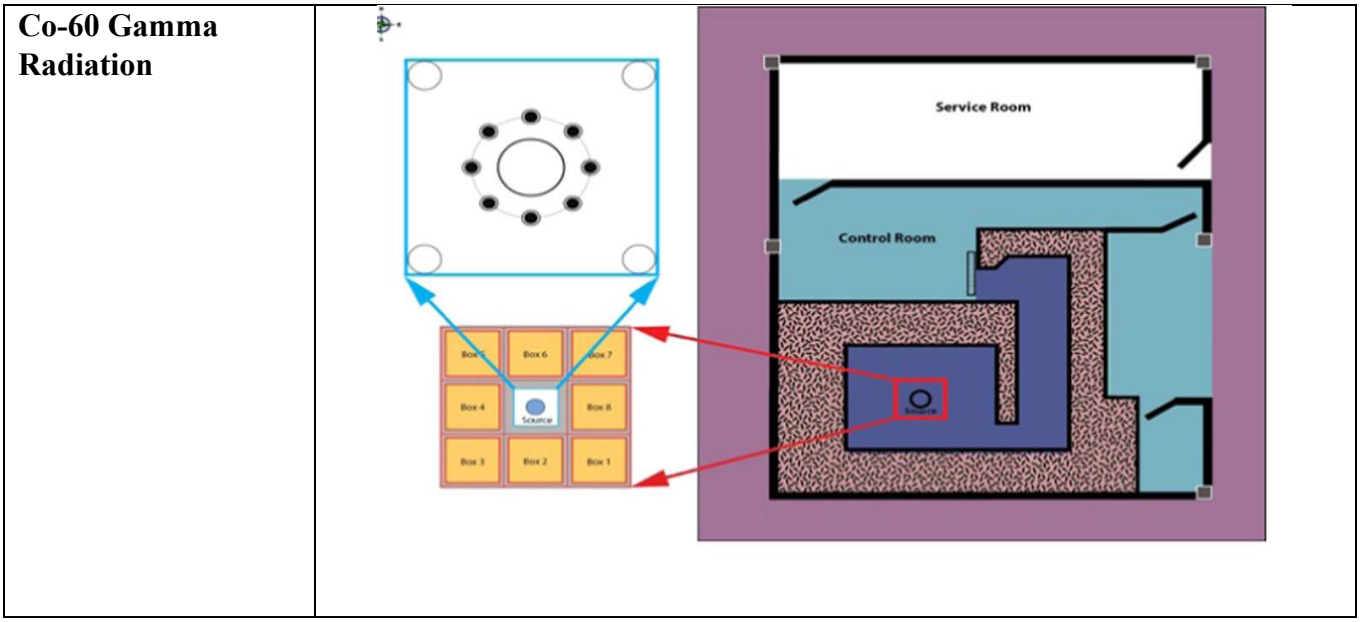

Figure 3. 4 Gamma radiation chamber used for irradiating chemically treated jute fabric samples [79].

3.4.5 Measurement of Moisture Content and Moisture Regain

Test Method: BS-4784

i) The test sample was cut in a specific measurement (1X1) square inch

ii) Conditioned the samples at 27˚C and maintain relative humidity (RH) at (65±2) %.

iii) Then, the samples were weighted and dried at (105±2) ˚C till a constant weight was attained by drying and weighing. The samples were weighed several times until the change between consecutive readings was less than 0.05%.

iv). Weighted should be carried out at intervals of 15 minutes [71].

3.4.6 Water Absorption and Hydrophilicity Study of Jute Fibre

The water absorption percentage of the research samples was calculated by the following method: ASTM Standard D570-98. The equation involved in-

Water uptake (%) = [(W2-W1)/W1] X100

Where W1 is the initial weight of the woven dried samples,

W2 is the weight of the jute fabric after water absorption.

Water absorption of jute fabric decreases after chemical modification. Water absorption depends on the oven dry weight, followed by temperature (105±2) °C. The samples were repeatedly dried until a constant weight was reached. The constant weight was attained by drying and weighing. The weight was measured several times until the variation between successive measurements was less than 0.05%. These testing methods require that successive weightings be carried out at 15-minute intervals. The raw jute fabric and chemically treated jute fabric samples were immersed in water for 10 minutes, and the weight of the immersed sample was then calculated to determine water absorption using the above formula [71].

Model No: **Brand Name:** And-Gulf. **Country of Origin:** England **Manufacturer Name:** A & D company Ltd.	

Figure 3. 5 Electronic balance used for accurate measurement of fabric and chemical sample weights.

Name: Convection Oven **Manufacturer:** Binder **Country of origin:** Germany	

Figure 3. 6 Oven dryer used for drying treated jute fabric samples under controlled temperature conditions.

3.4.7 Measurement of Fabric Thickness

Test method: ISO 5084: 1997

- The fabric samples were arranged on the table.
- As a result, the thickness gauge and pressing a lever the presser foot moved.
- The sample was put between the anvil and the presser foot.
- The lever removed the pressure carefully as a result the presser foot came down slowly.
- Finally recorded the dial gauge reading and the thickness was measured at multiple locations on the same sample.
- The same methods were followed for the remainder of the sample [80].

Dial indicator thickness Gauge **Manufacturing company: Mitutoyo** **Country of origin: Japan** **Model no**. 7301 **Functions:** Measure fabric, paper, tube wall film thickness etc.	

Figure 3. 7 Thickness gauge used to measure the thickness of jute fabric samples.

3.4.8 Scanning Electron Microscopy (SEM)

SEM was used to obtain a microscopic view of the research samples, which revealed their surface morphology. To measure surface morphology, samples were coated with a thin gold layer and sputtered in the SEM instrument before imaging. The machine model is JS-6490 LV, and the magnifications are X50, X100, and X200, with scales of 500 μm and 100 μm [80].

SEM Scanning Electron Microscopy **Model No:** JSM 6490-LA **Manufacturer:** JEOL **Country of origin: Japan**	

Figure 3. 8 Scanning Electron Microscope (SEM) used to observe the surface morphology of untreated and treated jute fibres.

3.4.9 Fourier Transform Infrared Analysis

Fourier transform infrared (FT-IR) spectra were obtained with the spectrophotometer, which analyzes the functional groups of chemicals or materials. The model number of the spectrophotometer is IR Prestige-21, and the manufacturer is Shimadzu Corporation, Japan. It is designed with ATR (Attenuated Total Reflection) technology, which enables the identification of specific reactive groups in the jute fabric and their interactions with the polymer mixture. [82]Since these samples were polymer-based, it was not possible to properly mix them with KBR to make pellets. As a result, the samples were directly placed in the sample holder. FT-IR (ATR) Spectra

were recorded on a Shimadzu FT-IR spectrophotometer over the wavenumber range of 4000-700 cm^{-1}, with a resolution of 4 cm^{-1} and around 20 scans.

FTIR spectrophotometer **Model No:** IR prestige-21 **Country of origin: Japan** **Manufacturer Name:** SHIMADZU	

Figure 3. 9 Spectrophotometer used for analyzing optical and chemical properties of treated jute samples.

3.4.10 X-ray Diffractometer

X-ray diffraction (XRD) analysis was performed to determine the crystalline structure of jute fibers before and after treatment. X-ray diffractometer analysis of the crystallinity and amorphous condition of the research specimen. X-ray diffraction analysis was performed using a Rigaku Ultima-IV (Rigaku Americas Corporation, Japan) diffractometer designed with Cu-Kα radiation. The measurement was taken at 5°/min, and the scanning diffraction angle 2θ ranged from 10 to 80 °[83].

.**X-ray Diffractometer (XRD)** **Model No:** ULTIMA-IV **Brand name:** Rigaku Ltd **Manufacture:** Tokyo, Japan	

Figure 3. 10 An X-ray diffractometer is used to analyze the crystalline structure of jute fibres.

3.4.11 TGA Analysis

The thermal decomposition behavior of the materials was evaluated by a Thermogravimetric analyzer (TGA). The machine's model number is PerkinElmer STA 8000. The process was completed at room temperature, with a heating rate of 10 °C per sample. Maximum temperatures reached 600 °C. A nitrogen gas flow maintained the heating rate, and thermal degradation was measured as weight loss due to the formation of volatile products [22] [82].

TGA and DSC analyzer **Manufacturer:** PerkinElmer **Model No:** STA 8000 **Country of origin:** American global corporation.	

Figure 3. 11 A thermogravimetric analyzer (TGA) was used to evaluate the thermal stability of jute fibre samples.

3.4.12 Antibacterial Activity Assessment

Method: AATCC standard 147-2004 (Parallel Streak Method)

Procedure:

i) The assessment of antimicrobial activity using a two-layer agar plate for every sample. The bottom layer of the agar plate showed no bacterial growth, and the top layer was inoculated with bacteria individually. Medium was made with TSA 80 g/L tryptone soya agar.

ii) Approximately (10±.1) ml of TSA was dispensed into sterile Petri Plates, then the plates were autoclaved at 122˚C for 15 minutes.

iii) The same procedure was used to make tryptone soya broth (TSB) solution.

iv) An appropriate quantity of bacteria was cultured and inoculated in 5 ml tryptone soya broth in a test tube using an inoculating loop.

v) Then incubated the test tube and petri plates at 37˚C for 18-24 hours.

vi) After 24 hours, a 4 mm inoculating loop was used to trans fer one loopful of the diluted inoculum onto the surface of the TSA plates. Five streaks, each approximately 60 mm long and spaced 10 mm apart, were made across the central area of a standard petri plate without reloading the loop.

vii) Cut the test specimen into rectangular pieces (25X 50) mm and position them on the TSA surface, and lay them transversely across the five inoculum streaks.

viii) The Petri plates were incubated at 37˚C for 18-24 hours.

ix) Bacterial growth was examined on the incubated plates. On the other hand, the inoculum streaks are located beneath the research sample, which showed interrupted growth, and a distinct zone of inhibition was observed around the edge of the samples. [70], [84].

Incubator **Model No:** LIB-060M **Country of Origin:** Korea **Manufacturer Name:** Daihan Labtech Co., Ltd	

Figure 3. 12 Laboratory incubator used during biological or soil burial durability testing of jute fabric samples.

3.4.13 Accelerated Weathering Test:

According to **ASTM G154-16**, an artificial weathering simulation was conducted in a laboratory using a specialized machine, a QUV/Spray accelerated weathering tester (Model QUV/Spray, Q-Lab, USA). The scheduled weathering cycle lasted 12 hours. Each cycle requires 6 hours of UVA radiation (0.8 W/m², 340nm wavelength) at 60°C, followed by 4 hours of water condensation at 40°C, and 2 hours of water spray at ambient temperature. Irradiation was performed using a fluorescent UVA 340 lamp. Every day (24 hours),02 (two) weathering cycles were carried out. From the sample holder, all samples were removed and characterized after exposure to weathering conditions for 1, 3, 7, 14, and 28 days. Then, the sample holders were collected from the aging chamber and stored in a refrigerator at 4°C in a plastic bag until characterization [85].

Accelerated Weathering Tester (QUV/Spray) **Model No:** JSM 6490-LA **Country of Origin:** Japan **Manufacturer Name:**	

Figure 3. 13 QUV accelerated weathering tester used to simulate environmental weathering conditions for durability analysis.

The accelerated weathering test simulates long-term environmental exposure by subjecting materials to controlled conditions of UV radiation, moisture, and temperature variations inside a weathering chamber. In this process, fabric samples are cyclically exposed to UV light (to mimic sunlight), condensation (to simulate rain or humidity), and heating (to replicate thermal ageing) for varying durations. In the present study, both raw jute and chemically treated jute fabrics were characterized after 1, 3, 7, 14, and 28 days of exposure. The raw jute fabric deteriorated rapidly due to its hydrophilic cellulose structure and the absence of protective layers. In contrast, treated fabrics (bitumen, polyester resin, HEMA, BP, and γ-radiation) demonstrated significantly reduced degradation due to polymer coating, free-radical crosslinking, and hydrophobic surface modification, thereby improving mechanical durability and environmental resistance**.**

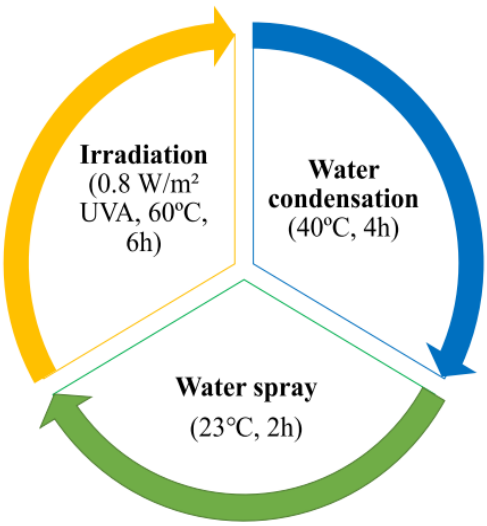

(a) [85]

(b)

Figure 3. 14 (a) Weathering cycle and (b) Sample in the specimen holder of the weathering machine.

Table 3. 4 Weathering cycle [75].

Observation	Accelerated weathering tests	Outdoor/real weather test
One cycle	Two-Four (2-4) hours	1 day (24 hours)
Cycles in every day	Six-Ten (6-10) cycles	One (1) cycle
Period of darkness	Available	All-time
Cycle constancy	Identical all the time	Various all-time

3.5. Biodegradability and Durability Considerations

Biodegradability is an important characteristic of natural fiber geotextiles. However, excessive biodegradation can reduce the functional lifespan of the material when used in erosion control applications.

The objective of this research is therefore not to eliminate biodegradability but to control the degradation rate so that the geotextile maintains sufficient strength during the critical period of soil stabilization.

Coating materials such as bitumen emulsion and polyester resin act as protective barriers that delay microbial attack and moisture absorption, thereby improving the durability of the jute geotextile while still allowing eventual environmental degradation.

This balance between durability and biodegradability is essential for sustainable erosion control systems.

Chapter 4: Results and Discussion

The research work was discussed in the four segments to present the study well, as follows:

4.1 Selection of optimum polymer mixture formula by soil burial test.

4.2 Selection of optimum radiation dose.

4.3 Pre-treatment of jute fabric, then chemical modification.

4.4 Measurement of durability by weathering test.

4.1 Selection of Optimum Polymer Mixture Formula by Soil Burial Test

4.1.1 Working Procedure

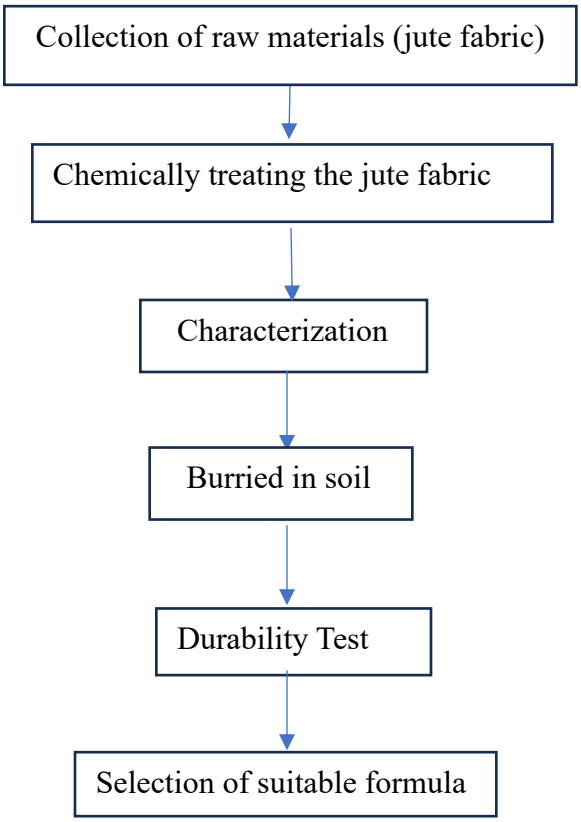

Figure 4.1. 1 Working Procedure of the Selection of Polymer Mixture.

4.1.2 Sample Preparation

Raw jute fabric was taken for chemical treatment. Every fabric sample size was (5 x 10) inches and weighed 150 grams. Various formulations were developed by blending BE (bitumen emulsion) and UPR (unsaturated polyester resin) in varying proportions. In the polymer mixture, MEKP (methyl ethyl ketone peroxide) served as the initiator, cobalt naphthenate acted as the curing accelerator, and styrene monomer functioned as the solvent for all samples. The fabric was passed through a mini padder machine under 0.2 MPa pressure to ensure complete impregnation and an optimum pick-up percentage, then cured in a dryer for 2 hours at 80 °C. After chemical treatment of the jute fabric, various mechanical and chemical tests were conducted. The samples were then buried 6 inches deep in soil for 15, 45, and 90 days. After each exposure time, samples were retrieved, washed with clean water, and air-dried in sunlight. Lastly, the durability of the fabrics was evaluated based on the extent of degradation, as indicated by weight loss and reduced tensile strength.

Table 4.1. 1Formulation of the chemical % used to treat the jute samples

Chemical % (v/v)	Raw jute Fabric (UJF)	Sample 1 (TJF1)	Sample 2 (TJF2)	Sample3 (TJF3)	Sample4 (TJF4)
Bitumen Emulsion (%)	0	100	30	20	10
UPR (%)	0	0	10	15	20
MEKP (%)	0	0	5	5	5
Cobalt Naphthenate (%)	0	0	1	1	1
Styrene Monomer (%)	0	0	54	59	64

4.1.3 Analysis of Tensile Resistance

The tensile resistance of all selected research samples was measured using a Titan universal strength tester in accordance with ASTM D5035. The strength (TS) of chemically treated jute fabric increased with increasing unsaturated polyester resin percentage. Every treated sample exhibited higher tensile strength than raw jute fabric, except for the bitumen emulsion-treated jute fabric.

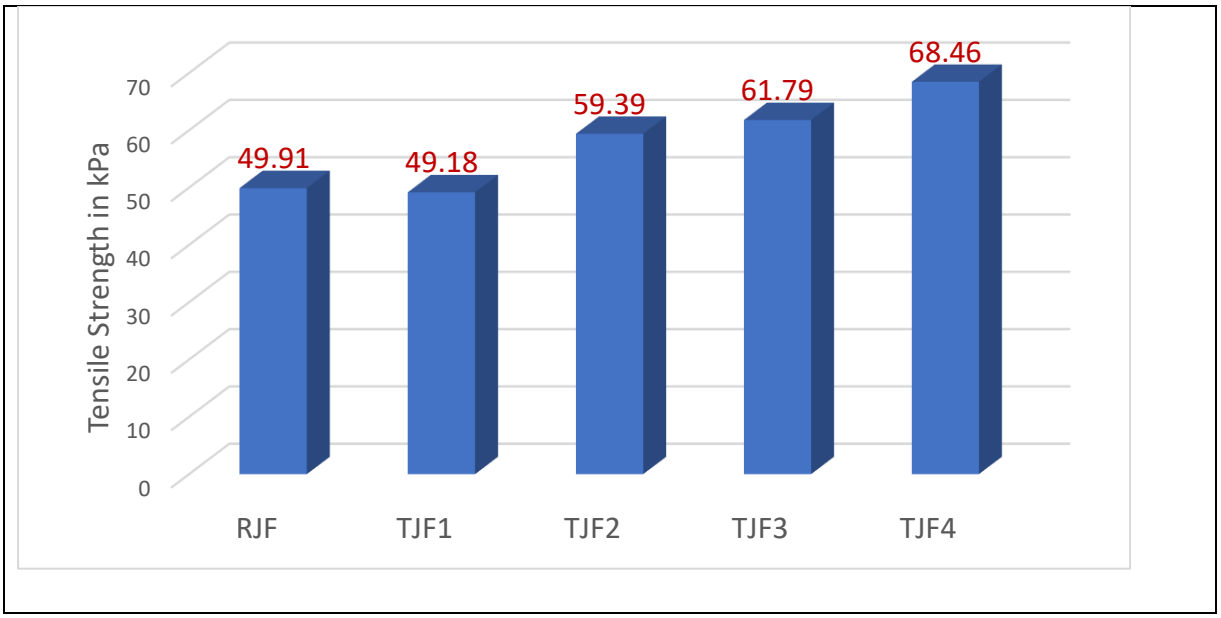

Figure 4.1. 2 Comparison of tensile strength.

(TJF1) did not show significant improvement in tensile strength. The bitumen emulsion was stiffening the fabric and not improving its stability. Increasing polyester resin (UPR)% and styrene monomer (%) progressively enhanced the tensile strength due to cross-linking and reinforcement. The high UPR (%) and Styrene monomer (%) further enhance bonding and reinforcement. The optimal condition in this study is TJF4, which increases tensile strength by about 37% compared to raw fabric (UJF)**.** The addition of Unsaturated Polyester Resin (UPR) and Styrene Monomer, along with catalysts (MEKP + Cobalt Naphthenate), initiates polymer cross-linking with the fabric, thereby enhancing its strength.

4.1.4 Analysis of Fabric Weight

GSM cutters were used to measure the sample's weight in g/m², in accordance with **ASTM D3776**. Jute fabric weight increased with the increasing polyester resin %. The weight of grey (raw) jute fabric is less than that of all the chemically treated jute fabrics.

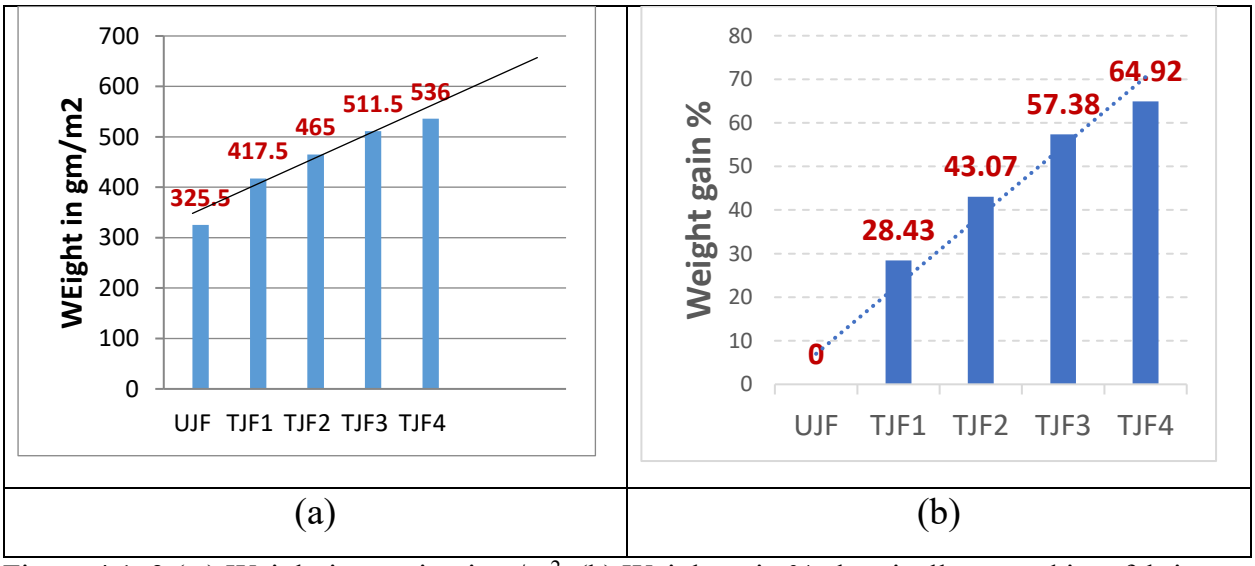

Figure 4.1. 3 (a) Weight increasing in g/m^2, (b) Weight gain % chemically treated jute fabric.

The weight gain (%) remained highest for the treated jute fabric (TJF). As the polyester resin percentage (%) increases, the fabric's stiffness and weight increase. With the increase in chemical (%) (bitumen, UPR, styrene monomer, MEKP, cobalt naphthenate), the fabric weight rises progressively. The progressive increase in fabric weight indicates greater polymer/resin

absorption and crosslinking within jute fabric, making it more durable, rigid, and chemically modified. This is due to a higher content of polyester resin and styrene monomer, as well as increased fabric weight resulting from more extensive polymer impregnation. Bitumen-only (TJF1) results in a moderate weight increase; however, the polymer mixture (BE) and UPR in TJF4 provide the greatest improvement, as the polymers fill pores and coat fibers.

4.1.5 Analysis of Water Absorbency by Measuring Moisture Regain%, Content%, and Water Uptake%

Chemical treatment of jute fabric gradually decreases moisture regain % (MR%), moisture content % (MC%), and water uptake % (WU%) as the chemical concentration increases. Hydrophilic –OH groups of cellulose in jute fabric are progressively blocked/covered by bitumen emulsion,

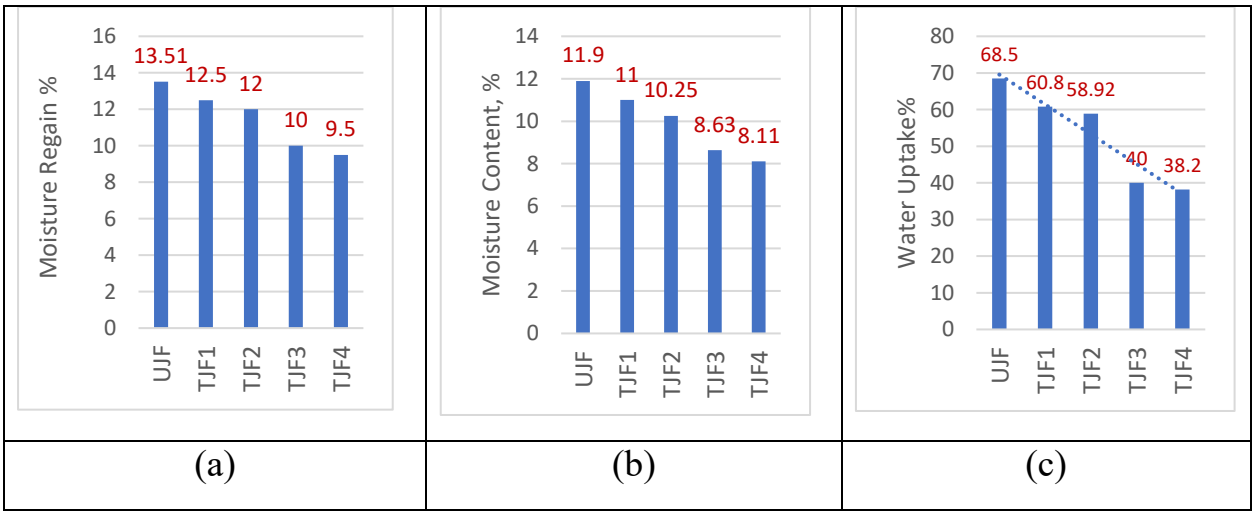

Figure 4.1. 4 Comparison of water absorbency of untreated and chemically treated jute fabrics showing (a) MR%, (b) MC%, and (c) WU%. The gradual decrease in MR%, MC%, and WU% indicates reduced hydrophilicity due to polymer impregnation and crosslinking within the jute structure.

UPR, and crosslinked styrene polymers, reducing the fabric's ability to absorb moisture from the air. MR%: chemical impregnation reduces the water-holding capacity within the fabric matrix. Polyester resin and styrene form a hydrophobic crosslinked layer. Bitumen coating (TJF1) moderately reduces water penetration. Cross-linking of UPR and styrene monomer from TJF2–TJF4 drastically blocks pores, forming a hydrophobic polymer matrix inside the jute structure. TJF4, with the highest resin content (20% UPR + 64% styrene), shows the lowest water absorption.

4.1.6 Analysis of Surface Morphology by SEM Images

The SEM images clearly show that the fibers of the raw jute fabric are compact, smooth, and have open pores. The surface is also comparatively clean, displaying hydrophilic cellulose microfibrils. The treated jute fabric has a rough, filled, and polymer-coated surface. Fiber bundles are clearly covered in bitumen and crosslinked resin.

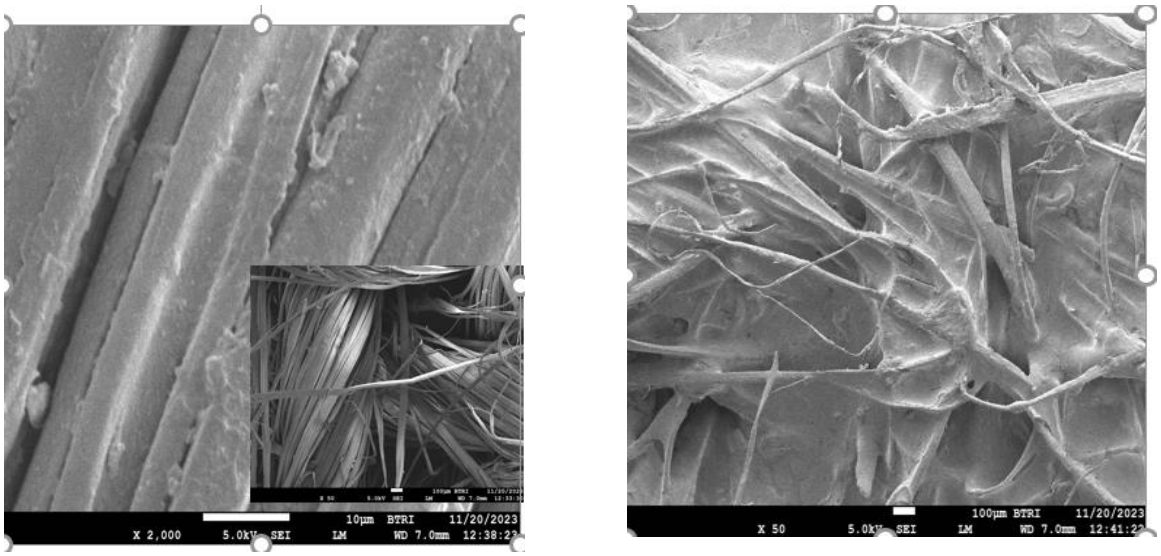

(a) Raw Jute fabric (b) Polymer treated jute fabric

Figure 4.1. 5 SEM images showing the surface morphology of (a)Raw jute fabric and (b) polymer-treated jute fabric.

A dense and uneven shape is produced by the reduction or blockage of voids between two adjacent fibers. This occurs because the hydroxyl (-OH) groups are covered, and pores are closed. Surface of jute fabric changed from being smooth and porous (hydrophilic) to being thick and rough (hydrophobic) for the polymer mixture of BE (bitumen emulsion), UPR (unsaturated polyester resin), and styrene monomer. This microstructural alteration explains why treated jute fibers lost their capacity to absorb water and gained weight and tensile strength, while also validating the chemical composition data.

4.1.7 Analysis of Infrared Spectral (FT-IR) Analysis

From the spectra of the Fourier transform infrared (FT-IR) graph, it could be said that the curve of raw jute fabric Broad band near 3400 cm^{-1} was observed, which indicates O–H stretching, and this O-H band comes from cellulose, hemicellulose, and lignin from jute fabric. Peaks around 2900

cm^{-1} indicate C–H stretching of aliphatic groups in cellulose**.** Bands near 1730 cm^{-1} are very weak and indicate C=O stretch from hemicellulose and ester (RCOOR´) groups. Peak intensity at 1020–1050 cm^{-1} indicates C–O–C stretching (polysaccharides). Raw jute exhibits strong hydrophilic –OH groups, consistent with its high moisture absorption capacity. The blue curve of bitumen emulsion, the peaks around 2920 and 2850 cm^{-1}, indicates C–H stretching of alkanes. A band near 1600–1700 cm^{-1} specifies the aromatic C=C stretching vibration. The strong peak around~1450 cm^{-1} means the bending of CH_2, and the Region below 1000 cm^{-1}, which is out-of-plane aromatic bending vibrations. The peaks of the blue curve from bitumen emulsion confirm the presence of aliphatic hydrocarbons and aromatic structures typical of bitumen, as seen in the green curve of UPR (unsaturated polyester resin). The strong peak near 1720–1735 cm^{-1} was observed, which indicates the C=O stretching vibration of ester functionalities from the polyester backbone. From the green curve of unsaturated polyester resin, the peaks around 1630-1650 cm^{-1} indicate the C=C stretching vibration of unsaturated bonds, and the broad band near 3000–3100 cm^{-1} indicates the aromatic C–H stretching vibration of styrene monomer. Finally, the peaks range of 1250–1050 cm^{-1} , which identifies C–O–C stretch of esters—the clear evidence of ester linkages and unsaturated double bonds for crosslinking. The purple curve of treated jute fabric shows that the broad O–H peak at 3400 cm^{-1} is reduced, meaning hydroxyl groups of cellulose are partly masked. The C=O ester peak (~1725 cm^{-1}) appears firmer and indicates UPR crosslinking onto jute fibers. C=C bands (1640 cm^{-1}) are visible and contribute from styrene/UPR. The new peaks around 1250–1050 cm^{-1} indicate C–O–C ester linkages from the polymer matrix. The reduced intensity at 1020–1050 cm^{-1} compared to raw jute indicates cellulose –OH reactivity and bonding. This FT-IR graph shows the successful combination of polymer impregnation and cross-linking of jute fibre, bitumen emulsion, and unsaturated polyester resin (UPR). This FT-IR graph confirms the surface modification of jute fabric by chemical treatment with gamma radiation, which reduces the OH groups on the jute fabric cellulose and introduces hydrophobic ester crosslinks, decreasing moisture regain, moisture content, and water uptake percentage and also increasing durability properties.

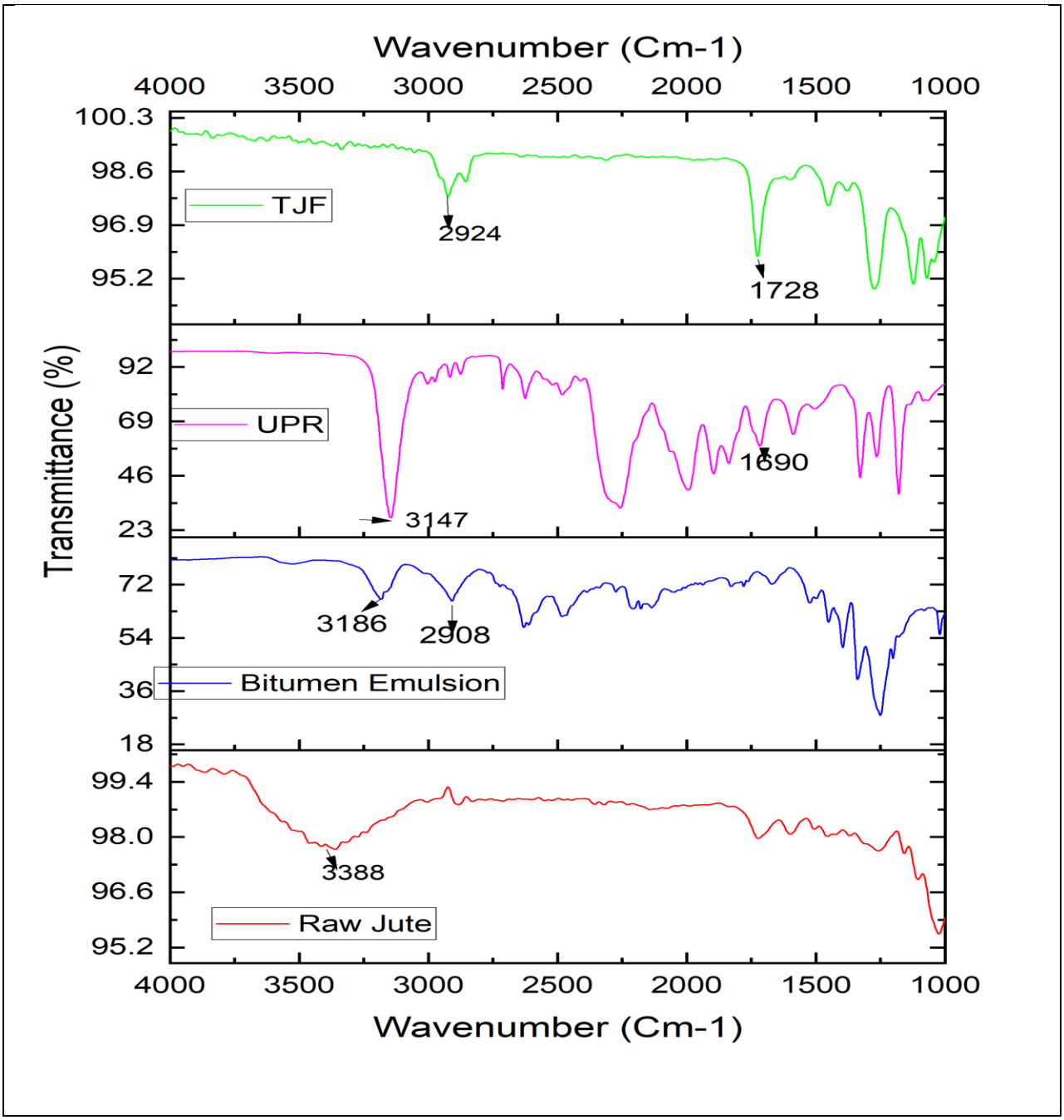

Figure 4.1. 6 FTIR spectra of raw jute fabric, bitumen emulsion, unsaturated polyester resin (UPR), and polymer-treated jute fabric. The untreated jute shows a strong O–H stretching band (~3400 cm^{-1}) and characteristic cellulose peaks, indicating its hydrophilic nature. In the treated fabric, the reduced O–H intensity and the appearance of strong C=O (~1725 cm^{-1}) and C–O–C (1250–1050 cm^{-1}) bands confirm ester formation and crosslinking between the jute cellulose and the polymer components, indicating successful polymer impregnation and increased hydrophobicity.

4.1.8 Analysis of X-ray diffraction curve

The X-ray diffraction (XRD) patterns provide information on the crystalline and amorphous phases present in the jute fibers [86] The diffraction data for raw and chemically treated jute fabrics are summarized in Tables 4.1.2 and 4.1.3, and the corresponding diffraction patterns are presented in Figure 4.1.7.

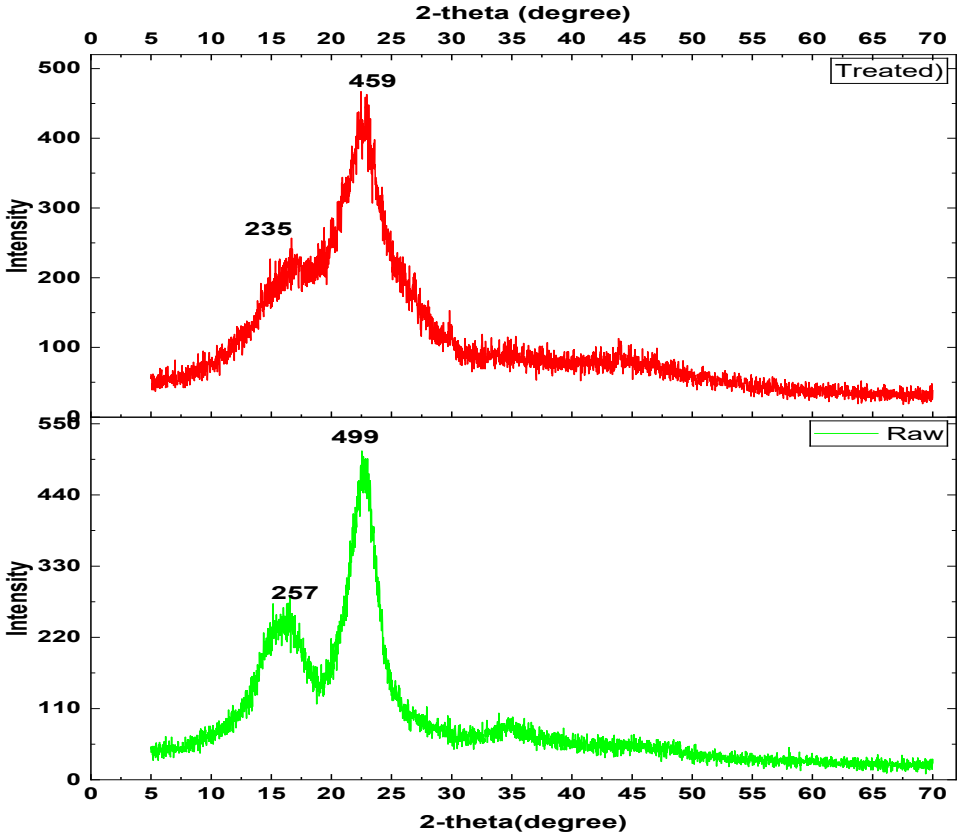

Figure 4.1. 7 XRD patterns of raw jute fabric (lower) and chemically treated jute fabric (upper). The raw jute shows characteristic diffraction peaks at 2θ ≈ 16.1°, 22.8°, and 34.8°, corresponding to the semi-crystalline Cellulose I structure. In the treated fabric, the broadened and reduced peak around 2θ ≈ 22° indicates decreased crystallinity due to crosslinking between cellulose hydroxyl groups and the polymer matrix (bitumen emulsion and unsaturated polyester resin), confirming the structural modification of the jute fibers.

Table 4.1. 2 Value of XRD graph for raw jute fabric

No.	2-theta(degree)	FWHM (degree)	Int. I (counts degree)	Size(ang.)	Rel. int. I(a.u.)
1	16.10(6)	4.50(7)	617(7)	18.6(3)	69.23
2	22.85(3)	2.87(3)	891(9)	29.5(3)	100.00
3	34.8(3)	2.0(3)	23(3)	44(6)	2.57

Table 4.1. 3 Value of XRD graph for chemically treated jute fabric

No.	2-theta(degree)	FWHM (degree)	Int. I(counts degree)	Size(ang.)	Rel. int. I(a.u.)
1	16.25(16)	8.3(4)	1466(104)	10.2(5)	73.21
2	22.85(4)	4.60(14)	2002(148)	18.4(5)	100.00

The raw jute fabric exhibits three characteristic diffraction peaks at $2\theta = 16.10°$, 22.85°, and 34.8°, which are typical reflections of Cellulose I. The most intense peak appears at $2\theta = 22.85°$ with a relative intensity of 100%, confirming the semi-crystalline nature of cellulose in jute fibers. The peak at 16.10° shows a relative intensity of 69.23% with a FWHM of 4.50° and a calculated crystallite size of approximately 18.6 Å, while the peak at 22.85° has a FWHM of 2.87° and a crystallite size of about 29.5 Å. A weaker peak at 34.8° with 2.57% relative intensity, FWHM of 2.0°, and a crystallite size of about 44 Å also appears, corresponding to the ordered regions of cellulose microfibrils.

After chemical treatment, noticeable changes in the diffraction parameters are observed. The treated jute fabric shows diffraction peaks at $2\theta \approx 16.25°$ and 22.85°, but the peaks become broader and less sharp, indicating a reduction in crystallinity. The FWHM values increase, for example from 4.50° to about 8.3° for the peak near 16°, while the calculated crystallite size decreases from about 18.6 Å to approximately 10.2 Å. Similarly, the peak near 22.85° shows an increased FWHM of about 4.60° and a reduced crystallite size of approximately 18.4 Å, although it still retains the maximum relative intensity (100%) among the observed peaks.

The increase in FWHM and reduction in crystallite size indicate partial disruption of the ordered cellulose structure due to chemical modification and crosslinking reactions between cellulose hydroxyl groups and the polymer matrix composed of bitumen emulsion and unsaturated polyester resin. These structural changes suggest that the treatment introduces additional amorphous regions within the fiber structure while preserving the basic cellulose framework.

Overall, the XRD analysis confirms that chemical treatment modifies the crystalline structure of jute fibers by reducing crystallite size and increasing structural disorder. This modification supports the formation of polymer–cellulose crosslinked networks, which contribute to reduced hydrophilicity, improved dimensional stability, and enhanced durability of the treated jute fabric for geotextile applications.

4.1.9 Determination of Thermal Degradation by Thermogravimetric (TGA) Analysis

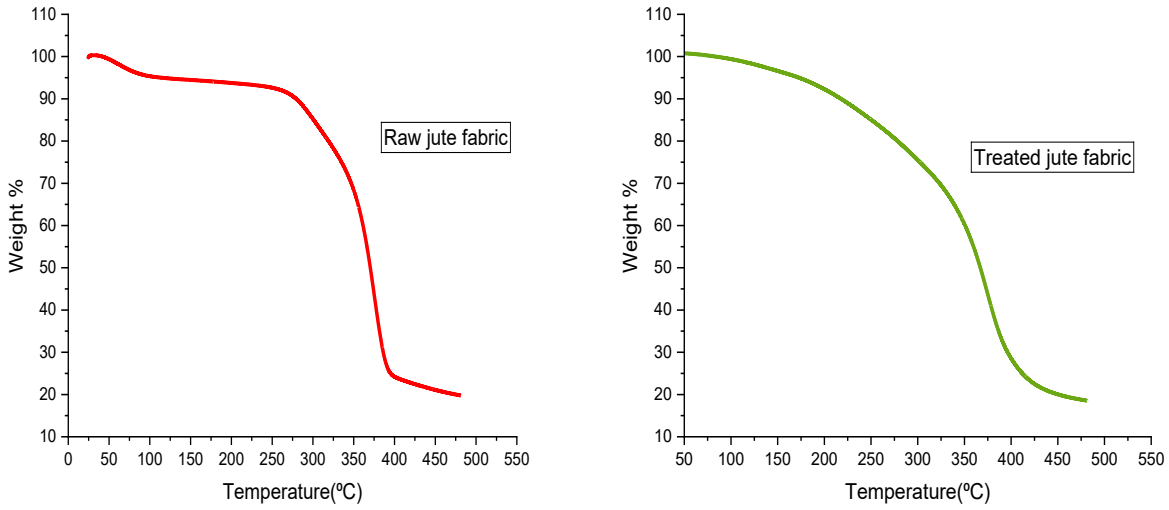

Figure 4.1. 8 Thermogravimetric analysis (TGA) curves of raw jute fabric and chemically treated jute fabric. The treated sample exhibits reduced initial moisture loss and improved thermal stability compared with raw jute, indicating that the polymer coating and crosslinking affect the thermal degradation behavior of the fibers.

The thermogravimetric (TGA) profiles of raw and chemically treated jute fabrics presented in Figure 4.1.8 illustrate their thermal degradation behavior over the temperature range up to about 550 °C. In the initial stage (below ~100 °C), both samples exhibit a small weight loss of approximately 2–5%, attributed to the evaporation of physically adsorbed moisture. The treated jute fabric shows slightly lower weight loss in this region, indicating reduced hydrophilicity due to polymer coating.

The main degradation stage occurs between ~200 °C and 350 °C, during which the raw jute fabric undergoes a rapid decrease in mass due to the thermal decomposition of hemicellulose and cellulose. In contrast, the treated jute fabric demonstrates a comparatively slower degradation rate,

suggesting improved thermal stability resulting from polymer impregnation and crosslinking with the cellulose structure.

At higher temperatures (> 350 °C), both samples undergo gradual decomposition, accompanied by lignin degradation and char formation. The final residual masses of the raw and treated jute fabrics are comparable; however, the treated sample exhibits a more gradual degradation profile, indicating enhanced thermal stability due to chemical modification. A summary of the thermogravimetric analysis of untreated jute fabric (UJF) and treated jute fabric (TJF) is presented in Table 4.1.4.

Table 4.1. 4 Summary of thermogravimetric analysis of raw jute (UJF) and treated jute (TJF)

Feature	**Raw Jute (UJF)**	**Treated Jute (TJF)**
Moisture loss	Higher (hydrophilic)	Lower (hydrophobic surface)
Main decomposition	Sharp (280–360°C)	Broad, multi-step (200–450°C)
Residue (char yield)	~15–20%	~30–35%
Thermal stability	Lower	Higher (delayed degradation)

4.1.10 Analysis of Weight Loss at Different Time Durations after Soil Burial

Figure 4.1.9 shows the weight loss (g/m²) of raw jute (UJF) and chemically treated jute (TJF) during soil burial degradation tests (before burial and at 15, 45, and 90 days). It supports evaluating the biodegradability and durability of the treated samples compared to raw jute fabric. From the bar diagram, it is noticeable that the degradation of raw jute fabric is more than that of other treated jute fabrics. Only bitumen emulsion does not improve durability because it forms a coating on the jute fabric surface without polymerization.

However, applying a composite mixture (Bitumen emulsion, polyester resin, and styrene monomer) to the jute fabric decreases biodegradability and improves its durability. The result is due to the composite mixture, which promotes polymerization through cross-linking. The higher the resin, the less biodegradable it becomes.

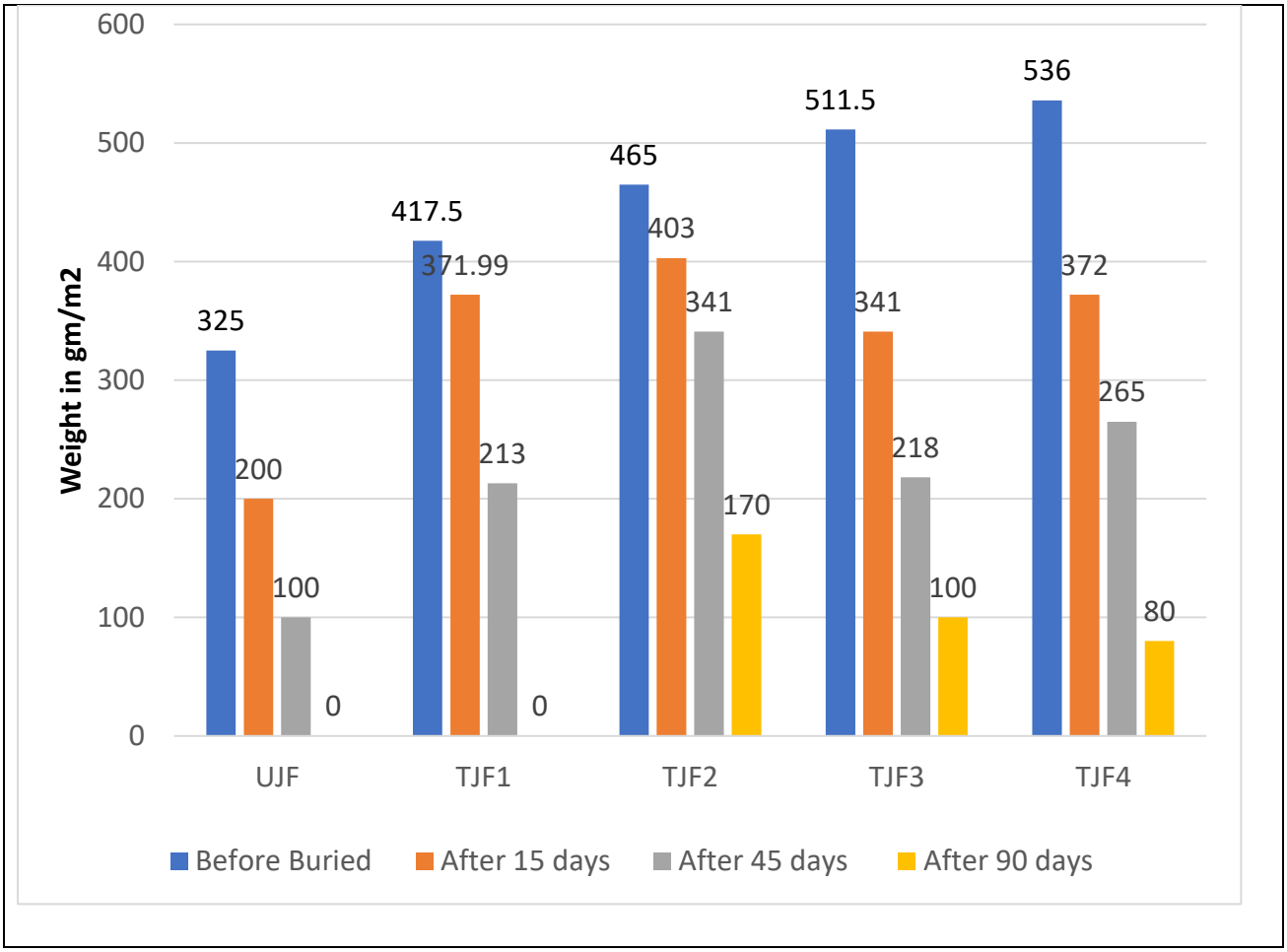

Figure 4.1. 9 Comparison of weight loss (g/m²) of untreated jute fabric (UJF) and chemically treated jute fabrics (TJF1–TJF4) during soil burial tests at 0, 15, 45, and 90 days. The treated samples exhibit reduced weight loss compared to raw jute, with increasing resistance to biodegradation observed at higher resin content due to polymer crosslinking and protective coating effects.

From the above discussion, it can be said that chemical treatment of jute fabric prominently increases its durability by reducing biodegradability and increasing resin content, leading to greater soil degradation resistance.

4.1.11 Analysis of Tensile Strength (TS) in Different Time Durations after Soil Burial

Figure 4.1.10 shows that the TS of both raw jute (UJF) and treated jute (TJF) decreased due to degradation after burial for different time durations. The raw jute fabric was demolished within 45 days, but the TJF was not demolished within the 90-day timeframe. TJF4 showed more durability properties than other treated jute fabrics.

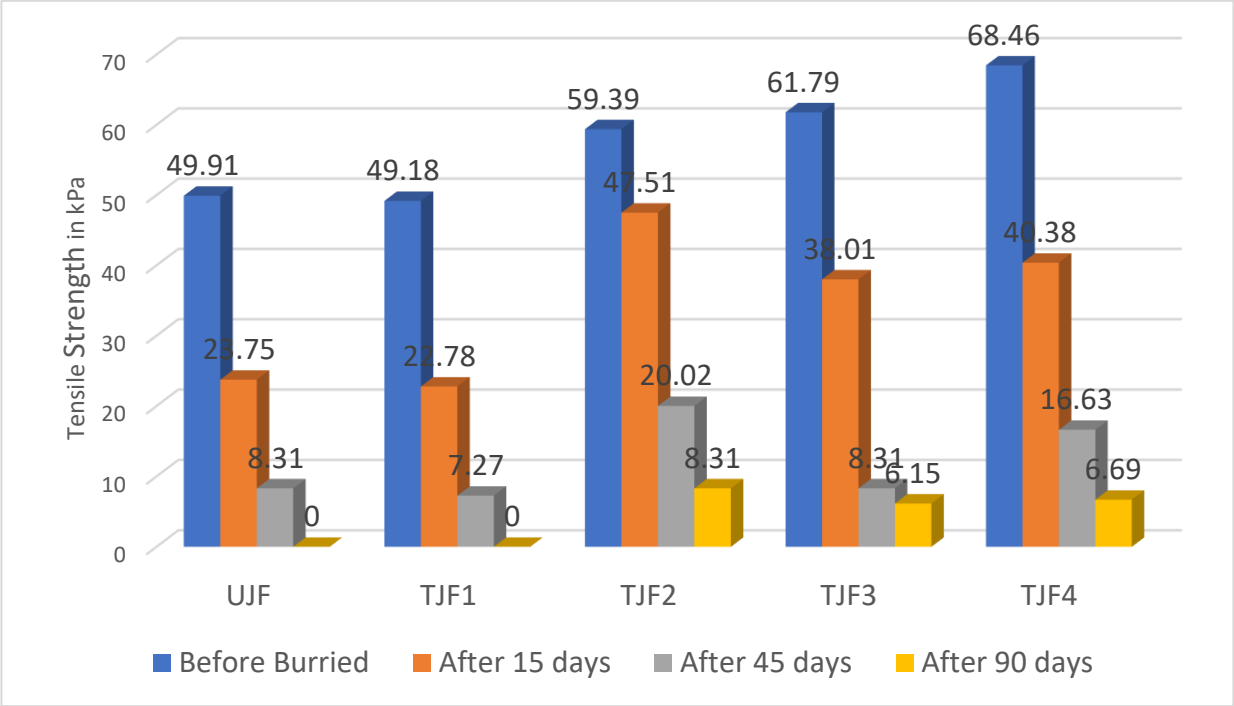

Figure 4.1. 10 Variation of tensile strength (kPa) of untreated jute fabric (UJF) and chemically treated jute fabrics (TJF1–TJF4) during soil burial tests at 0, 15, 45, and 90 days. The treated samples exhibit improved tensile-strength retention compared to raw jute, with higher polymer content resulting in enhanced durability through crosslinking and reduced biodegradation.

The result is due to cross-linking a polymer mixture with jute fabric, which decreases the number of O-H groups from cellulose, hemicellulose, and lignin, and also blocks the fibers' pores. As a result, when the resin % increases, biodegradability decreases.

4.1.12: Key Findings

1. The tensile strength (TS) of the raw jute (UJF) and treated jute (TJF) gradually increases with the increase in chemical (%).) The concentration of unsaturated polyester resin (UPR within the polymer mixture is crucial for enhancing TS. When the concentration of UPR increases, the tensile strength (TS) of treated jute (TJF) progressively increases.
2. Gradually, Moisture regains (MR%), moisture content (MC%), and water uptake (WU%) also decrease from UJF to TJF4 with the increase of UPR (%). Unsaturated polyester resin has plastic properties. As the unsaturated polyester resin (%) increases, the bitumen emulsion percentage decreases, thereby reducing the jute fabric's absorbency. Consequently, the MR (%), MC (%), and WU (%) percentages also decrease.
3. From the FTIR analysis, the hydroxyl (OH) group of raw jute (UJF) fabric also decreases from the cellulose, hemicellulose, and lignin, which reduces the formation of hydrogen bonds by moist air and also protects against microbial attack. As a result, the breaking force and water absorbency decrease.
4. The soil burrier test measured the durability properties of the jute fabric. After burying the samples in soil for 15, 45, and 90 days, they were retrieved, washed thoroughly, and the weight loss and TS (Tensile strength) of treated jute (TJF) and raw jute (UJF) were measured at different time points. Treated jute (TJF2) showed better durability properties compared to other treated jute (TJF). The result is due to the unsaturated polyester resin (%) making the jute fabric more plastic than a lower (%) of UPR. However, the coating material, bitumen emulsion (%), decreases the direct contact with moist air. As a result, the 30% bitumen emulsion and 10% polyester resin-treated jute fabric demonstrated greater durability than other jute fabrics.

4.1.13: Comments

This investigation aims to enhance the durability characteristics of jute fabric, without compromising its biodegradability. Based on the above discussion and analysis of the results, the treated jute fabric (TJF2) exhibits a good balance between strength and partial biodegradability.

4.2 Selection of Optimum Radiation Dose

4.2.1 Working Procedure

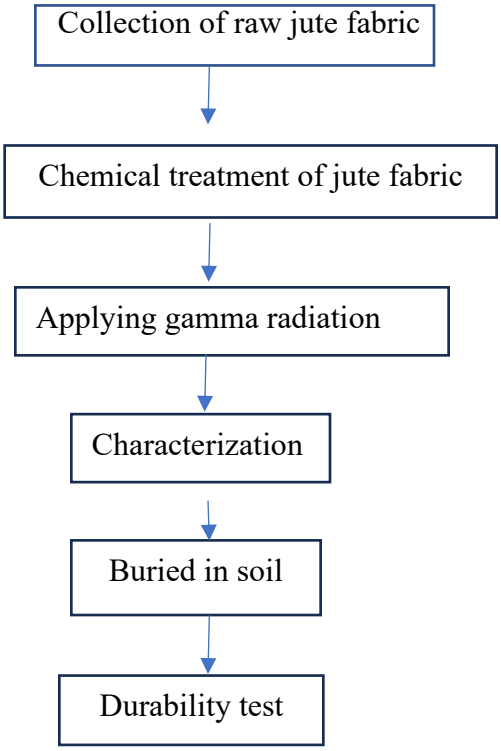

Figure 4.2. 1 Working procedure of radiation dose selection.

4.2.2 Sample Preparation

Raw jute fabric was taken for chemical treatment. Every fabric sample size was (5X10) inches and weighed 150 g. The chemical treatment of jute fabric was performed according to the TJF2 recipe (30% bitumen emulsion, 10% polyester resin, 54% styrene monomer, 5% MEKP, 1% cobalt naphthenate). Mini padders were used for uniform chemical pickup and drying at 40°C in a woven dryer. Applying γ-radiation over chemically treated jute fabric (30% bitumen emulsion + 10% polyester resin) was reported to expose it to high-energy gamma radiation by a cobalt-60 irradiator. Samples were exposed to varying doses of gamma radiation, specifically 2.5, 5, 7.5, and 10 kGy. Then cool and dry the samples under natural weathering conditions for a full day. After treating the jute fabric, various mechanical and chemical tests were conducted. Treated jute (TJF) and untreated fabrics (UJF) were buried under a 6-inch-deep soil bed and retrieved over the next 120 days. When samples were withdrawn from the soil bed, they were cleaned with water and then dried in the sunlight. Finally, the amount of degradation loss was measured by weight loss and strength loss.

4.2.3 The γ-Radiation Effect on Cellulose of Jute Fabric

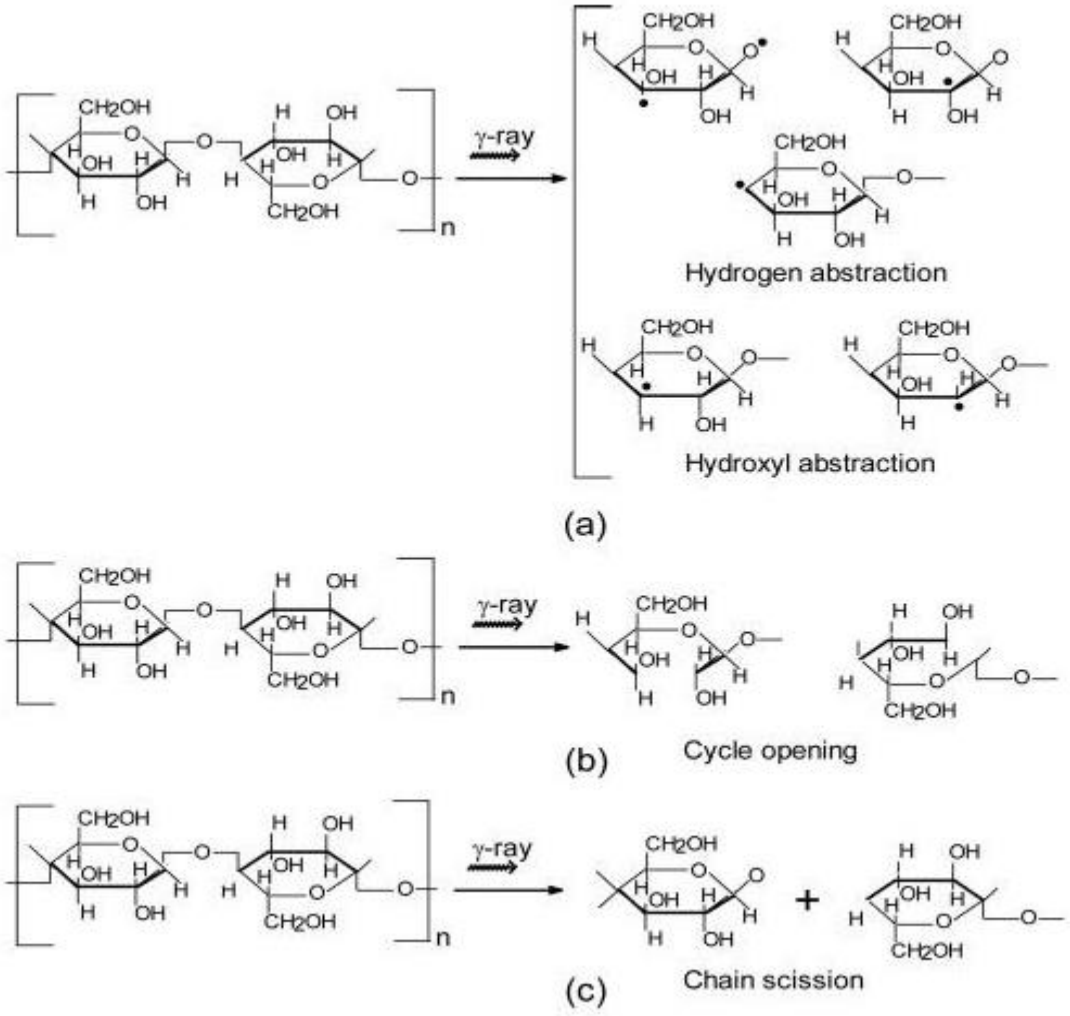

Figure 4.2. 2 (a) Abstraction of H and OH (b) Open the cellulose cycle (c) Chain scission after γ-irradiation. (Reused from [9])

High-energy gamma (γ-ray) radiation directly hits cellulose and breaks down the C-H and O-H bonds, creating free radicals (•) on the backbone side or side group of cellulose. This free radical played a vital role in the cross-linking of jute fabric and a polymer mixture (bitumen emulsion + polyester resin) during polymerization. Radiolysis of H from the -CHO_2OH or -CHOH group leaves a carbonyl radical. Hydroxyl group abstraction leads to reactions such as oxidation or cleavage chain scission, resulting in a weaker cellulose chain. Cellulose units are made of a glucose ring structure, and the ring-opening reaction creates aldehyde and carboxyl end groups.

4.2.4 Analysis of the TS Between TJF and UJF After Applying Gamma(γ) Radiation

Figure 4.2.3 express change of tensile strength for applying γ-irradiation over raw jute fabric (UJF) and chemically treated jute fabric (TJF). Chemical treatment and γ-irradiation gradually increase the tensile strength. The tensile strength of raw jute fabric is approximately 49.91 kPa, and that of chemically treated jute fabric is 59.39 kPa, confirming the reinforcing effect of polymer impregnation.

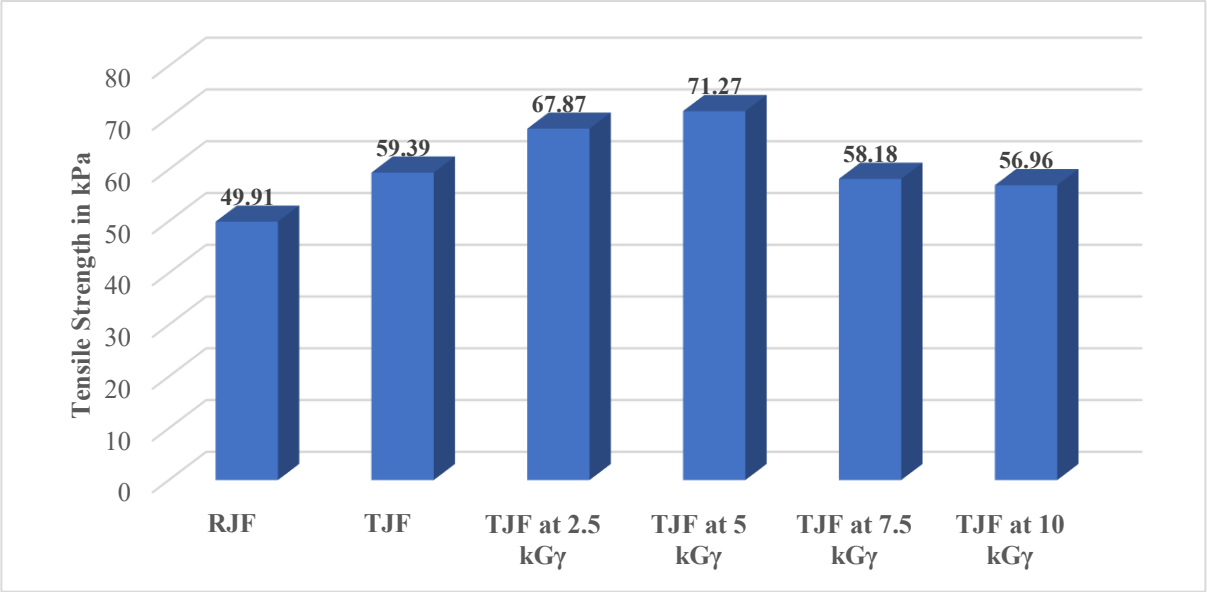

Figure 4.2. 3 Variation of tensile strength (kPa) of untreated jute fabric (UJF) and treated jute fabric (TJF) under different γ-radiation doses (2.5–10 kGy). The tensile strength increases to an optimum dose (5 kGy) due to radiation-induced crosslinking, followed by a decrease at higher doses due to chain scission and degradation.

After applying γ-radiation, the tensile strength (TS) of treated jute (TJF) improved from 67.87 kPa at 2.5 kGγ to 71.2 kPa at 5 kGγ. The Gamma radiation breaks weak bonds and creates free radicals, which induce cross-linking between the jute fabric cellulose and polymer. The cross-linking increases interfacial bonding and improves mechanical strength and stiffness. The tensile strength decreases with increasing γ-irradiation dose from 58.18 kPa at 7.5 kGγ to 56.96 kPa at 10 kGγ. Excessive γ-radiation causes severe chain scission, oxidation, and degradation of cellulose, which reduces mechanical strength and weakens the treated jute fabric. Gamma radiation initially improves breaking force by inducing cross-linking, but excessive doses cause degradation and loss of strength. Gamma radiation improves tensile strength up to an optimal dose. After applying a 5

kGy radiation dose, the highest tensile strength of 71.2 kPa was observed, indicating an optimal balance between crosslinking and degradation.

4.2.5 Analysis of Moisture Content, Moisture Regain, and Water Uptake% After Applying γ-Radiation

Moisture regain (MR), moisture content (MC), and water uptake (WU) are key parameters for assessing the hydrophilicity and durability of geotextile materials in soil environments. Natural fibers such as jute contain abundant hydroxyl (–OH) groups in cellulose, hemicellulose, and lignin, which interact strongly with water molecules through hydrogen bonding, resulting in a high moisture affinity. Excessive moisture absorption can accelerate microbial degradation and reduce the mechanical stability of natural geotextiles used for erosion control.

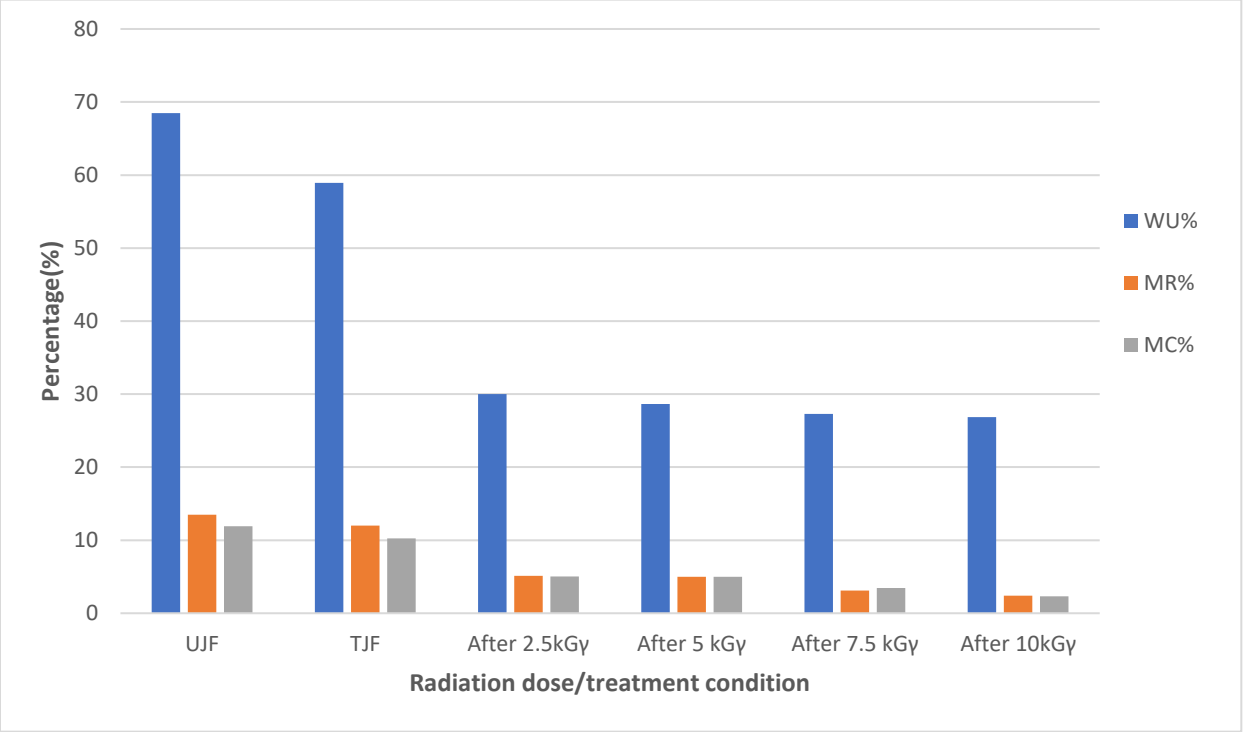

Figure 4.2. 4 Single bar diagram showing the comparison of Moisture Regain (MR), Moisture Content (MC), and Water Uptake (WU) of untreated and chemically treated jute fabrics under different γ-irradiation doses.

For clearer comparison, the values of MR, MC, and WU are presented together in a single bar diagram rather than in three separate diagrams (Figure 4.2.4). The results show that untreated jute fabric (UJF) exhibits the highest values due to the large number of accessible hydrophilic sites.

After chemical treatment and polymer coating, these values decrease markedly. Moisture regain decreased from 13.51% for untreated jute to 2.4% after 10 kGy γ-irradiation, while moisture content decreased from 11.9% to 2.3%, and water uptake decreased from 68.5% to approximately 26.85%.

This reduction in hydrophilicity is attributed to the formation of a cross-linked polymer network on the fiber surface. The bitumen emulsion and unsaturated polyester resin (UPR) coating partially blocks capillary pores and limits the accessibility of cellulose hydroxyl groups. In addition, γ-irradiation generates free radicals within the cellulose structure, promoting grafting and crosslinking reactions at the cellulose–polymer interface. These interactions strengthen interfacial bonding and hinder the diffusion of water molecules into the fiber matrix.

Consequently, the treated jute fabrics exhibit improved water resistance and enhanced durability, which are desirable characteristics for geotextile applications in soil erosion control.

4.2.6 SEM Analysis of Chemically Treated, and Chemically Treated with Gamma - Irradiated Jute Fabric

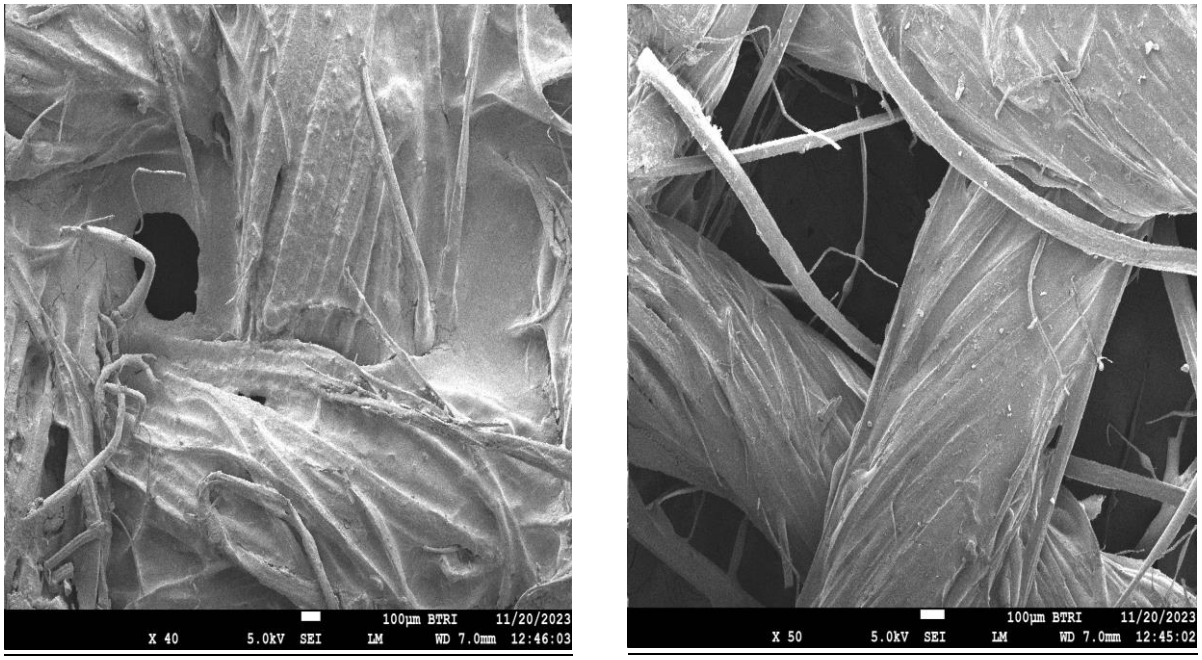

(a) (b)

Figure 4.2. 5 Morphological view of (a) Chemically treated and (b) Chemically treated with γ-radiated jute fabric.

The surface morphology of untreated and chemically treated jute fabrics was analysed using scanning electron microscopy (SEM).

The micrographs show that untreated jute fibres exhibit a rough, fibrillated structure with visible gaps between fibre bundles. These voids facilitate moisture penetration and contribute to the high-water uptake observed in untreated jute fabrics.

After chemical treatment with the polymer mixture (bitumen emulsion + UPR) and subsequent γ-irradiation, the SEM images reveal a more uniform polymer film covering the fibre surfaces. The polymer layer bridges adjacent fibres and fills some surface grooves, thereby improving fibre–matrix adhesion and reducing inter-fibre gaps.

Although SEM images clearly illustrate morphological changes and partial densification of the fibre network, the micrographs were not acquired under the calibrated imaging conditions required for quantitative pore size measurement. Therefore, precise pore-size distributions and numerical porosity values could not be determined from the SEM images.

Instead, SEM observations were used qualitatively to assess structural modification of the fibre surface. The images confirm that polymer deposition and γ-irradiation reduce excessive voids while still preserving some inter-yarn spacing. This residual porosity is beneficial for geotextile applications because it allows water permeability and vegetation growth while maintaining sufficient mechanical stability.

4.2.7 Analysis of FT-IR of Raw Jute Fabric, Chemically Treated Jute Fabric, and Chemical Treatment with Gamma-Irradiated Jute Fabric.

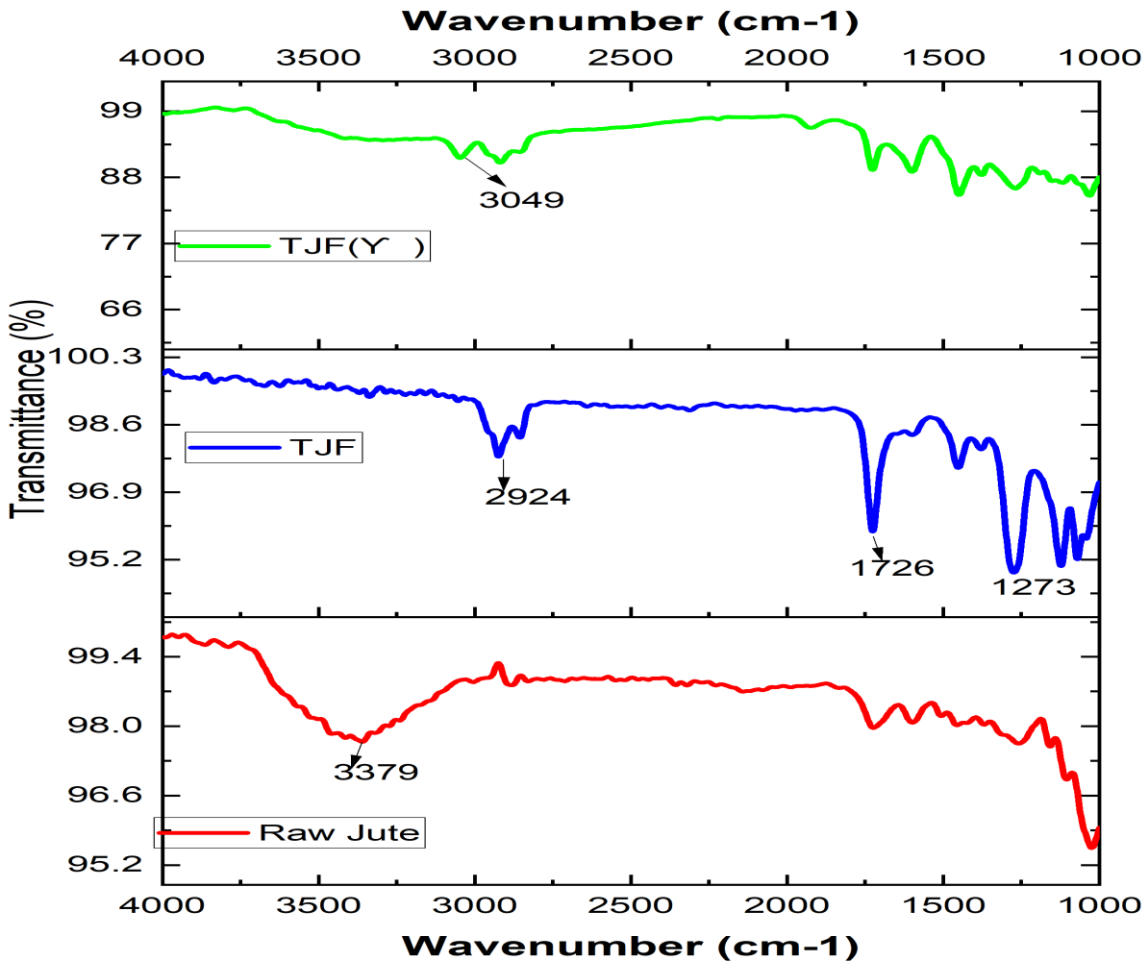

Figure 4.2. 6 FTIR graph of raw, chemical-treated, and γ-radiated jute fabric.

The 3379 cm^{-1} wavelength from FTIR indicates that the O-H bond of raw jute fabric cellulose is present. Nevertheless, after applying chemical and Γ-Radiation to the jute fabric, the reduction of the O-H groups improves the fabric's durability. The 3049 cm^{-1} peak intensity ensures cross-linking of the polymer with the jute fabric cellulose. FTIR confirms that the combined chemical treatment and γ-radiation reduce hydrophilicity by both chemical substitution (esterification, aromatic grafting) and structural sealing (crosslinking, densification). The proper discussion of wavenumber is given below in a table:

Table 4.2. 1 Comparative data from the FTIR graph

Wavenumber (cm^{-1})	Assignment	Interpretation here
3379	O–H stretch (cellulose/H_2O)	High in raw; reduced after treatment/γ ⇒ fewer accessible –OH
3049	=C–H (styrene ring)	Clear after γ; confirms styrene-containing network
2924	C–H stretching	Polymer phase (bitumen/UPR/styrene) is present on treated fabrics
1726	C=O stretching of ester (polyester)	Polyester/esterification persists after γ-radiation, with a possible subtle shift.
1273	C–O (ester, acyl–O)/aryl–O	Part of the ester fingerprint region; indicates polyester linkage

4.2.8 XRD Analysis of Raw, Chemically Treated, and Chemical Treated with Gamma-Irradiated Jute Fabric

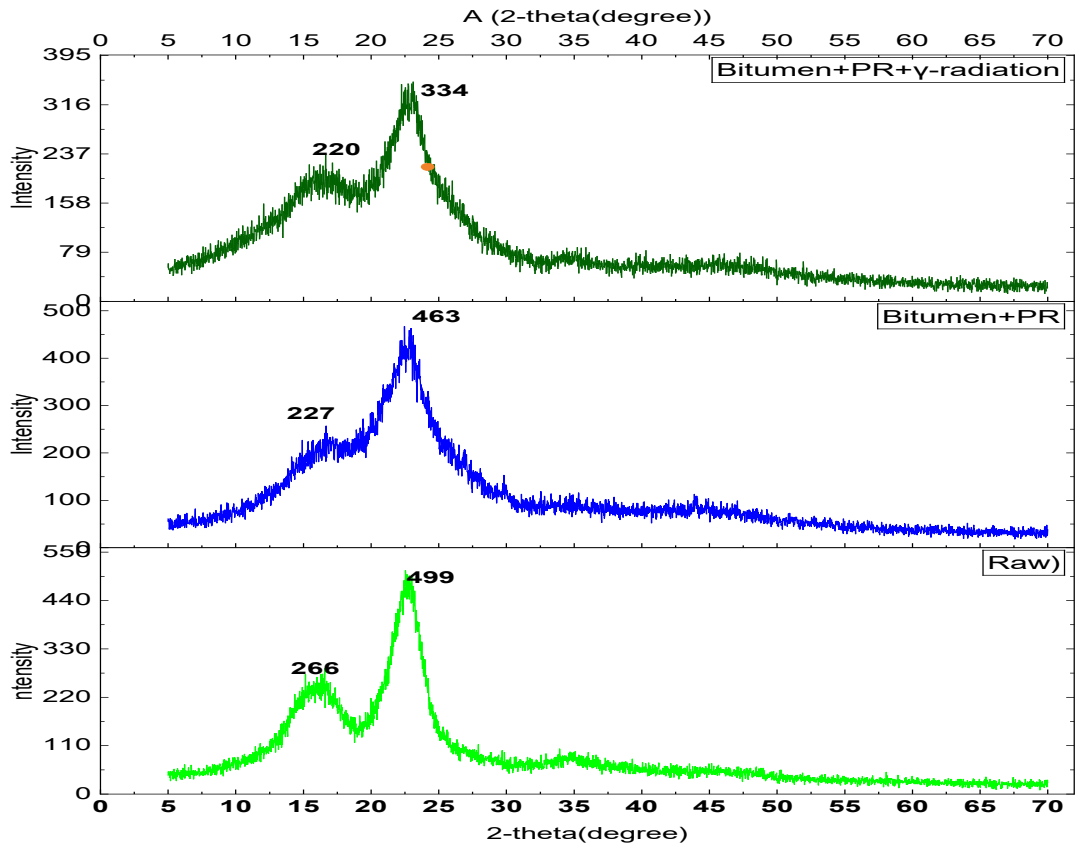

Figure 4.2. 7 XRD graph of raw, chemical-treated, and γ-radiated jute fabric.

This graph shows that the peak intensity of the raw jute (UJF) is more than that of the other TJF. It indicates that crystallinity decreases due to the cross-linking of jute fabric cellulose with the unsaturated polyester resin (UPR) from the polymer mixture, generated by free radicals via γ-radiation. The peak intensity at 2θ (22°) represents the crystalline cellulose in jute. A decrease in peak intensity indicates lower crystallinity, a more amorphous structure, and higher polymer impregnation and cross-linking. The Γ-Irradiation effect breaks some hydrogen bonds in cellulose, enabling polymer penetration and reduced water absorption, as observed in earlier results.

4.2.9 TGA Analysis of Raw, Chemically Treated, and Chemical Treated with Gamma-Irradiated Jute Fabric

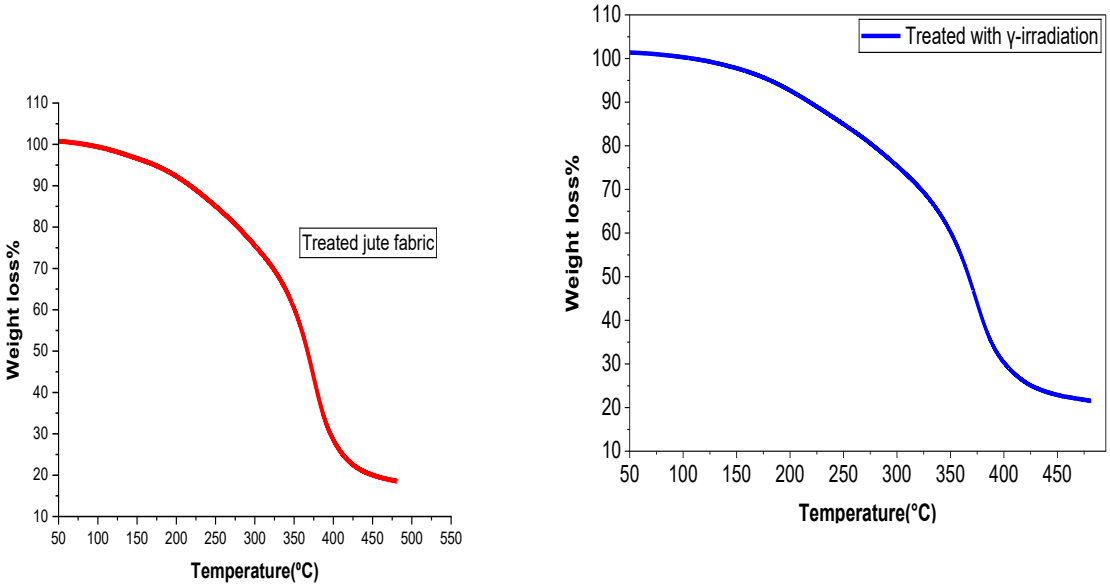

Figure 4.2. 8 TGA analysis of raw, chemically treated, and chemical treated with gamma-irradiated jute fabric.

TGA thermograms of treated jute fabric and the same fabric after 5 kGγ γ-irradiation. Both show (i) minor moisture loss below ~120 °C, (ii) hemicellulose/low-MW volatilization between ~150–260 °C, (iii) a primary decomposition step of hemicellulose/cellulose with overlapping polyester degradation at ~330–390 °C, and (iv) a slow tail attributed to lignin/aromatic residues up to 500–550 °C. The γ-irradiated sample exhibits a higher onset temperature and slightly increased char yield, indicating enhanced thermal stability due to radiation-induced crosslinking and densification of the polymer–cellulose network.

4.2.10 Analysis of Durability by TS (Tensile Strength) Loss

In this bar diagram, it is clear that the 5 kGγ γ-irradiated chemically treated sample exhibited less strength loss than the other samples after burial in soil for 120 days.

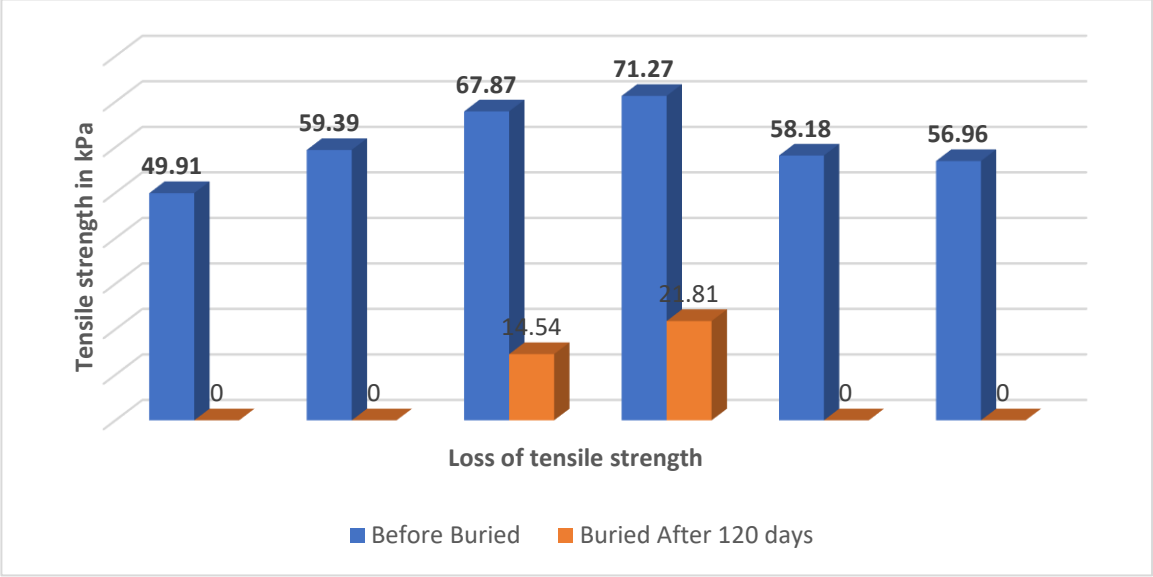

Figure 4.2. 9 Analysis of loss of tensile resistance after soil burial.

The breaking force of untreated jute (RJF), chemically treated jute (TJF), and TJF2 after γ-irradiation (2.5–10 kGγ). Strength increases with treatment, peaking at 5 kGy (71.27 kPa), and then decreases at 7.5–10 kGy toward the treated baseline, indicating an optimum crosslink density. The improvement at moderate doses is attributed to radiation-assisted grafting/crosslinking and better interfacial adhesion (SEM/FTIR), while higher doses introduce chain scission/embrittlement that offsets the gains.

4.2.11 Key Findings

1. Gamma radiation reduces the excess amount of polymer mixture (BE+UPR) from the fabric surface, and the space between two adjacent yarns is opened. As a result, the fabric's porosity was determined by SEM analysis. Gamma radiation also creates free radicals from jute cellulose, which exhibit cross-linking with cellulose and polyester resin and reduce hydroxyl groups; as a result, tensile strength increases, along with the improvement of durability properties of grey jute.

2. Porosity of chemically treated jute fabric proves that tree plantation is possible over the chemically treated jute fabric after its use for geo-technical purposes.

3. From the FTIR result, the extension of tensile strength faces a problem due to the high radiation dose, because it breaks down the original chemical structure of the jute fabric, resulting in a decrease in the strength of the jute fabric. Chemically treated with 5 kGy gamma-irradiated jute fabric showed better durability properties than those with other gamma radiation doses.

4. Durability test of jute fabric in the soil has proven that the 5kGy radiated jute fabric showed better results than the high and low-dose radiated jute fabric.

4.3 Pre-Treatment of Jute Fabric, Then Chemical Modification

4.3.1 Work Flow Diagram

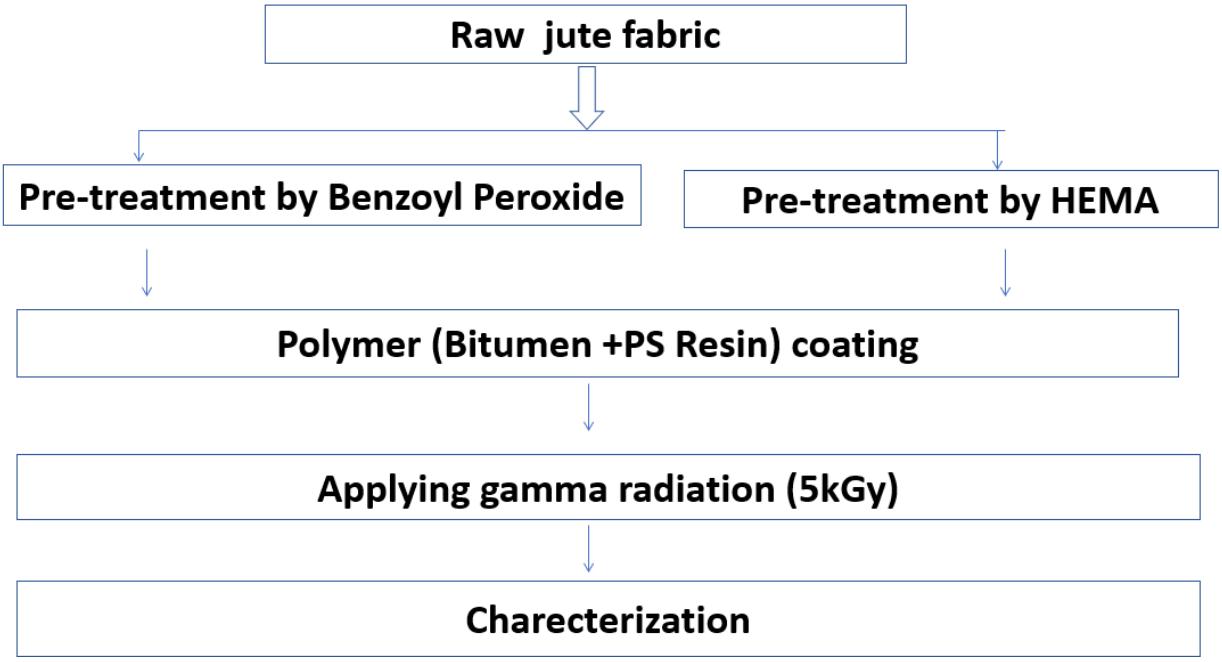

Figure 4.3. 1 Workflow diagram of pre-treatment and chemical modification.

4.3.2 Preparation of the Research Sample

Initially, the raw jute (UJF) was pre-treated using two separate processes. After pretreatment, all research samples were coated with a polymer coating using a selected recipe of the polymer mixture from 3.1. 1where bitumen emulsion (30%), Polyester resin (10%), Styrene monomer (54%), MEKP (4%) as initiator, and 1% cobalt naphthenate as curing agent. After polymer coating/chemical treatment, gamma radiation (5 kGy) was applied to the treated jute fabric, and the samples were characterized for physical and chemical properties. The pre-treatment process was done in two ways. At pre-treatment process -1, raw jute fabric was treated with benzoyl peroxide, whereas acetone was used as a solvent, and at pre-treatment process -2, jute fabric was treated with HEMA+benzoyl peroxide. After pre-treatment, the jute fabric is coated with a polymer mixture and then irradiated with 5 kGy γ-radiation.

4.3.3 Pre-Treatment Process-1: Benzoyl Peroxide Treatment

The pre-treatment of jute fabric using benzoyl peroxide (BP) was carried out to enhance the reactivity of cellulose fibres and improve their compatibility with polymer coatings.

Benzoyl peroxide was selected as a free-radical initiator because it decomposes thermally to generate benzoyloxy radicals, which can abstract hydrogen atoms from the cellulose backbone. This reaction produces active radical sites on the jute fibre surface, which promote graft polymerization and crosslinking with the unsaturated polyester resin.

The following steps were involved with the above-stated process:

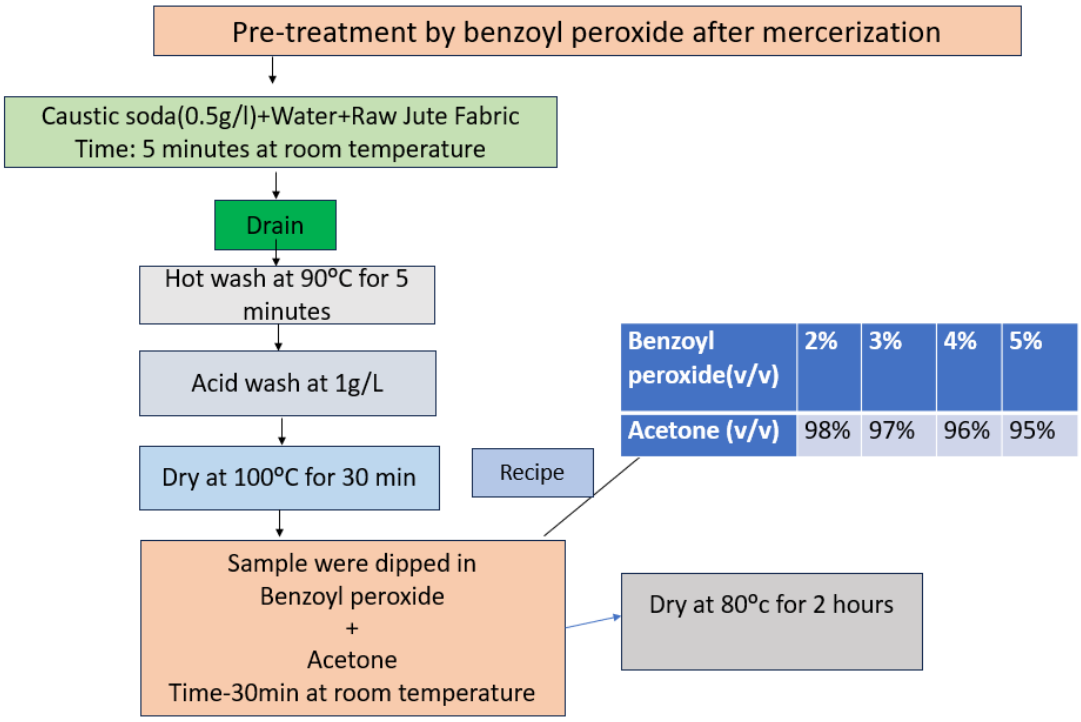

Figure 4.3. 2 Working procedure of the diagram of the pre-treatment process-1.

4.3.3.1 (a) Selection of Benzoyl Peroxide (%) by the change of tensile strength

The optimum concentration of benzoyl peroxide was determined experimentally by evaluating the tensile strength of treated jute fabrics at different BP concentrations, as represented in Figure 4.3.3.

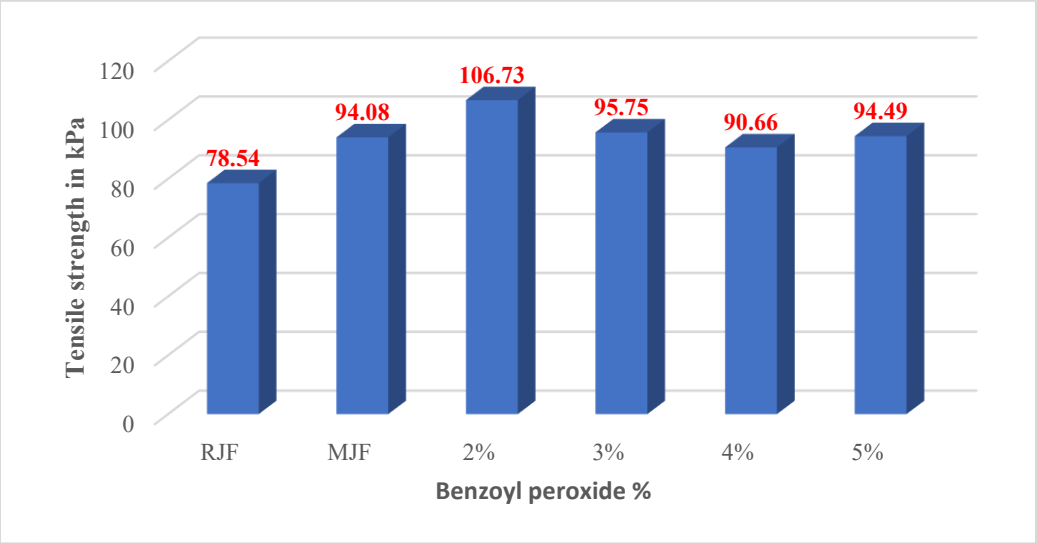

Figure 4.3. 4 Tensile strength v/s benzoyl peroxide % of mercerized jute fabric.

The tensile strength initially increased with increasing benzoyl peroxide concentration, reaching a maximum at 2% BP, then gradually decreased. The highest tensile strength was 106.73 kPa for the 2% benzoyl peroxide treatment, compared with 78.54 kPa for the raw jute fabric.

The improvement in tensile strength at 2% BP can be attributed to the formation of free radicals that initiate cross-linking between cellulose chains and the polymer matrix. This enhances interfacial bonding and improves load transfer between fibres and the polymer coating.

The optimum percentage observed from the above bar diagram is 2(%). The result was due to benzoyl peroxide, which enhanced interfacial bonding by promoting free radicals that induced cross-linking. This, in turn, led to more free radicals, which further enhanced cross-linking and structural brittleness.

4.3.3.1(b) Reaction involved in pre-treatment process-1

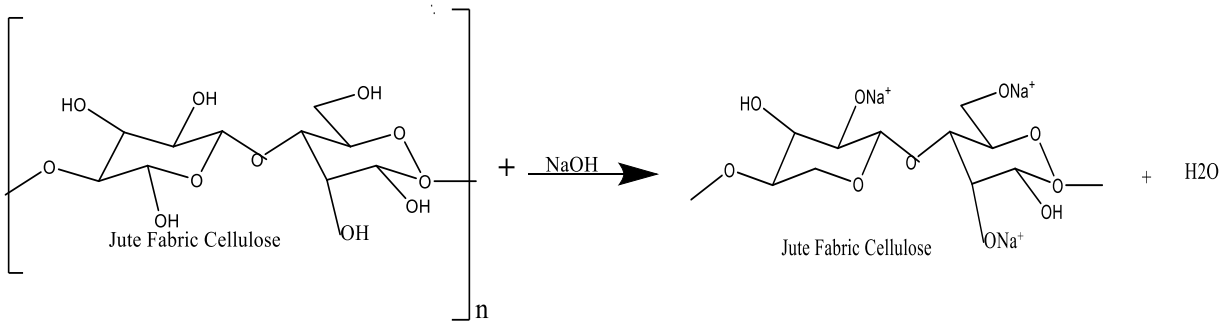

(i)

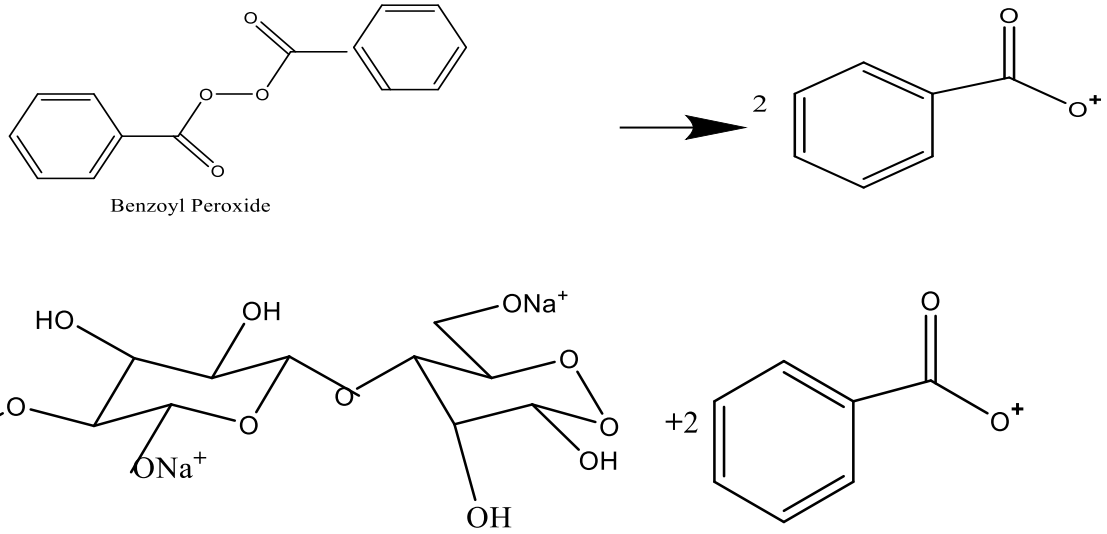

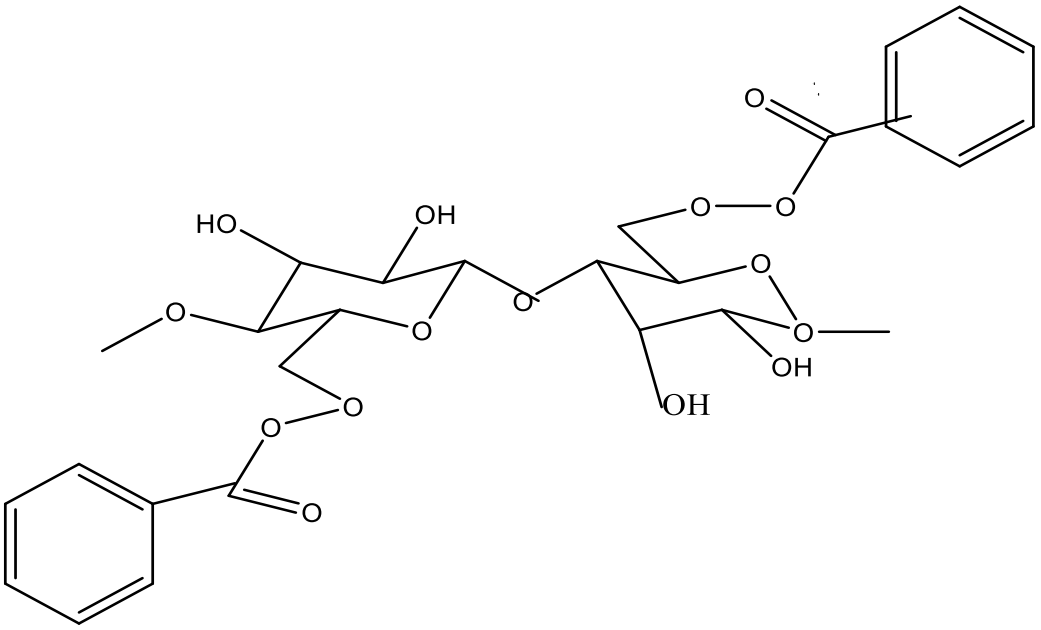

(ii)

Step-1(i) Mercerization of jute fabric cellulose (ii) Reaction with mercerized cellulose and Benzoyl peroxide [87].

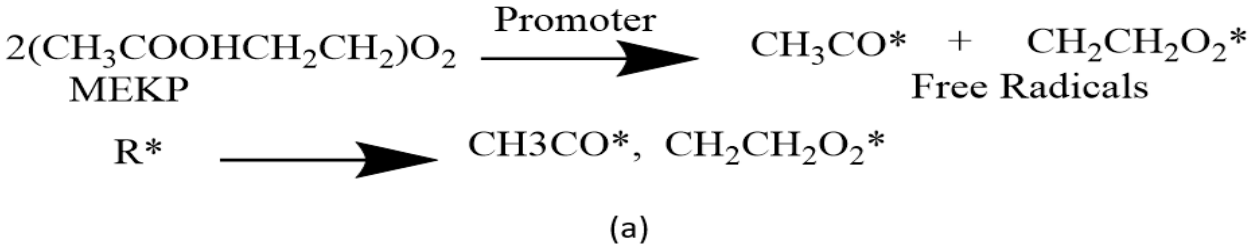

Step-2 (a) Formation of a free radical by decomposition of MEKP (b) Double bond opening of PR

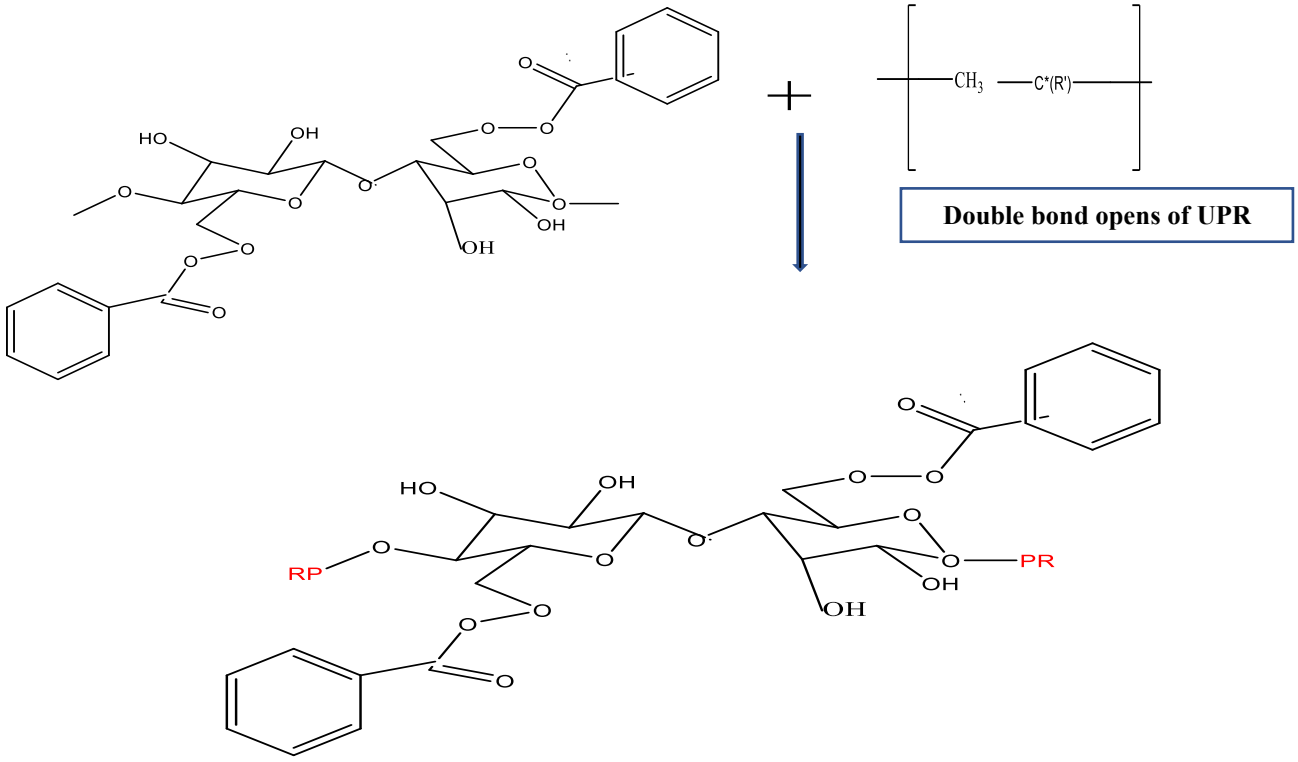

Step-3 Possible Polymerization of Benzoyl Peroxide-treated cellulose of jute fabric and PR

4.3.3.2 Proposed Cross-Sectional View of Benzoyl Peroxide Pre-Treated Jute Fabric

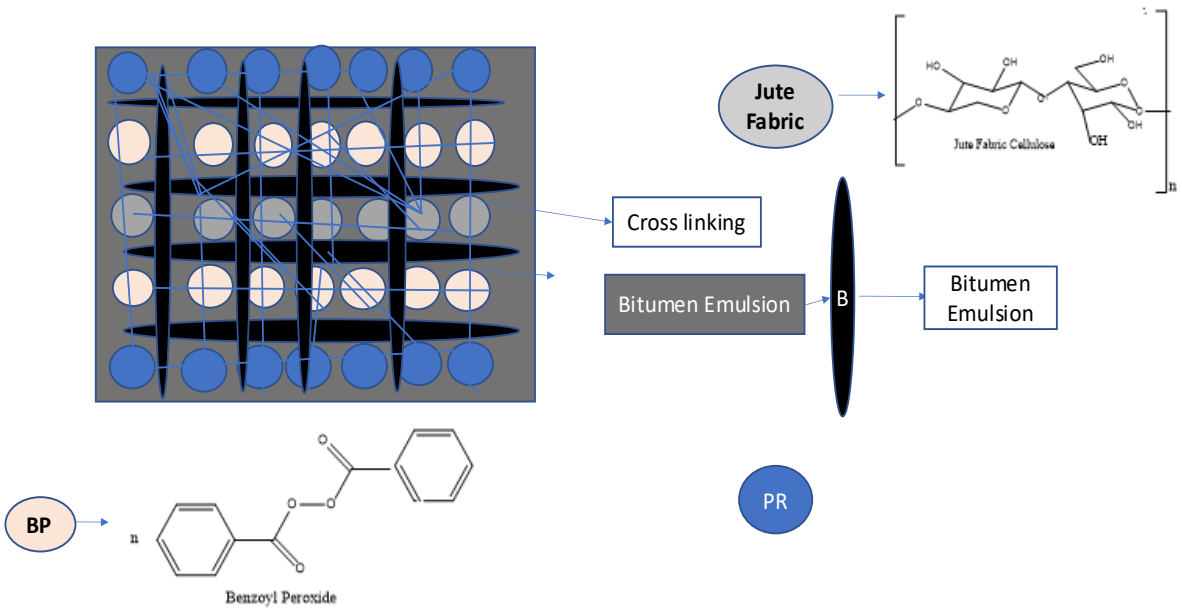

Figure 4.3. 5 Possible cross-sectional view of benzoyl peroxide pre-treated with chemically treated jute fabric.

4.3.3.3 FTIR Analysis of Benzoyl Peroxide Pre-Treated Jute Fabric with Raw Jute Fabric

The broad absorption band at approximately 3414 cm^{-1} corresponds to the O–H stretching vibration of cellulose hydroxyl groups. After treatment, the intensity of this band decreases noticeably, indicating partial consumption or shielding of hydroxyl groups due to chemical reactions and polymer coverage. Similar reductions in O–H band intensity have been widely reported in modified cellulose-based natural fibers after chemical treatment and polymer grafting.

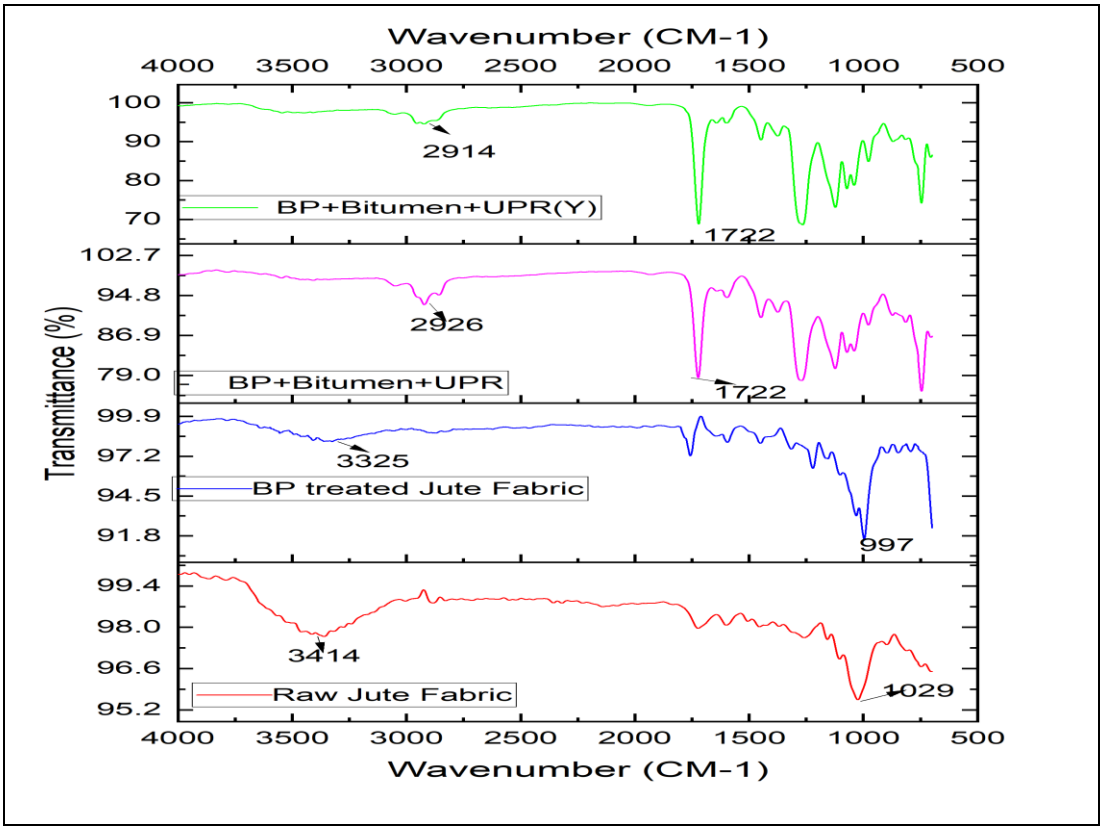

Figure 4.3. 6 FTIR spectral comparison of raw and benzoyl peroxide pre-treated jute fabric showing esterification and polymer–cellulose crosslinking.

The appearance and intensification of the band at 1722 cm^{-1}, attributed to C=O stretching vibrations, confirm the formation of ester linkages between the unsaturated polyester resin and the cellulose surface. This band is also commonly associated with carbonyl groups from esterified hemicellulose or polyester matrices, indicating successful interfacial bonding between the fiber and the polymer coating.

The absorption peaks in the 2914–2926 cm^{-1} region correspond to aliphatic C–H stretching vibrations originating from methylene groups present in bitumen and unsaturated polyester resin, indicating the incorporation of hydrophobic polymer chains onto the fiber surface. In addition, the characteristic band near ~997 cm^{-1}, typically assigned to C–O–C stretching of the β-1,4-glycosidic linkage in cellulose, remains present, confirming that the fundamental cellulose backbone is preserved although its surface chemistry has been modified.

These spectral changes indicate that benzoyl peroxide acts as a radical initiator, generating free radicals that promote grafting and crosslinking reactions between cellulose and the unsaturated polyester resin matrix. Consequently, a cross-linked polymer network forms on the jute fiber surface, reducing the accessibility of hydroxyl groups and restricting the diffusion of water molecules into the fiber structure.

Overall, the FTIR results confirm that the treatment process chemically modifies the jute fiber surface through esterification and crosslinking, thereby decreasing hydrophilicity, increasing crosslink density, and enhancing the water resistance and durability of the treated jute fabric for geotextile applications. Table 4.3.1 compiles the different peaks with relevant interpretations,

Table 4.3. 1 Peak intensity analysis from the FTIR graph

Wavenumber (cm^{-1})	Peak Position	Functional Group	Interpretation
~3414	Broad peak	O–H stretching (hydroxyl group in cellulose)	Present in raw jute; decreases after BP, Bitumen, UPR treatment due to bonding/crosslinking.
3325	Broad/Medium	O–H/N–H stretching	Hydrogen bonding or hydroxyl groups in jute cellulose
2914–2926	Medium	C–H asymmetric stretching (aliphatic $–CH_2$)	Indicates alkyl groups from bitumen/polyester resin incorporation
1722	Strong	C=O stretching (ester group)	Formation of ester linkages after polyester resin and BP treatment
997	Medium	C–O stretching, β-glycosidic linkages in cellulose	Cellulose backbone characteristic peak

4.3.3.4 Analysis of X-Ray Diffraction (XRD) of Benzoyl Peroxide Pre-Treated Grey Jute

XRD graphs revealed two primary peaks at $2\theta = 16–17°$ and 22–23°, corresponding to the cellulose I structure in jute fabrics. Raw jute exhibited the highest crystallinity, indicating more ordered cellulose chains and high hydrophilicity. Chemical treatments with Bitumen and PR, followed by γ-irradiation, reduced peak intensities, suggesting partial amorphization due to crosslinking and polymer deposition. Benzoyl peroxide (BP)- treated samples exhibited moderate crystallinity, with improved interfacial bonding, thereby balancing hydrophobicity and mechanical stability and enhancing durability compared to untreated jute.

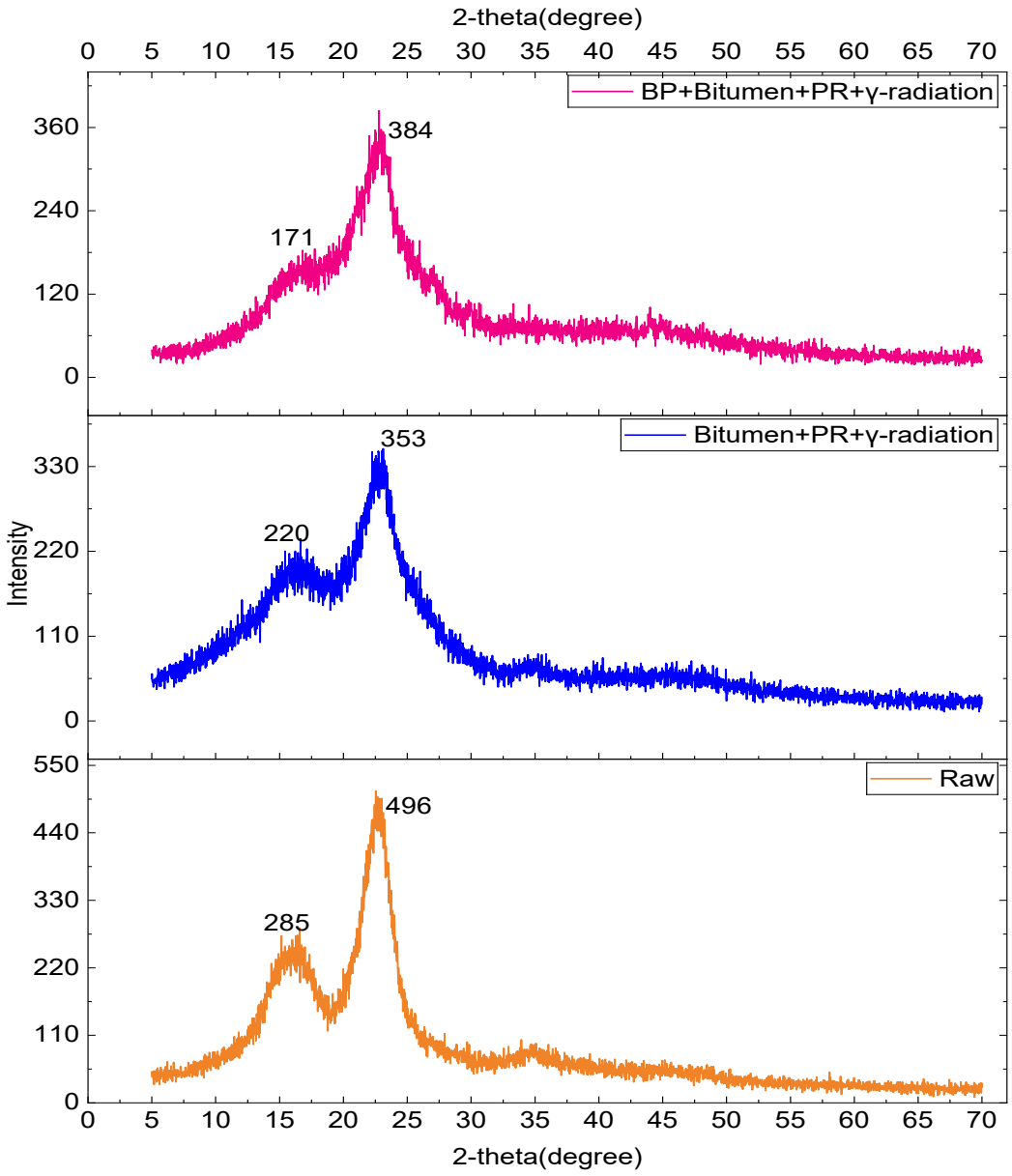

Figure 4.3. 7 X-ray diffraction (XRD) patterns of raw jute, bitumen/PR/γ-radiation treated jute, and benzoyl peroxide (BP) pre-treated jute composites, illustrating variations in cellulose I crystallinity and structural modification induced by chemical treatment and irradiation.

4.3.4 (a) Pretreatment Process-2 (Pre-Treatment of Jute by HEMA (2-Hydroxyethyl Methacrylate)

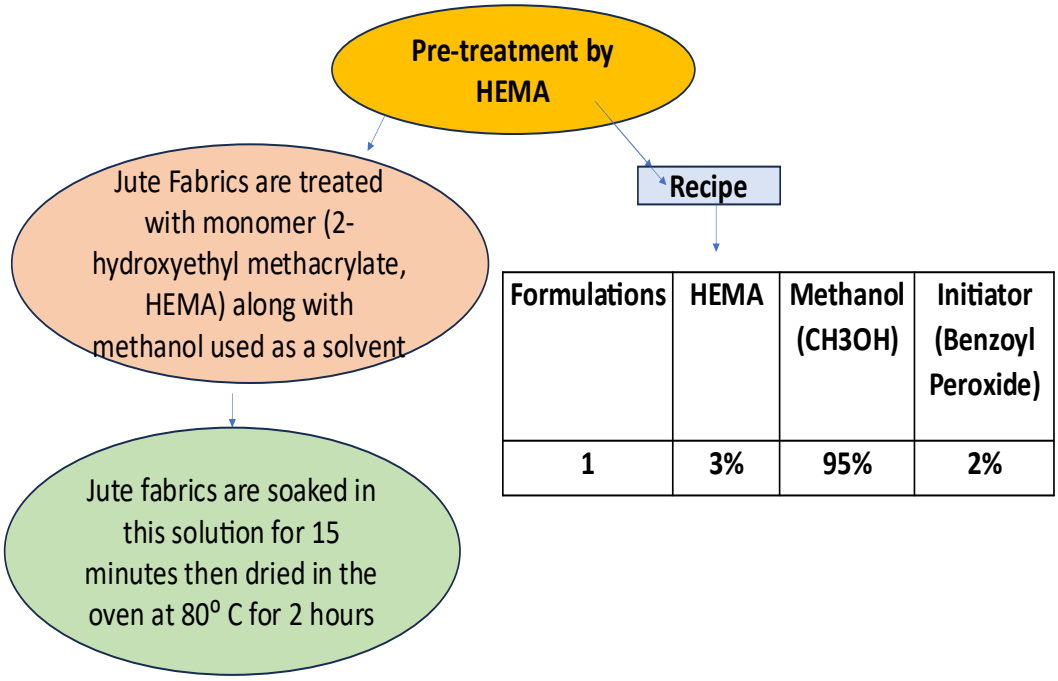

Figure 4.3. 8 Workflow diagram of the Pre-treatment process-2.

4.3.4.1 Reaction Involved in Pre-Treatment Process-2

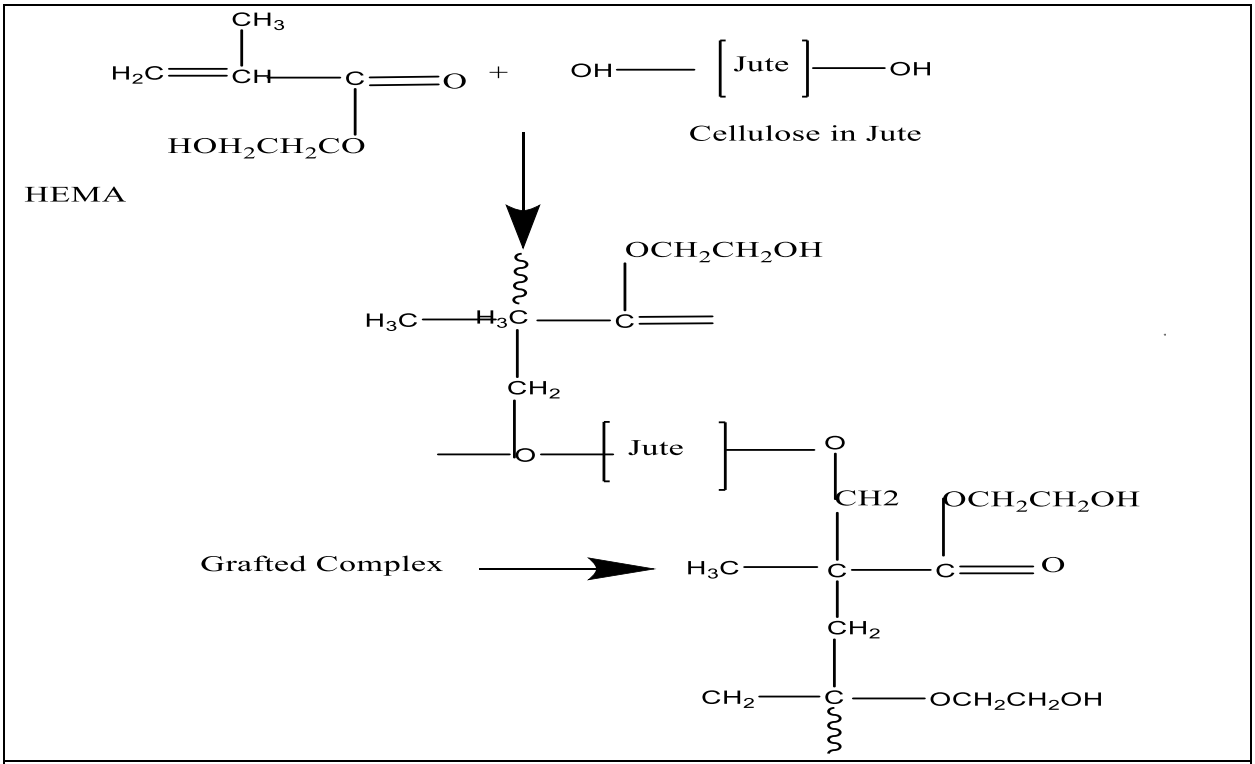

(a) Formation of grafted complex HEMA and Jute fabric

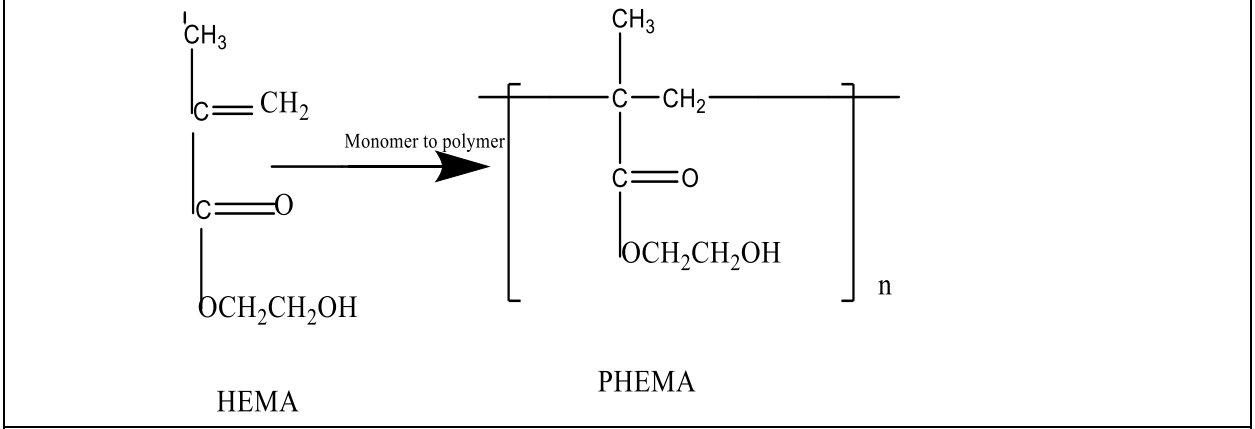

(b) **Polymer (poly-HEMA) formation**

Step -1 (a) Formation of grafted complex with HEMA and jute fabric, and (b) Polymer (poly-HEMA) formation. (Adopted from [20])

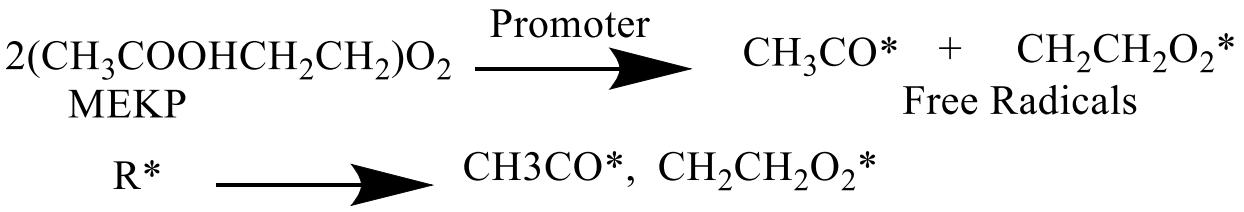

(a)

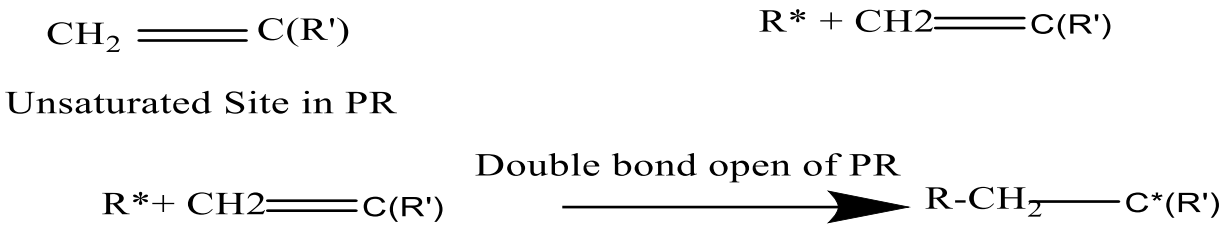

(b)

Step-2 (a) Formation of a free radical by decomposition of MEKP (b) Double bond opening of PR

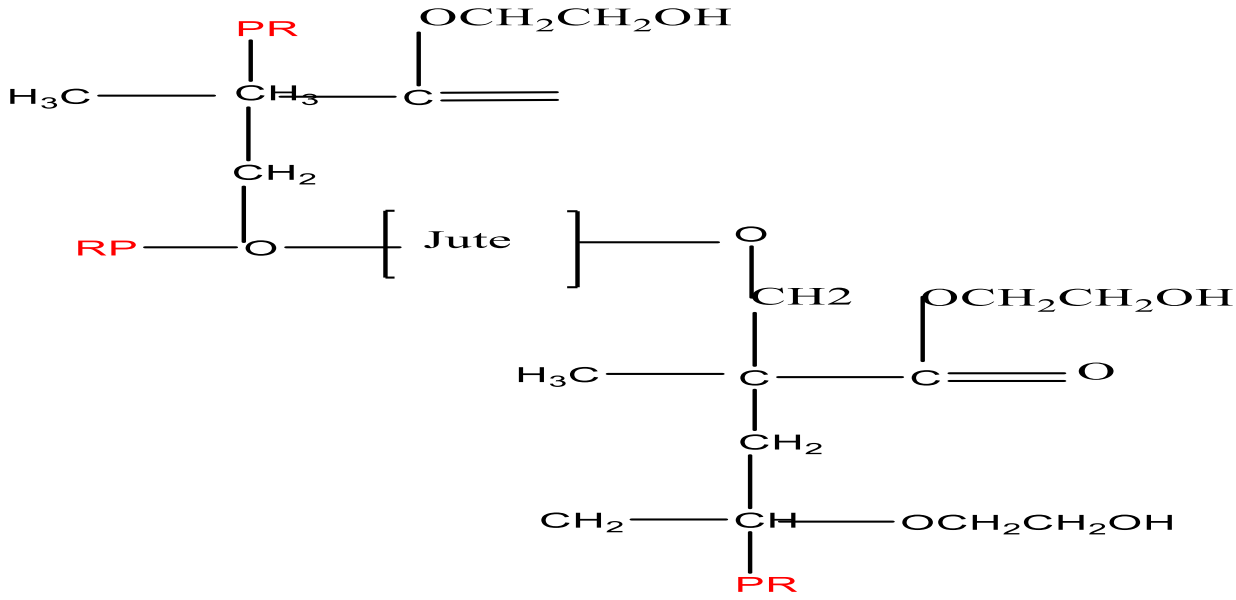

Step-3 Polymerization of HEMA-treated jute fabric cellulose with PR

4.3.4.2 Possible Cross-Sectional View of HEMA Pre-Treated Jute Fabric

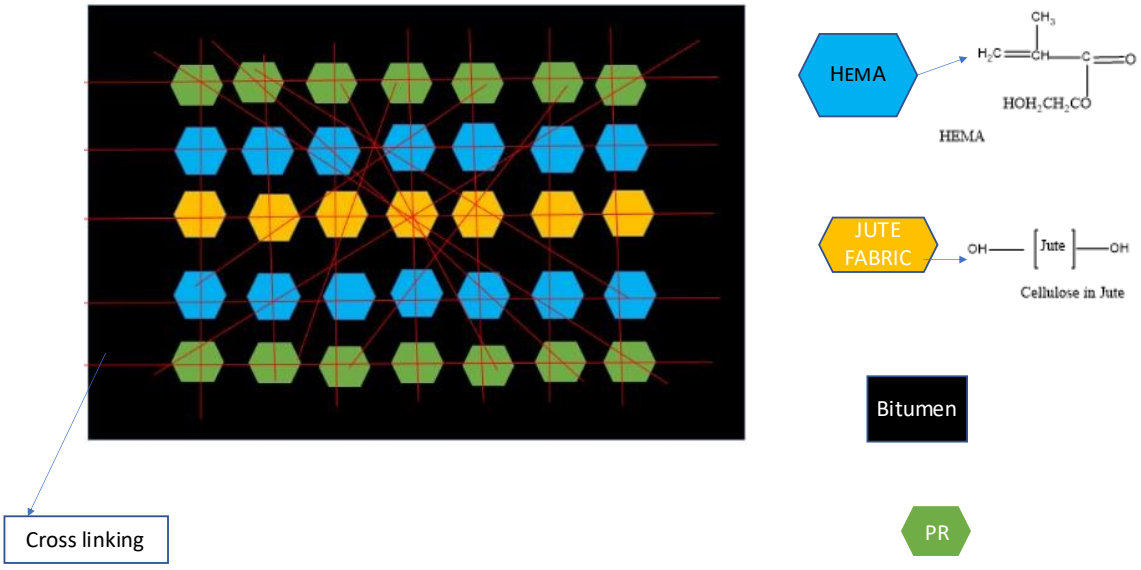

Figure 4.3. 9 Possible cross-sectional view of HEMA pre-treated jute fabric.

4.3.4.3 FTIR Analysis HEMA Pre-Treated Jute Fabric

The peak intensity at 3359-3338 cm^{-1} indicates that the –OH band intensity in treated samples decreases relative to that in raw jute fabric, suggesting esterification or bonding with HEMA and UPR. The new peak at 1720cm confirms cross-linking/polymerization of cellulose in the jute fabric. The peak intensity of the alkyl group 2956 cm^{-1} appears in the presence of bitumen, indicating hydrophobicity. The peak at 1268 cm^{-1} indicates successful polymerization of the cellulose surface. HEMA (2-hydroxyethyl methacrylate) contains both a hydroxyl (–OH) and a vinyl group. Benzoyl peroxide, through thermal initiation, triggers free-radical polymerization of HEMA, forming polymer chains that attach to jute cellulose hydroxyl groups. Ester bonds (C=O) and ether linkages (C–O–C) appear. Also, the addition of UPR + Bitumen introduces hydrophobic chains, reducing hydrophilicity, improving dimensional stability, and possibly enhancing mechanical strength.

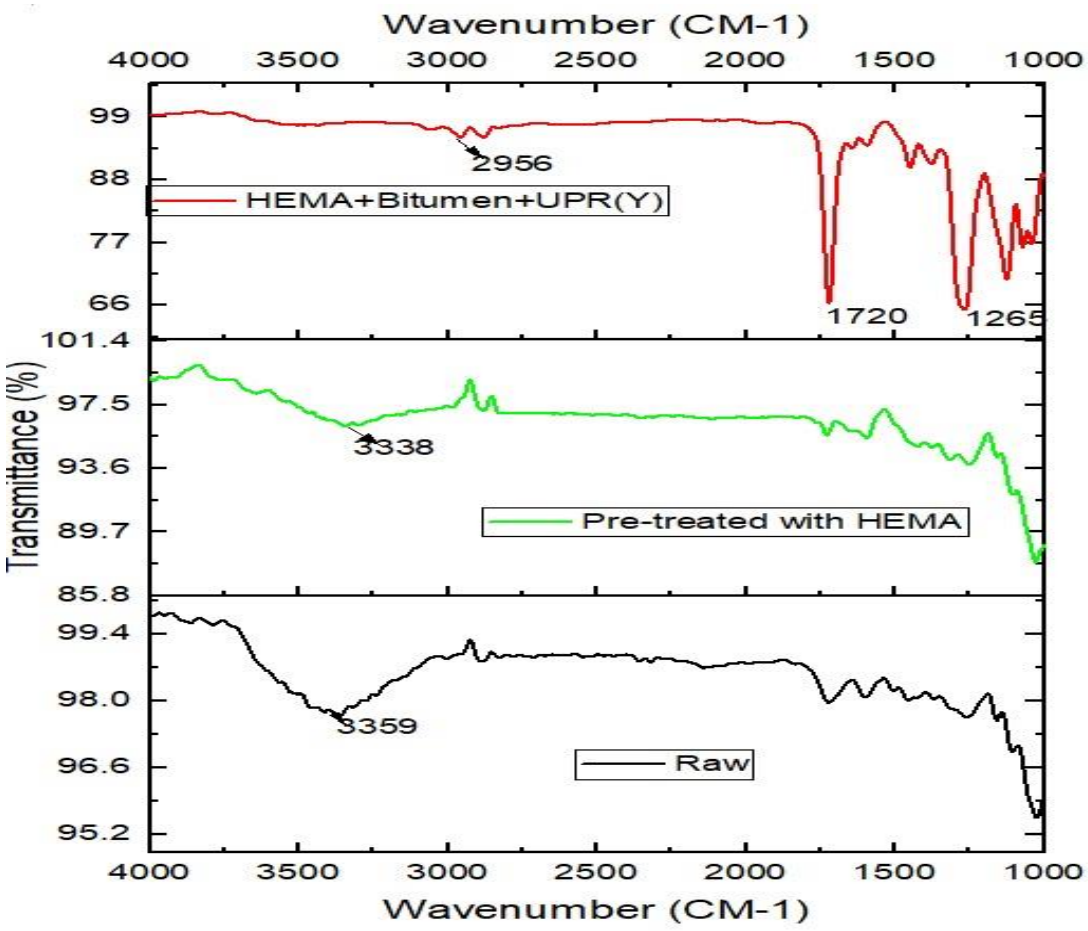

Figure 4.3. 10 FTIR spectra of raw and HEMA pre-treated jute fabric composites, showing the change of functional groups, including reduction of hydroxyl (–OH) intensity and formation of ester (C=O) and ether (C–O–C) linkages, confirming successful graft polymerization and crosslinking with HEMA, UPR, and bitumen.

Table 4.3. 2 Analysis of peak intensity from FTIR graph

Wavenumber (cm^{-1})	**Peak Intensity**	**Functional Group**	**Interpretation**
3359–3338	Broad peak	O–H stretching (hydroxyl in cellulose, HEMA)	Hydrogen bonding decreases after HEMA treatment, showing reaction with –OH groups
2956	Medium	C–H asymmetric stretching ($–CH_2$, $–CH_3$ groups)	Indicates alkyl chains from HEMA and bitumen

Wavenumber (cm^{-1})	Peak Intensity	Functional Group	Interpretation
1720	Strong	C=O stretching (ester or acrylate groups in HEMA/UPR)	Confirms ester linkage formation after polymerization
1268	Sharp	C–O–C stretching (ester/ether linkage)	New crosslinking between HEMA and cellulose

4.3.4.4 XRD Analysis of HEMA Pre-Treated Jute Fabric

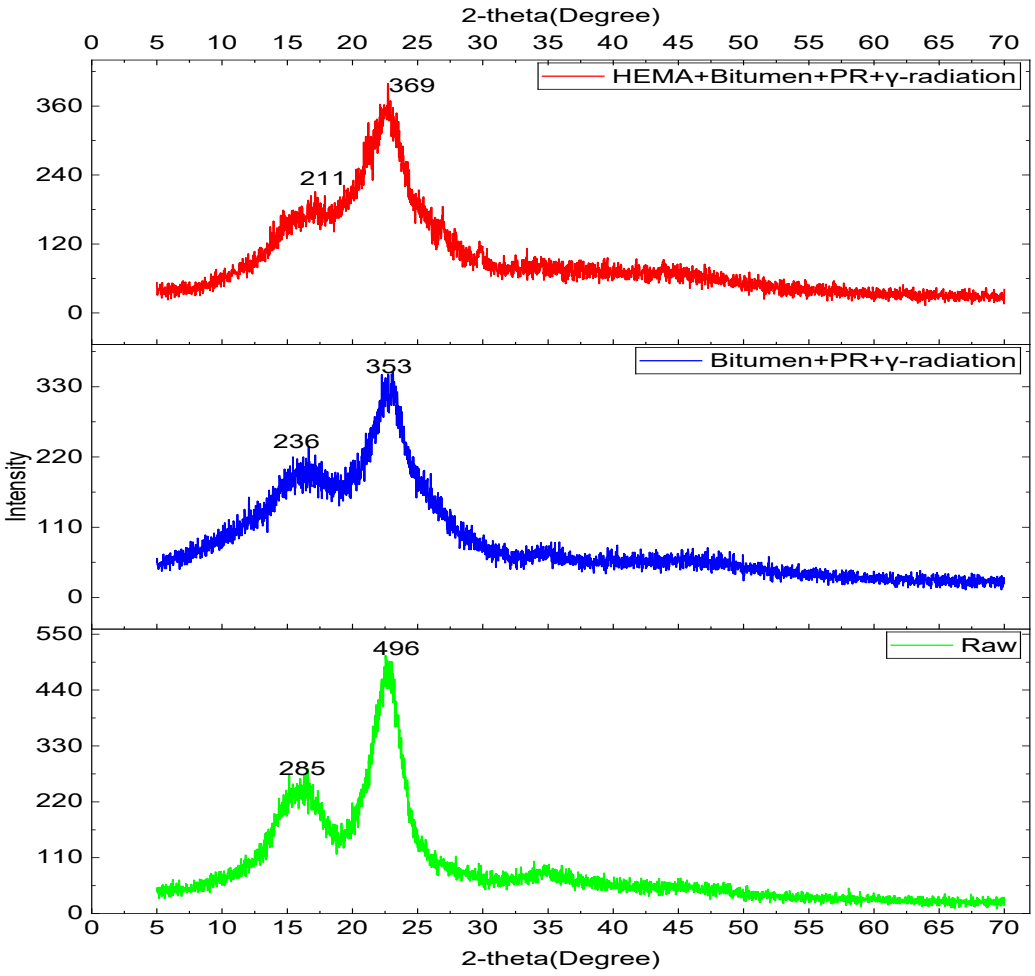

Figure 4.3. 11 Comparative X-ray diffraction (XRD) patterns of raw, bitumen–polyester resin treated, and HEMA-modified jute fabrics under γ-irradiation indicating structural transformation and crystallinity variation.

XRD analysis revealed two major peaks at 2θ = 16–17° and 22–23° associated with the cellulose I structure of raw jute fibers. Raw jute exhibited the highest crystallinity index, indicating highly ordered cellulose chains with increased hydrophilicity. Treatment with Bitumen emulsion and polyester resin (PR) followed by γ-irradiation decreased peak intensity, suggesting partial amorphization due to polymer deposition and irradiation-induced crosslinking. The hydroxyethyl methacrylate (HEMA)- treated samples showed the lowest peak intensities and the highest amorphous content, indicating extensive disruption of crystalline domains, improved hydrophobicity, and superior dimensional stability.

4.3.5 Key Findings

1. Pre-treatment of jute fabric by benzoyl peroxide (Pre-treatment-1) and HEMA (Pre-treatment-2) increases the hydrophobicity of jute fabric and also creates free radicals, which help the formation of polymerization/ cross-linking with polymer mixture (bitumen emulsion, polyester resin) and jute fabric cellulose.
2. Pre-treatment of jute fabric more activates the cross-linking of the polymer mixture with the jute fabric cellulose, which increases the hydrophobicity of the jute. Finally, pre-treatment improves the durability of grey jute fabric by increasing tensile strength
3. HEMA Pretreated jute fabric showed more hydrophobicity than other treated jute fabrics. The durability of jute fabric increases through cross-linking with bitumen emulsion, polyester resin, and cellulose.

4.4 Measurement of Durability Properties by Weathering Test.

4.4.1 Comparative Analysis of Physio-Mechanical Properties

Table 4.4. 1 Data table for comparison of tensile strength:

Sl.	Observation	TS in kPa
1.	Raw jute fabric**(J0)**	49.81
2.	Jute fabric treated with Bitumen + PR **(J1)**	59.39
3.	Jute fabric treated with Bitumen + PR **(J2)**	67.39
4.	Jute fabric treated with HEMA+ Bitumen+ PR + γ-irradiation **(J3)**	74.78
5.	Jute fabric treated with BP + Bitumen+ PR + γ-irradiation **(J4)**	69.87

4.4.2 Analysis of Tensile Strength

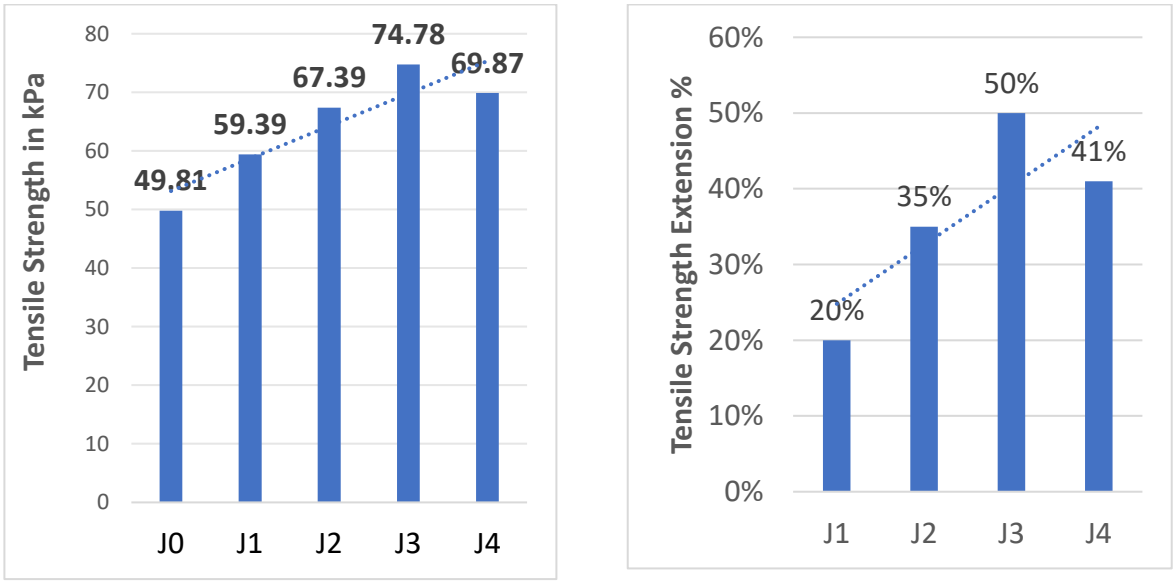

(i) (ii)

Figure 4.4. 1 Comparative evaluation of (i) tensile strength and (ii) percentage elongation of raw and chemically modified jute fabrics (Bitumen + PR, Bitumen + PR + γ-irradiation, HEMA + Bitumen + PR + γ-irradiation, and BP + Bitumen + PR + γ-irradiation systems).

The bar diagram above shows that pre-treating jute fabric increases its tensile strength compared to raw jute fabric. Pre-treatment with HEMA showed better results than other samples. HEMA introduces additional hydroxyl groups and double bonds, enhancing interfacial bonding between polymer mixtures and jute fibers, and exhibits maximum tensile strength (TS). Benzoyl peroxide (BP) initiates the creation of free radicals for crosslinking but might cause localized degradation

at high concentrations, resulting in slightly less improvement than HEMA. A polymer mixture (Bitumen + PR) alone enhances hydrophobicity and dimensional stability, but has a lower crosslink density than HEMA- or BP-treated systems.

4.4.3 Analysis of Fabric Weight

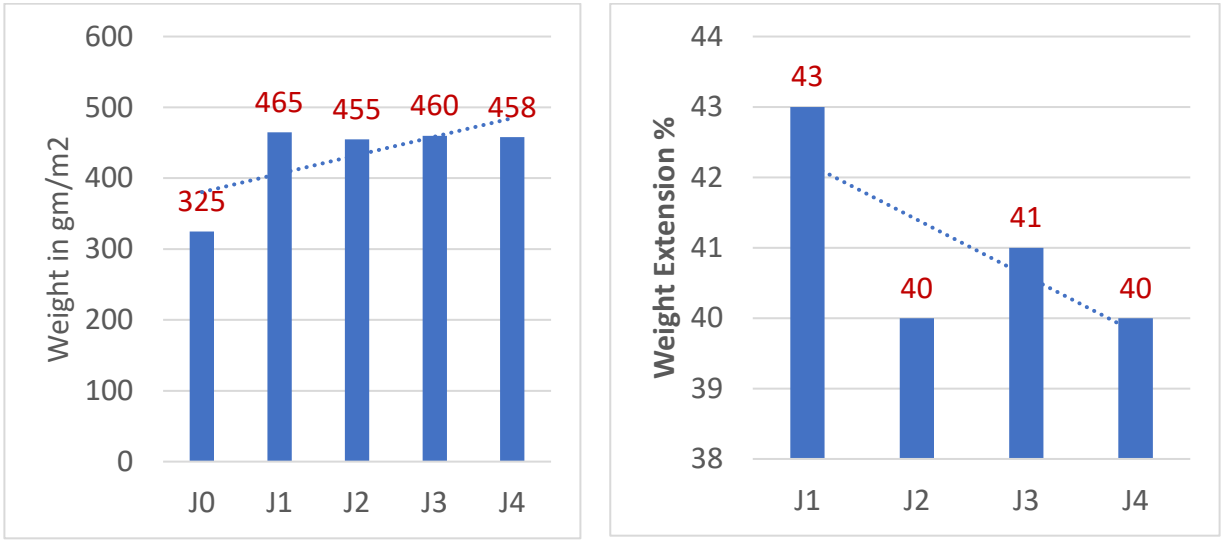

(a) **(b)**

Figure 4.4. 2 (a) Weight gain and (b) Weight Extension (%).

This bar diagram illustrates the weight of raw jute (UJF) and chemically treated jute (TJF). The fabric weight increases significantly after treatment due to the deposition and cross-linking of polymers on the fiber surfaces. The maximum weight gain is observed for J1 (43%), indicating the highest material deposition during polymer coating (bitumen + UPR). γ-irradiation samples (J2, J3, J4) exhibit a slightly lower weight gain (40–41%), possibly because irradiation enhances crosslinking while limiting excessive polymer buildup**.** Final weight sequence: J1 > J3 > J4 > J2 > J0.

4.4.4 Analysis of Fabric Thickness

The thickness increases after chemical treatments compared to the raw fabric (J0). Maximum thickness in J1 (2.0 mm) due to polymer deposition from Bitumen + PR. The slightly lower thickness in irradiated samples (J2, J3, J4) suggests that γ-irradiation enhances crosslinking while reducing excessive polymer buildup. J3 shows high tensile strength despite having the thinnest coating, indicating that bonding quality matters more than layer thickness**.**

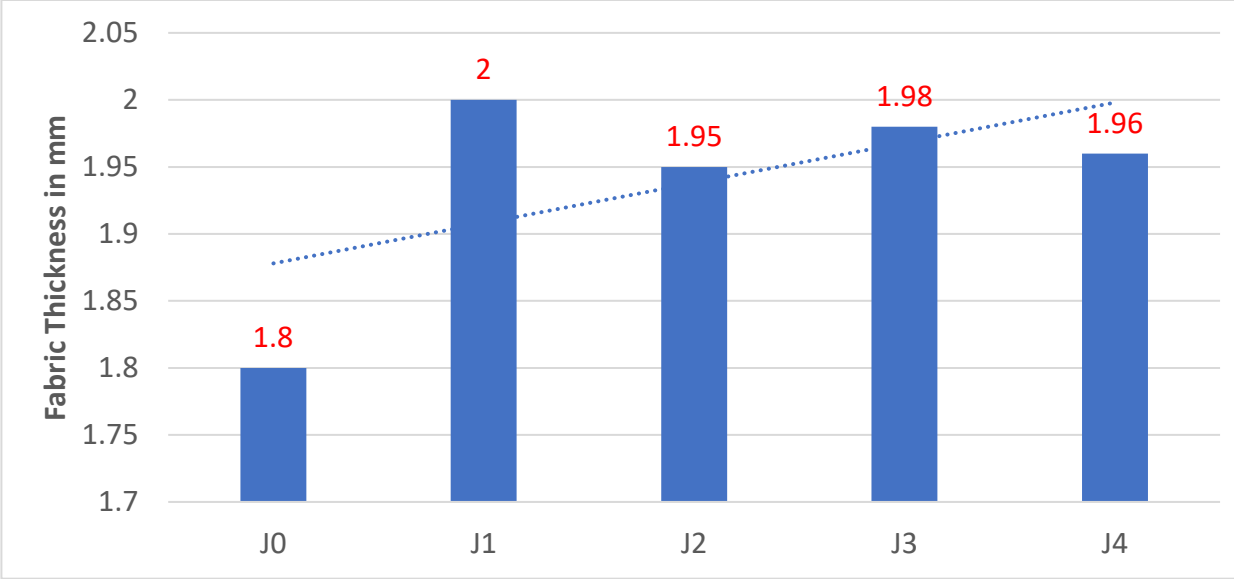

Figure 4.4. 3 Comparison of thickness.

4.4.5 Analysis of Moisture Regain, Moisture Content, and Water Uptake%

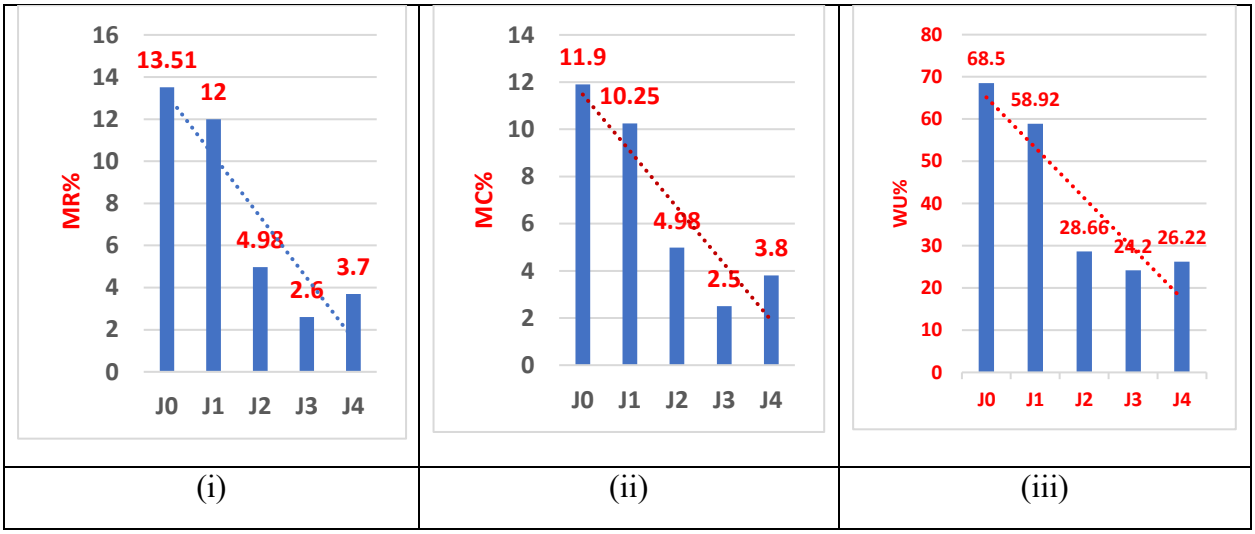

(i) (ii) (iii)

Figure 4.4. 4 Changes of (i) MR (moisture regain) %, (ii) MC (moisture content) %, and (iii) WU (water uptake) %.

This bar diagram illustrates the deviations in water absorbency of raw jute (UJF) and chemically treated jute (TJF) using the MR%, MC%, and WU% curves. HEMA-pre-treated jute fabric (J3) showed the lowest water absorbency percentage among J0, J1, J2, and J4. Combinable pre-treatment, polymer coating, and γ-irradiation gradually decrease the water absorption % and

increase the hydrophobicity of jute fabric by reducing the O-H groups of cellulose, but do not make it 100% hydrophobic.

Table 4.4. 2 Statistical analysis of data from correlation

Observation	TS in (kPa)	MR (%)	MC (%)	WU (%)
J0	49.81	13.51	11.9	68.5
J1	59.39	12	10.25	58.92
J2	67.39	4.98	4.98	28.66
J3	74.78	2.6	2.5	24.2
J4	69.87	3.7	3.8	26.22

Table 4.4. 3 Pearson correlation

Variables	Tensile strength	Moisture regains	Moisture Content	Water Uptake
Jute fabric	1	-.96144	-.97419	-.96001

-(.20-00)	Almost no correlation/very low
-(.21-.40)	Low Negative Correlation
-(.41-.60)	Moderate Negative Correlation
-(.61-.80)	High Negative Correlation
-(.81-1.00)	Perfect Negative Correlation

Pearson's Correlation table exhibits a correlation matrix. Here, we can see a perfect negative correlation between tensile strength and water absorbency. Including moisture regain (r = -.96144), moisture content (r =-97419) and water uptake (r =-.96001). This indicates that the hydrophilicity of the jute fabric decreases with chemical treatment, while its tensile strength increases.

4.4.6 Analysis of Surface Morphology

The SEM images of untreated and treated jute fabrics reveal clear morphological differences resulting from chemical modification and γ-irradiation.

The micrographs of raw jute fabric (Fig. ia and ib) show fibres with rough, uneven, and fibrillated surfaces. Noticeable gaps between adjacent fibre bundles indicate a loose and highly hydrophilic structure. The absence of any protective or binding layer exposes a large number of hydroxyl (–OH) groups on the cellulose surface, which contributes to high moisture absorption and relatively low tensile strength

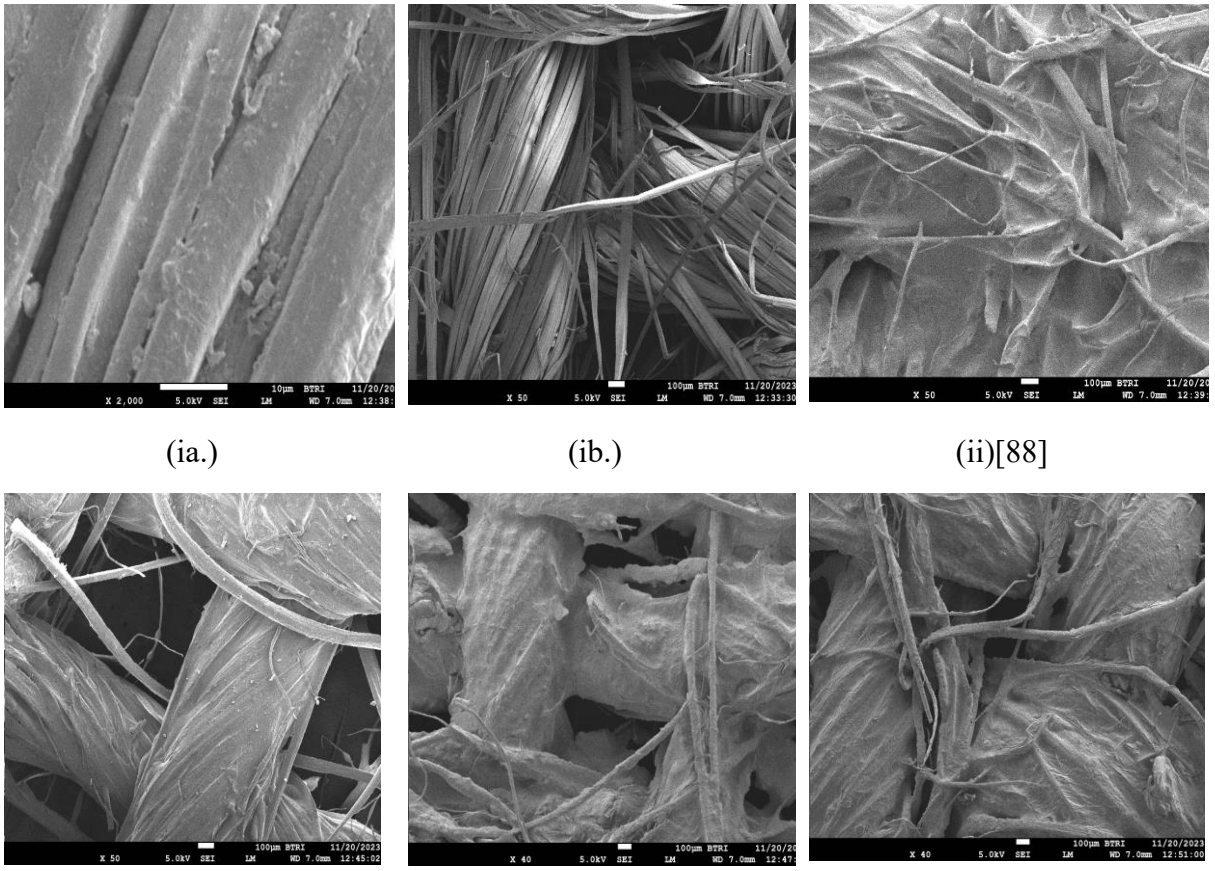

(ia.) (ib.) (ii)[88]

(iii)[88] (iv) (v)

Figure 4.4. 5 (ia.), (ib.) Raw jute fabric, (ii) bitumen +PR treated, (iii) bitumen + PR + γ irradiation (iv)HEMA+ Bitumen+ PR+ γ-radiation, (v) BP+ Bitumen+ PR+ γ-radiation.

After polymer treatment, the SEM images show the deposition of a polymeric film on the fibre surfaces. The coating makes the surfaces comparatively smoother and partially covers the exposed hydroxyl groups, thereby improving inter-fibre bonding, water resistance, and tensile properties. However, some voids remain between adjacent fibres, suggesting that the polymer coating does not completely fill the inter-fibre spaces.

The application of γ-irradiation further enhances the interaction between the polymer matrix and the cellulose structure of the jute fibres. Radiation-induced free radicals promote crosslinking between the unsaturated polyester resin and cellulose chains, thereby improving interfacial adhesion and stabilizing the composite structure. At the same time, excess polymer between neighbouring fibres is reduced, thereby preserving the fabric's intrinsic porosity.

The presence of controlled inter-fibre voids is beneficial for geotextile applications, as a certain degree of porosity is required for soil filtration, water drainage, and root penetration during vegetation growth in erosion control systems. Therefore, the treatment process does not aim to eliminate porosity entirely, but rather to optimise the balance between mechanical durability and functional permeability of the jute geotextile.

4.4.7 TGA Analysis

Thermogravimetric analysis (TGA) was carried out to evaluate the thermal stability of untreated jute fabric (UJF) and chemically treated jute fabrics (TJF).

In the temperature range below 100 °C, a small weight loss of approximately 2–5% is observed, which corresponds to the evaporation of physically absorbed moisture. Treated fabrics exhibit slightly lower weight loss in this region due to reduced hydrophilicity resulting from polymer coating and crosslinking.

A major degradation stage occurs between 200–300 °C, where untreated jute shows substantial weight loss (approximately 50–60%) due to the thermal decomposition of hemicellulose and cellulose. In contrast, the treated fabrics degrade more gradually because the cross-linked polymer networks formed by polyester resin, HEMA, and benzoyl peroxide (BP) provide additional thermal stability and delay the decomposition process.

At higher temperatures (350–500 °C), further degradation occurs mainly due to the decomposition of lignin and the breakdown of residual polymeric structures, leading to the formation of char. Among the treated samples, HEMA pre-treated jute fabric exhibits the highest thermal stability, as indicated by the slowest rate of weight loss, suggesting the formation of a relatively dense cross-linked network. The benzoyl peroxide pre-treated fabric also shows improved stability compared

with untreated jute, although its thermal resistance is slightly lower than that of the HEMA-treated sample.

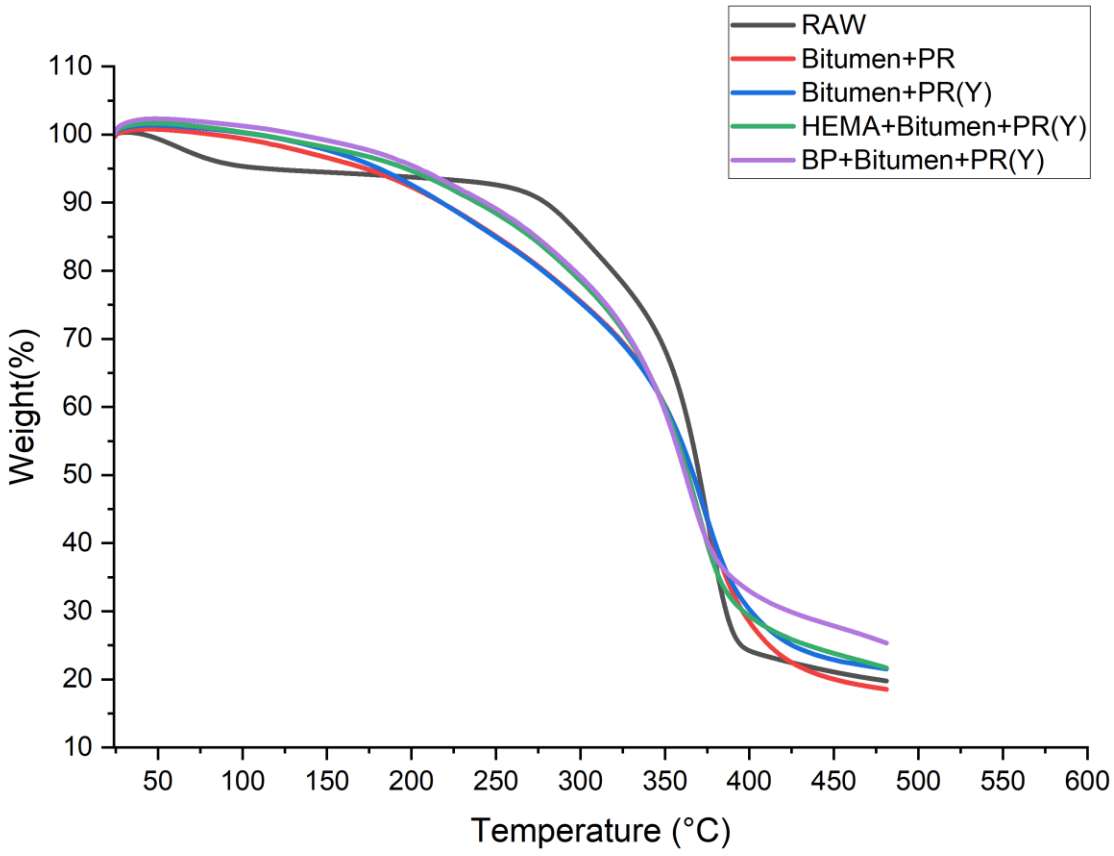

Figure 4.4. 6 Comparative thermogravimetric analysis (TGA) of untreated and chemically modified jute fabrics indicating thermal degradation behavior and stability.

Above 500 °C, treated fabrics retain a higher amount of residual char (approximately 20–25%), indicating improved char yield and enhanced thermal resistance. Overall, the results demonstrate that chemical modification and polymer crosslinking improve the thermal stability of jute fabrics while simultaneously reducing their hydrophilicity, which is advantageous for geotextile applications exposed to varying environmental conditions.

.

4.4.8 Antimicrobial Activity Assessment

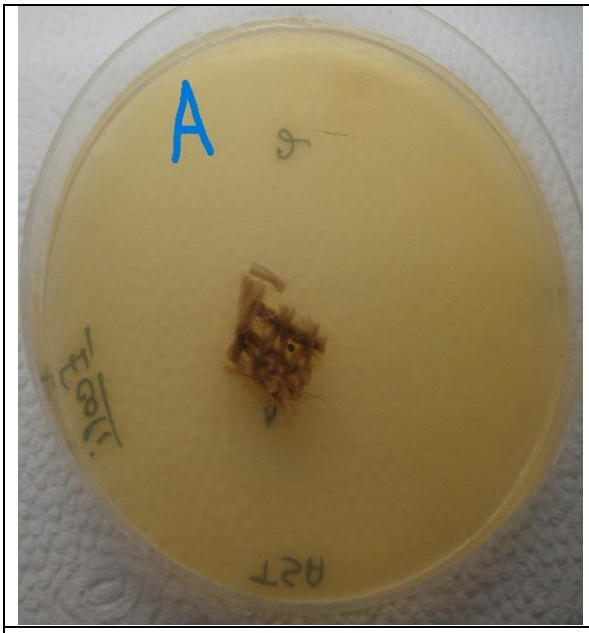

(i)[70]

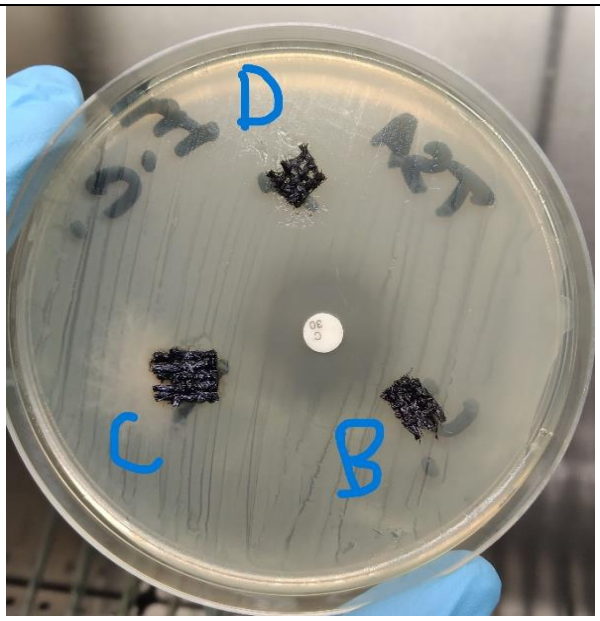

(ii)

Figure 4.4. 7 (i) raw jute fabric(A) (ii) Raw Jute+Bitumen+PR+ γ-radiation(B), Raw jute+HEMA+Bitumen +PR+ γ-radiation (C), Raw jute+ BP+Bitumen+PR+ γ-radiation (D**).**

Assessment of antimicrobial activity (Gram-positive Staphylococcus aureus)

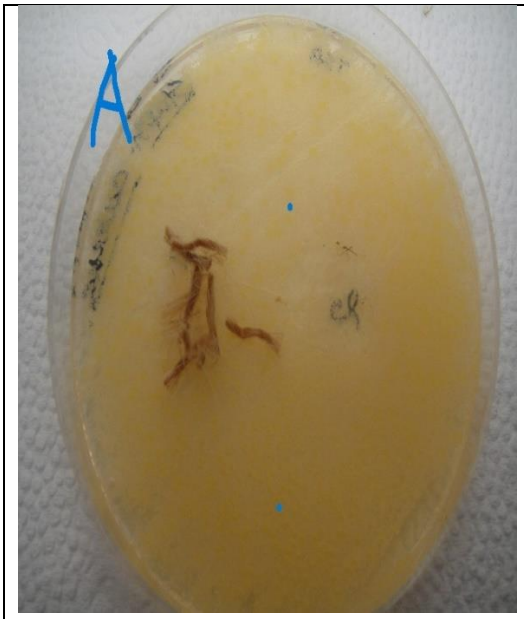

(i)[70]

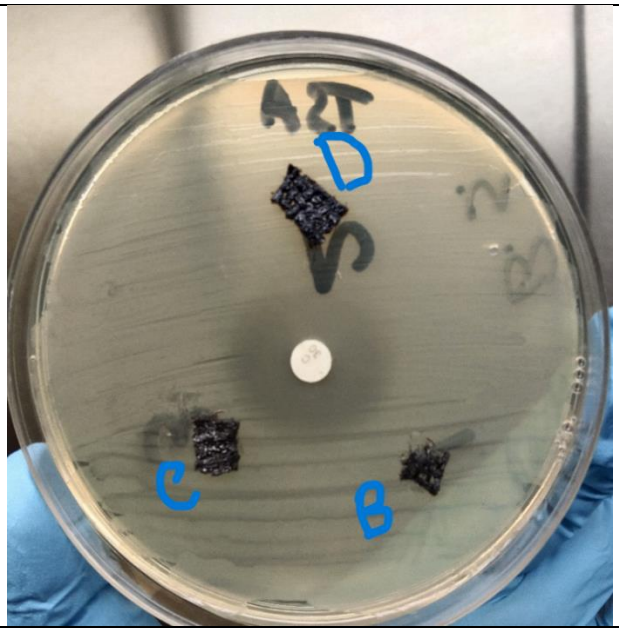

(ii)

Figure 4.4. 8 (i) raw jute fabric (A) (ii) Raw Jute+Bitumen+PR+ γ-radiation (B), Raw jute+HEMA+Bitumen +PR+ γ-radiation (C) Raw jute+ BP+Bitumen+PR+ γ-radiation (D).

Antimicrobial activity was evaluated using two bacterial strains: Gram-negative Escherichia coli and Gram-positive Staphylococcus aureus. From the above images, no bacterial inhibition was observed, suggesting that the antimicrobial properties of jute fabric or its modified form are not evident. Visible microbial growth was observed around or on the raw jute fabrics, indicating high moisture content and hydrophilicity, which make the fabrics prone to microbial attack. The chemically treated jute fabric surface appears darker and denser, possibly due to the polymer coating and crosslinking that occur after γ-radiation. Visible microbial growth is reduced, suggesting enhanced resistance due to chemical treatment and γ-radiation-induced crosslinking. Bitumen and polyester resin minimize water absorption, limiting microbial growth.

4.4.9. Analysis of Tensile Strength After Accelerated Weathering Test

After treatment, tensile strength increases due to polymerization, crosslinking, and coating effects**.** After 7, 14, and 28 days, all samples experience a slight loss of strength due to moisture absorption, environmental degradation, and microbial attack**.** However**,** treated samples (J2, J3, J4) retain higher strength compared to raw jute (J0).

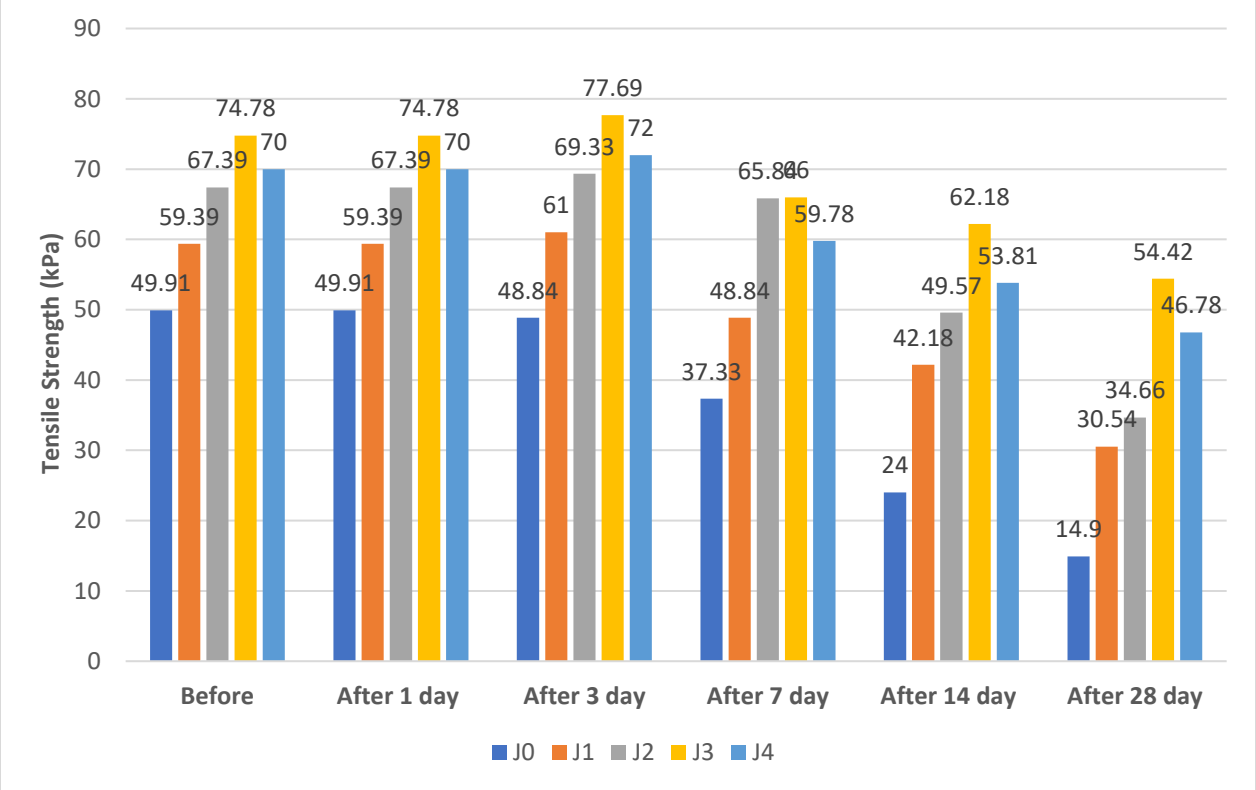

(a)

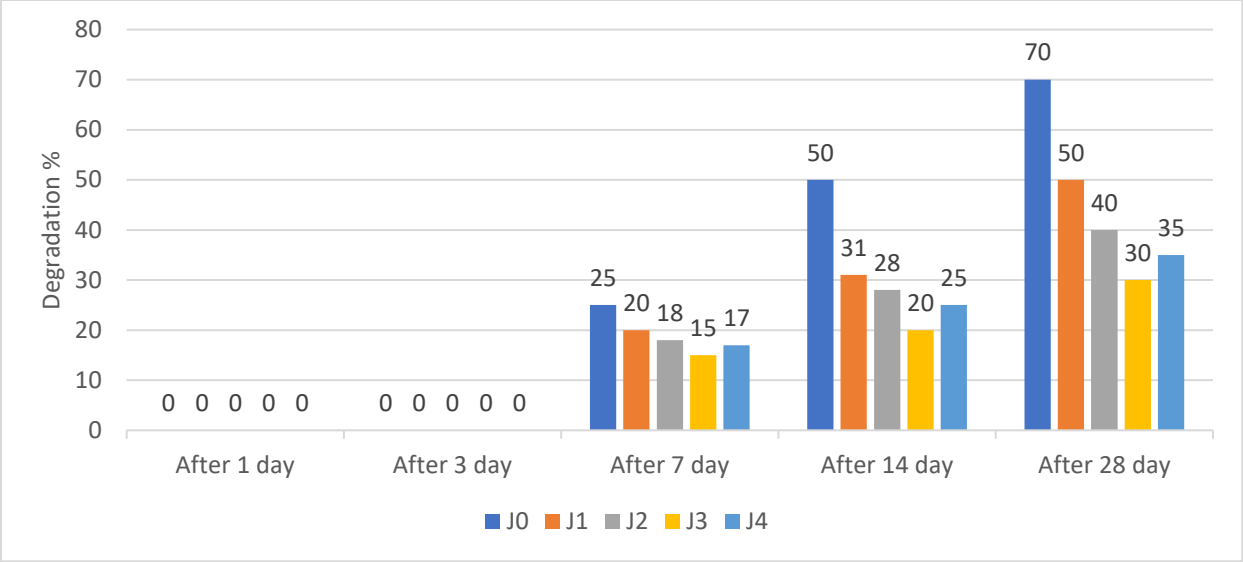

(b)

Figure 4.4. 9 (a) Loss of Tensile Strength (b)Strength Loss (%) after accelerated weathering exposure.

After 28 days, J3 and J4 still have significantly higher strength (54–46 kPa) than raw jute (14.9 kPa), confirming that the treatments substantially delay degradation**.** Chemical treatment combined with γ-radiation enhances tensile strength by cross-linking cellulose chains, reducing hydrophilicity, and forming a protective polymer matrix. Environmental exposure gradually reduces the strength of raw jute, but treated samples exhibit much slower degradation rates. The degradation percentage analysis shows that chemically treated and γ-irradiated jute fabrics exhibit superior durability compared to raw jute. The rapid strength loss in raw jute (J0) after 28 days (70%) is attributed to moisture absorption, microbial attack, and UV degradation of natural cellulose fibers. On the other hand, samples treated with bitumen, PR, and crosslinking agents such as HEMA and BP showed significantly lower degradation percentages due to:

1. Hydrophobic Coating: Bitumen and PR form a barrier that limits water penetration.
2. Crosslinking Effect: γ-radiation and reactive monomers (HEMA, BP) enhance molecular bonding, improving dimensional stability and weather resistance.
3. HEMA Advantage: The presence of vinyl groups in HEMA leads to higher crosslinking density, explaining why J3 retained tensile strength better than other treated samples.

4.4.10 Comparison of Weight After Accelerated Weathering Test

Chemically treated samples (J1–J4) showed significantly lower degradation percentages and slower weight loss throughout the weathering period. After 28 days, samples treated with bitumen,

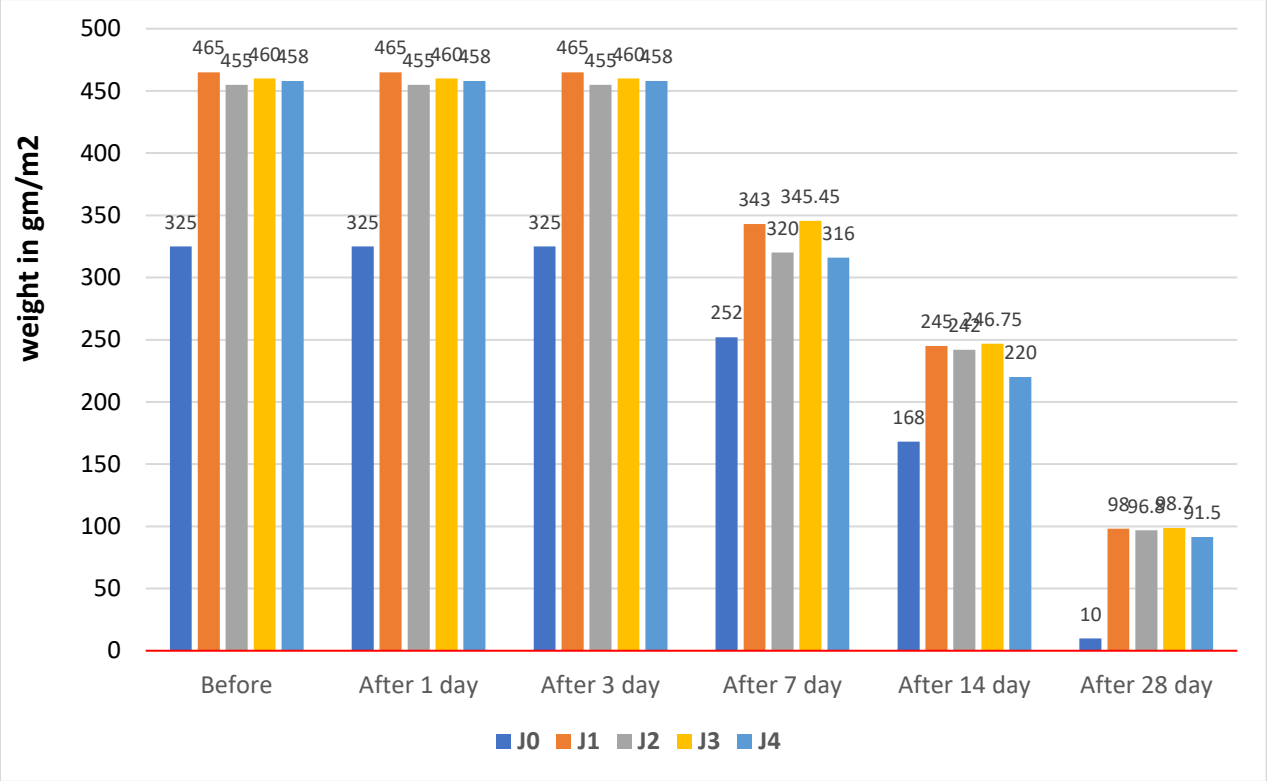

Figure 4.4. 10 Graphical analysis of fabric weight loss before and after weathering exposure.

Polyester resin (PR) and γ-radiation retained tensile strengths 30–40% higher than raw jute and greater residual weight, indicating improved structural integrity. Among all treatments, the HEMA + Bitumen + PR + γ-radiation (J3) sample performed best, with the lowest degradation (30%) and highest residual weight (~98 g/m²). The vinyl groups in HEMA provided additional reactive sites for free-radical polymerization, forming a denser, three-dimensional crosslinked network that imparted superior environmental stability. The incorporation of bitumen created a hydrophobic barrier. At the same time, γ-radiation enhanced crosslinking density by generating free radicals on both cellulose and polymer chains, thereby improving interfacial adhesion and reducing polymer leaching during weathering. As a result, treated fabrics exhibited greater tensile strength retention, reduced weight loss, and a longer service life than untreated raw jute.

4.4.11 Comparison of Thickness After Accelerated Weathering Test

Before weathering, treated fabrics showed higher initial thicknesses due to the polymer coating and crosslinking. After 1 and 3 days of weathering test, the thickness remains almost constant. No significant swelling or erosion occurs in the early stages of weathering. After 7 days, Polymer coatings slow down the thickness loss compared to raw jute. After 14 days, a sharp reduction

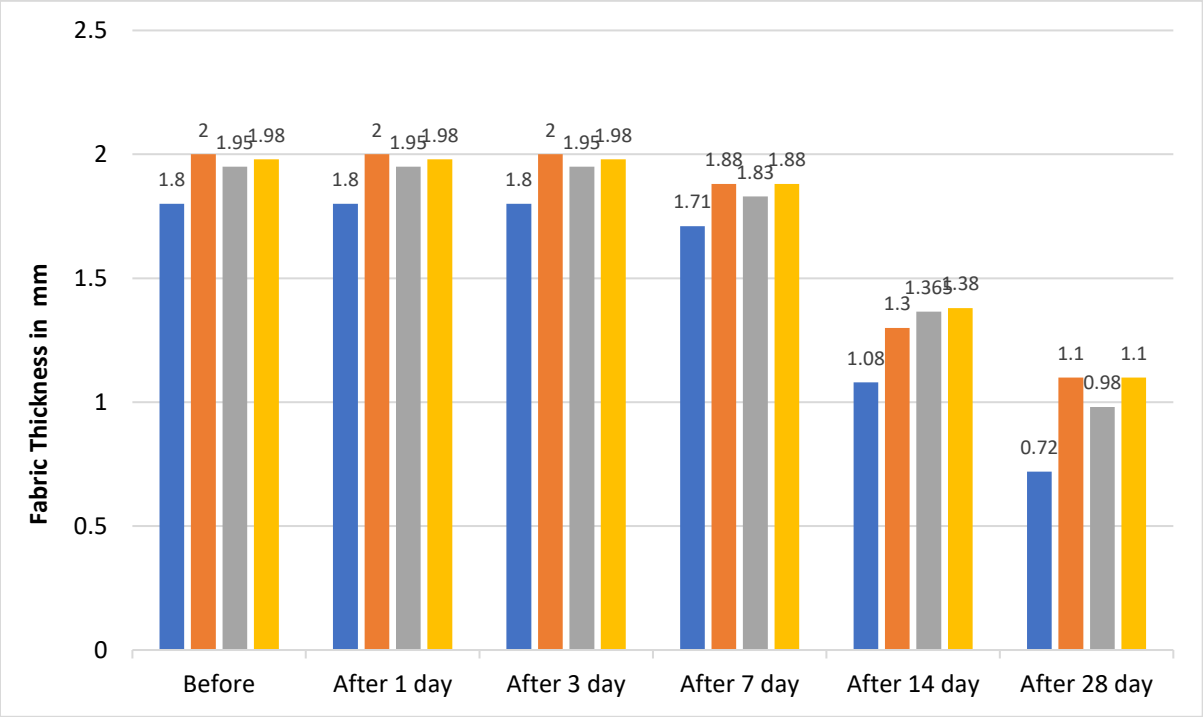

Figure 4.4. 11 Comparison of thickness before and after weathering exposure.

Raw jute fabric was the thickest, whereas modified jute fabric showed the best dimensional stability. After 28 days, severe weathering degradation was observed, and the modified jute fabric showed better resistance to weathering damage. The result is due to polymer deposition, which increases fabric thickness. Weathering exposure to UV radiation, water, temperature, etc. leads to fiber erosion, moisture swelling, and polymer leaching, resulting in a reduction in thickness. The γ-radiation crosslinking creates a dense network on cellulose surfaces, preventing rapid structural degradation. HEMA-pre-treated samples showed the most outstanding stability due to additional free-radical crosslinking sites, retaining better dimensional integrity even after 28 days.

4.4.12 Comparison of Cellulose Degradation from the FTIR Graph Before and After Accelerated Weathering Exposure

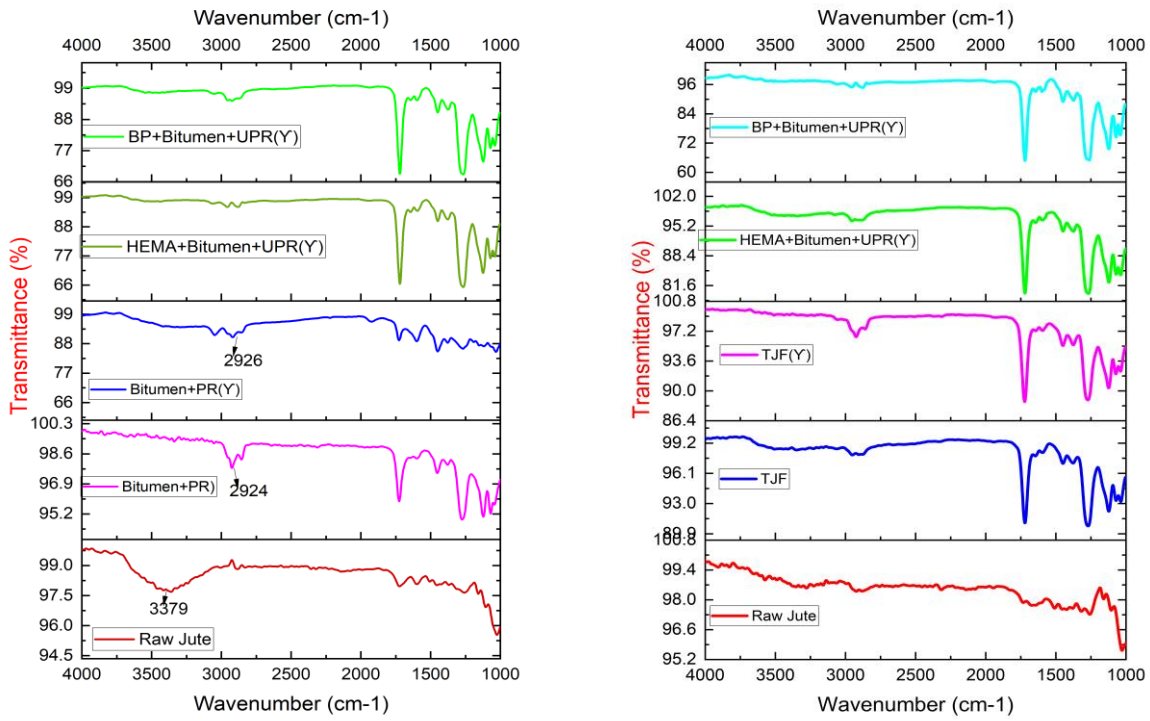

(a) **(b)**

Figure 4.4. 12 (a) FTIR graph of before weathering exposure, (b) FTIR graph of after weathering exposure.

Before weathering exposure: Raw jute fabric showed strong O–H and C–H peaks, indicating high cellulose hydroxyl content and, hence, high hydrophilicity. Treated jute fabric (bitumen, PR, HEMA, BP) exhibited additional peaks near 1720 cm^{-1} (C=O) and reduced O–H intensity, which suggests polymer coating and crosslinking over cellulose surfaces. Pre-treatment with HEMA- and BP showed the strongest ester and crosslinking peaks, confirming maximum chemical modification.

After weathering exposure: The Peaks become broader or weaker, indicating cellulose degradation and loss of hydroxyl groups due to UV/moisture exposure. The peaks of treated samples remain sharper, especially in pre-treated fabrics with HEMA and BP, confirming better structural stability and resistance to hydrolytic/oxidative degradation. Minor peak shifts suggest photo-oxidation, but crosslinked networks limit structural breakdown compared to untreated jute. After weathering, treated fabrics retain most functional groups, while raw jute loses intensity due

to chain scission, oxidation, and depolymerization. HEMA- and BP pre-treated fabrics provide maximum resistance because of higher crosslinking density and hydrophobic barriers**.**

4.4.13 XRD-Analysis Before and After Weathering Exposure

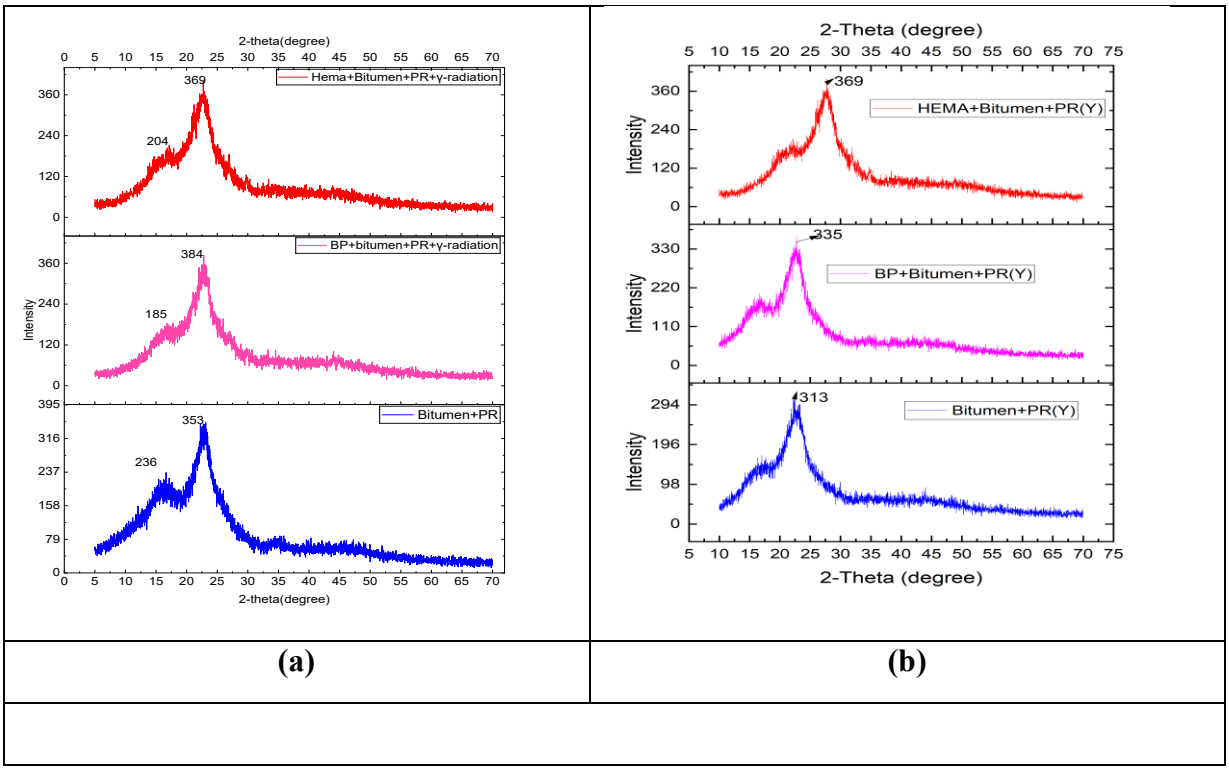

(a) **(b)**

Figure 4.4. 13 (a)XRD graph before weathering exposure (b) XRD graph after weathering exposure.

XRD analysis before weathering exposure revealed prominent peaks at 2θ = 16–17° and 22–23°, representing the cellulose I crystalline structure in jute composites. After weathering exposure, peak intensities decreased significantly, and amorphous background intensity increased, indicating degradation of crystalline cellulose domains due to UV radiation, oxidative stress, and moisture attack. HEMA-pre-treated samples exhibited better retention of crystallinity than BP-pre-treated and Bitumen-treated samples, suggesting enhanced structural stability and resistance to environmental degradation. Before weathering, all treated samples showed higher crystallinity, more potent mechanical properties, and better dimensional stability. After weathering, reduced crystallinity, increased amorphous content, lower strength, and higher degradation rate. Peak intensities drop significantly for all samples after weathering, due to UV degradation, oxidative reactions, and moisture penetration during environmental exposure.

4.4.15 Some Photographs of this Research Work

In this research, some practical work photographs were preserved for proper documentation. The following pictures are important for this [70-71].

		
Raw jute fabric	Pre-treatment of jute fabric	Drying at dryer
		
Mixing of BE and UPR	Padding the samples	Sample at AWE tester
		
Treated jute fabric	Buried the sample	Raw jute fabric after 45 days buried

		
Tree plantation over the buried sample	Treated jute fabric after 120 days buried	Treated jute fabric after 28 days at the AWE testing machine

4.5 Cost Analysis

Although the research was conducted in a laboratory, it required small quantities of different chemicals; as a result, the treatment cost per kg or per meter of jute fabric could not be calculated. The individual cost of chemicals is given below-

Table 4.5. 1 The cost of raw materials and different chemicals individually

Materials	**Price**
Jute Fabric	120/yards
Bitumen	190/kg
PR	280/lit
MEKP	950/Kg
Cobalt Naphthenate	1400/lit
Benzoyl peroxide	2500/kg
NaOH	352/kg
Methanol	3474/lit
Styrene monomer	200/kg
Acetic acid	1500/lit
Aceton	2800/lit
HEMA	3500/lit

Chapter 5: Conclusion

5.1 Conclusion

The capabilities of jute fabric exceed those of other natural fibres for use in geotechnical applications, enabling it to replace synthetic fibres. In comparison, synthetic fibres are used across all geotextile applications. The main limitation of jute fabric for geotechnical purposes is its low durability and environmental degradation from moist air and microorganisms. The potential use of jute fibre in geotechnical applications, such as soil erosion control, reinforcement, and slope stabilization, to improve the durability and mechanical performance of jute fabric is vital.

Surface modification of jute fabric is crucial for its use in geotechnical applications. This research work enhances the durability of jute fabric through surface modification using a pre-treatment process, chemical, and gamma radiation. Chemical treatment of jute fabric over pre-treated jute fabric by bitumen emulsion and unsaturated polyester resin with gamma radiation is a new concept. Satisfactory results were obtained following the research work. The research work was completed in four steps to better explain the results. In the first step, raw jute fabric was treated with bitumen emulsion and unsaturated polyester resin. Four formulations were prepared by mixing with bitumen emulsion and polyester resin at different percentages for the chemical modification of jute fabric. Chemically treated jute fabric TJF2 (30% bitumen emulsion and 10% UPR) demonstrated better durability properties than untreated jute fabric and other chemically treated jute fabrics, which were measured by the soil burial test. FTIR, XRD, and TGA analysis confirm the crosslinking of jute fabric cellulose with the polymer coating, which reduces the -OH groups of jute fabric cellulose. In the second step, gamma radiation was applied to the chemically treated jute fabric (TJF2) at various doses (2.5, 5, 7.5 and 10 kGy). Gamma radiation generates free radicals that facilitate polymerization through crosslinking; however, excessive gamma radiation can disrupt the chemical structure of the jute fabric. Applying 5 kGy gamma radiation to the chemically treated jute fabric resulted in better durability properties than the untreated samples, the chemically treated samples, and other radiated samples. The analysis of water absorbency, tensile strength, FTIR, XRD, and TGA, which ensures the more crosslinking of jute fabric cellulose with polymer coating, and the reduction of hydroxyl (OH) group from jute fibre cellulose, and the durability of jute fabric were measured by the soil burial test and the effect of gamma radiation. In the third step, the raw jute fabric was pre-treated in two different ways. Pre-treatment of raw jute fabric before surface modification with a polymer coating also plays a crucial role in enhancing its tensile strength and durability by reducing hydroxyl groups and accelerating

crosslinking. Two different pre-treatment processes were employed, and each had a significant effect on surface modification. Jute fabric was pre-treated with benzoyl peroxide over mercerized jute fabric, and another pre-treatment by HEMA with benzoyl peroxide. HEMA-pre-treated jute fabric showed good durability properties and higher tensile strength among all the treated and raw samples. Durability tests were conducted using an accelerated weathering tester. FTIR, XRD, and TGA analyses confirm that the pretreatment process enhances crosslinking of the jute fabric with the polymer coating. Finally, antimicrobial activity assessment confirmed the control of direct microbial attack of treated jute fabric. The accelerated weathering test provides greater exposure to weathering conditions than natural conditions. This investigation measures the durability properties using an accelerated weathering tester and compares them with those under outside weathering conditions. Gamma radiation treatment and pre-treatment of jute fabric improve its tensile strength by lowering water absorption and reducing the -OH group from jute fabric cellulose. The percentage increase in tensile extension of raw jute fabric is higher than that of treated fabric, reaching up to 50%. The durability test also showed better results than raw jute fabric; raw jute fabric deteriorates within 40-60 days, while treated jute fabric remains intact for 3 months. The accelerated weathering test followed a similar trend to the soil burial durability test. After 28 days of weathering exposure, the percentage of strength loss in HEMA-pre-treated jute fabric (J3) is the lowest at 30%, whereas raw jute fabric experienced a maximum 70% loss in strength. The HEMA-pre-treated samples(J2) showed a minimum 30% loss.

This study confirmed that the combined treatment of jute fabric by chemical and gamma radiation reduced the water absorbency properties, such as moisture regain, moisture content, and water uptake percentage, which significantly improve the durability properties of jute fabric and also decrease the microbial attack and environmental damage. As a result, the barrier to the potential use of jute fabric for geo-technical purposes, such as soil erosion control, slope stabilization, and temporary reinforcement of soil structure, has been reduced.

5.2 Key Findings of the Study

The major outcomes of this research work are given below:

1. The surface modification of jute fabric by bitumen emulsion and unsaturated polyester resin has significantly improved the durability properties of jute fabric compared to raw jute fabric.
2. Gamma radiation promotes cross-linking between the polymer mixture and jute fibres by creating free radicals, which improve the mechanical performance of the jute fabric.
3. Low and excess doses of gamma radiation do not enhance the cross-linking. Optimal gamma radiation dose: 5 kGy irradiated samples showed the greatest improvement in the mechanical properties of jute fabric compared to raw jute fabric.
4. Pre-treatment of jute fabric significantly improves the mechanical and durability properties of jute fabric. HEMA-pre-treated jute fabric showed a significant improvement over other treated and raw jute fabrics.
5. Durability test by soil burial and accelerated weathering tester confirms the structural stability of treated jute fabric over raw jute fabric.

5.3 Research Contribution

This study promotes the sustainable development of jute geotextiles by recommending an effective method to improve durability and mechanical properties by reducing the number of OH groups in jute fabric cellulose. In this research, a combined chemical and gamma radiation treatment of jute fabric is used to enhance its mechanical properties for geotechnical applications.

This work identifies the optimal chemical formulation and radiation dose that improve mechanical properties without damaging the jute fibre. In addition to different pre-treatment processes, which also enhance durability by generating free radicals and extending the cross-linking of jute fabric cellulose with chemicals. HEMA-based pretreatment significantly improves durability by enhancing mechanical properties and reducing water absorption. The durability of treated jute fabric was evaluated by soil burial test and accelerated weathering exposure.

5.4 Practical Implications for Geo-Textile Applications

The development of durable natural fibers, such as jute, for use in geotextiles contributes to sustainable development and reduces reliance on synthetic fibers in geotechnical applications. On

the other hand, the practical use of jute geotextile is environmentally and economically safe, particularly in countries where jute is abundantly available.

This research suggests that the treated jute fabric has significant practical use for jute geotextiles in geo-textile engineering applications, as it is biodegradable and environmentally safe. The improved mechanical properties, like tensile strength, durability, and low water absorption ability of treated jute, are suitable for soil erosion control, riverbank protection, subgrade reinforcement, and slope stabilization.

5.5 Limitations of the Study

Despite the promising results obtained in this research, several limitations were encountered.

Due to time and financial constraints, large-scale production and field-level testing of treated jute fabrics could not be conducted. The experimental samples were produced at the laboratory scale, limiting the ability to conduct full-scale cost analyses and practical installation studies.

Only plain-woven jute fabric was used in this investigation due to the limited availability of laboratory weaving equipment capable of producing different weave structures. In addition, different yarn counts could not be investigated, which may also influence mechanical performance.

Another limitation concerned SEM characterization. Due to the temporary unavailability of the scanning electron microscope, detailed pore-size measurements could not be obtained for all samples, although qualitative surface-morphology observations were performed on selected samples.

5.6 Recommendations for Future Research

This study offers a solution to enhance the durability of jute fabric, paving the way for the application of jute geo-textile. Though the experimental results were satisfactory, it would be better to bury the samples for 6 to 12 months.

Here, only γ-radiation is used to enhance the durability of jute fabric; comparative results will be obtained on the increase in durability when UV radiation is used.

This work has been carried out only in plain weave; other woven fabric structures could be used. I hope that, in the future, knitted and nonwoven fabrics can also be used for specific geo-textile applications.

Finally, large-scale production, practical field applications, and economic feasibility studies will be important for the practical implementation of the modified jute fabric in the real engineering sector.

References

[1] B. V. Wiewel and M. Lamoree, "Geotextile composition, application and ecotoxicology—A review," Nov. 05, 2016, *Elsevier B.V.* doi: 10.1016/j.jhazmat.2016.04.060.

[2] A. Rawal, T. Shah, and S. Anand, "Geotextiles: Production, properties and performance," *Textile Progress*, vol. 42, no. 3, pp. 181–226, Sep. 2010, doi: 10.1080/00405160903509803.

[3] S. C. Das, D. Paul, M. M. Fahad, T. Islam, and H. Nizam, "Geotextiles-A Potential Technical Textile Product," *Journal of Scientific and Engineering Research*, vol. 4, no. 10, pp. 337–350, 2017, [Online]. Available: www.jsaer.com

[4] M. H. Islam, M. R. Islam, M. Dulal, S. Afroj, and N. Karim, "iScience The effect of surface treatments and graphene-based modifications on mechanical properties of natural jute fiber composites: A review," *cell press*, Jan. 2022, doi: 10.1016/j.isci.

[5] H. A. H. Khan, M. A. Hossain, M. A. Khan, and R. A. Khan, "Effect of chemical modification of jute fabrics on the performance of urethane acrylate-based composites," *Journal of Reinforced Plastics and Composites*, vol. 29, no. 13, pp. 2027–2036, Jul. 2010, doi: 10.1177/0731684409341761.

[6] M. A. Khan, J. M. M. Islam, M. Arifur Rahman, R. A. Khan, and T. Islam, "Study on the effect of urea on the mechanical and morphological properties of jute/gelatin composites," *Polymer - Plastics Technology and Engineering*, vol. 49, no. 9, pp. 885–891, Jun. 2010, doi: 10.1080/03602551003681820.

[7] M. A. Khan, R. A. Khan, M. H. Rashid, and A. N. M. H. Kabir, "Modification and characterization of bio-blend of jiga resin/starch with vinyltrimethoxy silane by UV-radiation," *Polymer - Plastics Technology and Engineering*, vol. 48, no. 8, pp. 781–787, Aug. 2009, doi: 10.1080/03602550902824697.

[8] A. Khan, T. Huq, M. Saha, R. A. Khan, and M. A. Khan, "Surface modification of calcium alginate fibers with silane and methyl methacrylate monomers," *Journal of Reinforced Plastics and Composites*, vol. 29, no. 20, pp. 3125–3132, Oct. 2010, doi: 10.1177/0731684410367534.

[9] Khan M, Islam jahid, jubayer abdullah, and Rahman md, "Modification of jute fibers by radiation induced graft copolymerisation and their application," in *Cellulose-Based Graft Copolymers*, CRC Press, 2015, pp. 166–185. doi: 10.1201/b18390-12.

[10] M. F. Mina, M. H. S. Shohrawardy, M. A. Khan, A. K. M. M. Alam, and M. D. H. Beg, "Improved mechanical performances of triple super phosphate treated jute-fabric reinforced polypropylene composites irradiated by gamma rays," *J. Appl. Polym. Sci.*, vol. 130, no. 1, pp. 470–478, Oct. 2013, doi: 10.1002/app.39120.

[11] M. A. Khan, R. A. Khan, B. S. Aliya, and Z. Nasreen, "Effect of the pretreatment with UV and gamma radiations on the modification of plywood surface by photocuring with epoxy

acrylate," *J. Polym. Environ.*, vol. 14, no. 1, pp. 111–118, Jan. 2006, doi: 10.1007/s10924-005-8713-z.

[12] H.Kazemi Esfeh, B Ghanavati, and R shojaei Arani, "The Factors Affecting on Bitumen Emulsion properties," *International conferrence on Chemistry and Chemical Engineering*, 2010.

[13] A. A. Athawale and J. A. Pandit, "Unsaturated polyester resins, blends, interpenetrating polymer networks, composites, and nanocomposites: State of the art and new challenges," in *Unsaturated Polyester Resins: Fundamentals, Design, Fabrication, and Applications*, Elsevier, 2019, pp. 1–42. doi: 10.1016/B978-0-12-816129-6.00001-6.

[14] S. Manivannan, P. S. Khola, K. Kannan, P. K. Choudhury, and V. Kasthuri Thilagam, "National Jute Board," 2018.

[15] R. Ram, J. P. Shukla, E. Peters, S. Choudhary, and K. Prasad, "Application of Geotextiles in Erosion Control-A Field Experiment."

[16] V. K. Kaushik, A. Kumar, and S. Kalia, "Effect of Mercerization and Benzoyl Peroxide Treatment on Morphology, Thermal Stability and Crystallinity of Sisal Fibers," *International Journal of Textile Science*, vol. 1, no. 6, pp. 101–105, Jan. 2013, doi: 10.5923/j.textile.20120106.07.

[17] A. J. Khan, M. S. Islam, and S. S. Islam, "Laboratory Assessment of Soil-Jute Geotextile Interaction Behavior." [Online]. Available: https://www.researchgate.net/publication/270885052

[18] F. Sarker, P. Potluri, S. Afroj, V. Koncherry, K. S. Novoselov, and N. Karim, "Ultrahigh Performance of Nanoengineered Graphene-Based Natural Jute Fiber Composites," *ACS Appl. Mater. Interfaces*, vol. 11, no. 23, pp. 21166–21176, Jun. 2019, doi: 10.1021/acsami.9b04696.

[19] C. A. Correia, L. M. De Oliveira, and T. S. Valera, "The influence of bleached jute fiber filler on the properties of vulcanized natural rubber," in *Materials Research*, Universidade Federal de Sao Carlos, 2017, pp. 472–478. doi: 10.1590/1980-5373-mr-2017-0126.

[20] M. J. Miah, M. A. Khan, and R. A. Khan, "Fabrication and Characterization of Jute Fiber Reinforced Low Density Polyethylene Based Composites: Effects of Chemical Treatment," *Journal of Scientific Research*, vol. 3, no. 2, pp. 249–259, Apr. 2011, doi: 10.3329/jsr.v3i2.6763.

[21] N. Akter, S. C. Das, M. M. Fahad, D. Islam, M. A. Khan, and S. M. Shamsuddin, "Tailoring the performance of cellulosic textiles by chemical treatment and ionizing radiation: Assessment of physical, mechanical, thermal, crystal and morphological properties," *Next Materials*, vol. 7, Apr. 2025, doi: 10.1016/j.nxmate.2024.100372.

[22] M. H. S. Shohrawardy, M. K. Alam, M. F. Mina, and M. A. Khan, "Fabrication of strong and thermally more stable jute fabric/polypropylene composites by compression molding

along with γ-ray irradiation," *Polymer Bulletin*, vol. 71, no. 5, pp. 1219–1239, 2014, doi: 10.1007/s00289-014-1120-7.

[23] M. K. Gupta, R. K. Srivastava, H. Bisaria, M. K. Gupta, and R. K. Srivastava, "Potential of Jute Fibre Reinforced Polymer Composites: A review," *International Journal of Fiber and Textile Research*, vol. 5, no. 3, pp. 30–38, 2015, [Online]. Available: http://www.urpjournals.com

[24] H. N. Dhakal and S. O. Ismail, "Unsaturated polyester resins: Blends, interpenetrating polymer networks, composites, and nanocomposites," in *Unsaturated Polyester Resins: Fundamentals, Design, Fabrication, and Applications*, Elsevier, 2019, pp. 181–198. doi: 10.1016/B978-0-12-816129-6.00008-9.

[25] H. U. Zaman, M. A. Khan, and R. A. Khan, "Improvement of mechanical properties of jute fibers-polyethylene/polypropylene composites: Effect of green dye and UV radiation," *Polymer - Plastics Technology and Engineering*, vol. 48, no. 11, pp. 1130–1138, 2009, doi: 10.1080/03602550903147262.

[26] M. Ahmad Khan *et al.*, "Mechanical and electrical properties of photocured jute fabric with 2-Hydroxy Ethylacrylate," *Fibers and polymers*, vol. 11, no. 3, pp. 391–397, 2010.

[27] M. A. Khan, R. A. Khan, H. U. Zaman, M. Noor-A Alam, and M. A. Hoque, "Effect of surface modification of jute with acrylic monomers on the performance of polypropylene composites," *Journal of Reinforced Plastics and Composites*, vol. 29, no. 8, pp. 1195–1205, Apr. 2010, doi: 10.1177/0731684409103147.

[28] H. U. Zaman, M. A. Khan, R. A. Khan, M. Z. I. Mollah, S. Pervin, and M. Al-Mamun, "A comparative study between gamma and UV radiation of jute fabrics/polypropylene composites: Effect of starch," *Journal of Reinforced Plastics and Composites*, vol. 29, no. 13, pp. 1930–1939, Jul. 2010, doi: 10.1177/0731684409343325.

[29] F. Tanasă, M. Nechifor, M. Mauru¸sa-Elena Ignat, and C.-A. Teacă, "Geotextiles-A Versatile Tool for Environmental Sensitive Applications in Geotechnical Engineering," 2022, doi: 10.3390/textiles.

[30] H. U. Zaman, M. A. Khan, and R. A. Khan, "Surface modification of jute fabrics using acrylic monomers: Effect of additives," *International Journal of Polymeric Materials and Polymeric Biomaterials*, vol. 60, no. 10, pp. 754–765, Sep. 2011, doi: 10.1080/00914037.2010.551360.

[31] S. K. Ghosh, R. Bhattacharyya, M. M. Mondal, P. K. Choudhury, and T. Sanyal, "Design and development of woven jute geotextiles for potential applications in the field of geotechnical constructions," *Journal of the Textile Institute*, vol. 106, no. 5, pp. 550–563, May 2015, doi: 10.1080/00405000.2014.929272.

[32] V. Dr. Krishna Kumar and N. Dr. Gokarneshan, "A review of some significant trends in geotextiles," *International Journal of Research in Engineering and Science (IJRES) ISSN*, vol. 09, no. 10, pp. 62–71, 2021, [Online]. Available: www.ijres.org

[33] J. G. Zornberg and N. Thompson, “Title and Subtitle Application Guide and Specifications for Geotextiles in Roadway Type of Report and Period Covered Technical Report,” 2007. [Online]. Available: www.ntis.gov.

[34] J. R. Ajmeri and C. J. Ajmeri, “Developments in nonwoven as geotextiles,” *Advances in Technical Nonwovens*, pp. 339–363, Jun. 2016, doi: 10.1016/B978-0-08-100575-0.00012-7.

[35] E. M. Palmeira and R. J. C. Farias, “Geotextile performance as barriers for erosion control.”

[36] A. Daniel Supervisor, D. Kalumba Co-supervisor, L. Nolutshungu Co-supervisor, and J. Oriokot, “UNIVERSITY OF CAPE TOWN FACULTY OF ENGINEERING AND BUILT ENVIRONMENT Department of Civil Engineering An Investigation into the Effects of Asperities on Geomembrane/Geotextile Interface Shear Characteristics.”

[37] T. Sanyal and A. K. Khastagir, “PREPONDERANCE OF JUTE AS GEOTEXTILES,” 2012.

[38] U. Datta, “Application of Jute geotextiles,” *Journal of Natural Fibers*, vol. 4, no. 3, pp. 67–82, 2007, doi: 10.1300/J395v04n03_05.

[39] Khan Mubarak A *et al.*, “Mechanical and Electrical Properties of Photocured Jute Fabric with 2-Hydroxy Ethacrylate,” *Fibers and polymers*, vol. 11, no. 3, pp. 391–397, Jun. 2010, doi: 10.1007/s12221-010-0391-3.

[40] M. H. S. Shohrawardy, M. K. Alam, M. F. Mina, and M. A. Khan, “Fabrication of strong and thermally more stable jute fabric/polypropylene composites by compression molding along with γ-ray irradiation,” *Polymer Bulletin*, vol. 71, no. 5, pp. 1219–1239, 2014, doi: 10.1007/s00289-014-1120-7.

[41] P. Biswal[1], N. Patel[2], A. K. Samal[3], and M. Rao, “INVESTIGATION ON MECHANICAL PROPERTIES OF PONDASH/NATURAL FIBER BASED GEOPOLYMERIC PRODUCTS,” *International Journal of Research and Analytical Reviews*, 2019, [Online]. Available: www.ijrar.org

[42] A. K. Bledzki and J. Gassan, “Composites reinforced with cellulose based fibres,” *Prog. Polym. Sci.*, vol. 24, no. 2, pp. 221–274, May 1999, doi: 10.1016/S0079-6700(98)00018-5.

[43] Mohanty K. Amar, Misra Manjusri, and Drzal T. Lawrence, “NATURAL FIBERS, BIOPOLYMERS, AND BIOCOMPOSITES,” Boca Raton, Apr. 2005. doi: https://doi.org/10.1201/9780203508206.

[44] D. U. Shah, “Developing plant fibre composites for structural applications by optimising composite parameters: A critical review,” Sep. 2013. doi: 10.1007/s10853-013-7458-7.

[45] D. Ray, B. K. Sarkar, A. K. Rana, and N. R. Bose, “The mechanical properties of vinylester resin matrix composites reinforced with alkali-treated jute fibres,” *Compos.*

Part A Appl. Sci. Manuf., vol. 32, no. 1, pp. 119–127, Jan. 2001, doi: 10.1016/S1359-835X(00)00101-9.

[46] H. M. Feroz, J. Nahar, and M. Rahman, "ECO-FRIENDLY JUTE PROCESSING IN BANGLADESH," 2011.

[47] M. K. Biswas, M. Ridwan-Ul-Risty, and A. Datta, "A proposal of sustainable and integrated plant for jute fiber extraction in an eco-friendly manner," *Int. J. Sci. Eng. Res.*, vol. 10, no. 1, 2019, [Online]. Available: http://www.ijser.org

[48] A. Ali *et al.*, "Effect of jute fibre treatment on moisture regain and mechanical performance of composite materials," in *IOP Conference Series: Materials Science and Engineering*, Institute of Physics Publishing, Nov. 2017. doi: 10.1088/1757-899X/254/4/042001.

[49] L. Solhi *et al.*, "Understanding Nanocellulose-Water Interactions: Turning a Detriment into an Asset," Mar. 08, 2023, *American Chemical Society*. doi: 10.1021/acs.chemrev.2c00611.

[50] S. Sheikh, K. Hirogaki, S. Irie, and K. Nakane, "Preparation and characterization of jute cellulose nanocrystals using tetrabutylammonium fluoride and dimethyl sulfoxide solutions," *SPE Polymers*, vol. 6, no. 1, Jan. 2025, doi: 10.1002/pls2.10168.

[51] J. Gassan and A. K. Bledzki, "Thermal Degradation of Flax and Jute Fibers," 2001.

[52] M. Mozetič, "Surface modification to improve properties of materials," Feb. 01, 2019, *MDPI*. doi: 10.3390/MA12030441.

[53] P. Fabbri and M. Messori, "Surface Modification of Polymers: Chemical, Physical, and Biological Routes," in *Modification of Polymer Properties*, Elsevier Inc., 2017, pp. 109–130. doi: 10.1016/B978-0-323-44353-1.00005-1.

[54] G. A. El-Awadi, "Review of effective techniques for surface engineering material modification for a variety of applications," *AIMS Mater. Sci.*, vol. 10, no. 4, pp. 652–692, 2023, doi: 10.3934/MATERSCI.2023037.

[55] F. Fioresi, "Surface modification of different materials for biological and environmental applications." [Online]. Available: https://theses.hal.science/tel-03141546v1

[56] P. Panda and R. Mohapatra, "Transforming Polymers: Innovative Physical and Chemical Modification Techniques for Advanced Functional Applications," 2025, *Bentham Science Publishers*. doi: 10.2174/0118756298367223250112224739.

[57] S. K. Nemani *et al.*, "Surface Modification of Polymers: Methods and Applications," Dec. 21, 2018, *Wiley-VCH Verlag*. doi: 10.1002/admi.201801247.

[58] "POLITECNICO DI MILANO Metallization of Polymeric Substrates via Physical Vapor Deposition," 2017.

[59] S. Ebnesajjad and R. A. Morgan, “Use of Fluorinated Additives in Coatings,” in *Fluoropolymer Additives*, Elsevier, 2012, pp. 157–174. doi: 10.1016/b978-1-4377-3461-4.00009-x.

[60] A. Konijnenberg, A. Butterer, and F. Sobott, “Native ion mobility-mass spectrometry and related methods in structural biology,” Jun. 2013. doi: 10.1016/j.bbapap.2012.11.013.

[61] J. Moore, “ChemPRIME.” [Online]. Available: https://chem.libretexts.org/@go/page/241506

[62] I. Obodovskiy, “Nuclei and Nuclear Radiations,” in *Radiation*, Elsevier, 2019, pp. 41–62. doi: 10.1016/b978-0-444-63979-0.00002-1.

[63] S. G. Wi *et al.*, “Effects of gamma irradiation on morphological changes and biological responses in plants,” *Micron*, vol. 38, no. 6, pp. 553–564, Aug. 2007, doi: 10.1016/J.MICRON.2006.11.002.

[64] M. A. Malik, H. K. Sharma, and C. S. Saini, “Effect of gamma irradiation on structural, molecular, thermal and rheological properties of sunflower protein isolate,” *Food Hydrocoll.*, vol. 72, pp. 312–322, Nov. 2017, doi: 10.1016/j.foodhyd.2017.06.011.

[65] E. A. Glady, R. A. Kemalov, A. F. Kemalov, and O. M. Kornetova, “Obtaining of bitumen emulsions using nonionic surface-active substances,” *Indian J. Sci. Technol.*, vol. 9, no. 18, May 2016, doi: 10.17485/ijst/2016/v9i18/93770.

[66] L. Meknaci, A. Graziani, C. Mignini, A. D. Henni, and M. Miljković, “Influence of bitumen emulsion on the curing behaviour of standardised cold bitumen emulsion mortars,” *Road Materials and Pavement Design*, vol. 23, no. S1, pp. 99–115, 2022, doi: 10.1080/14680629.2021.2017329.

[67] R. N. Thakur, S. K. Gupta, A. Sinha, S. Chawla, and S. S. Vadavadagi, “A Durability Study of Jute Geotextile Treated with Bitumen Emulsion,” *Journal of Natural Fibers*, vol. 18, no. 3, pp. 400–418, 2021, doi: 10.1080/15440478.2019.1623749.

[68] A. Al-Mohammedawi and K. Mollenhauer, “Current Research and Challenges in Bitumen emulsion Manufacturing and its properties,” *Materials*, pp. 1–29, Mar. 2022.

[69] S. K. Ghosh, K. Ray Gupta, R. Bhattacharyya, R. B. Sahu, and S. Mandol, “Improvement of Life Expectancy of Jute Based Needlepunched Geotextiles Through Bitumen Treatment,” *Journal of The Institution of Engineers (India): Series E*, vol. 95, no. 2, pp. 111–121, Dec. 2014, doi: 10.1007/s40034-014-0036-y.

[70] N. Akter, S. C. Das, S. A. Grammatikos, J. Saha, and M. A. Khan, “Development of sustainable jute geotextiles by bitumen emulsion and polyester resin: Effect of gamma radiation,” *J. Eng. Fiber. Fabr.*, vol. 15, 2020, doi: 10.1177/1558925020957969.

[71] N. Akter, J. Saha, S. C. Das, and M. A. Khan, “Effect of bitumen emulsion and polyester resin mixture on the physico-mechanical and degradable properties of jute fabrics,” *Fibers*, vol. 6, no. 3, Sep. 2018, doi: 10.3390/fib6030044.

[72] P. Gañán *et al.*, “The Evolution and Future Trends of Unsaturated Polyester Biocomposites: A Bibliometric Analysis,” Jul. 01, 2023, *Multidisciplinary Digital Publishing Institute (MDPI)*. doi: 10.3390/polym15132970.

[73] H. N. Dhakal and S. O. Ismail, “Unsaturated polyester resins: Blends, interpenetrating polymer networks, composites, and nanocomposites,” in *Unsaturated Polyester Resins: Fundamentals, Design, Fabrication, and Applications*, Elsevier, 2019, pp. 181–198. doi: 10.1016/B978-0-12-816129-6.00008-9.

[74] J. Saha, S. Chandra Das, M. Rahman, Md. A. B. Siddiquee, and M. Ahmad Khan, “Influence of Polyester Resin Treatment on Jute Fabrics for Geotextile Applications,” 2016. doi: 10.4236/jtst.2016.24009.

[75] M. Crewdson, “OUTDOOR WEATHERING MUST VERIFY ACCELERATED TESTING.”

[76] P. Bhatia *et al.*, “Distinct levels in Pom1 gradients limit Cdr2 activity and localization to time and position division,” *Cell Cycle*, vol. 13, no. 4, pp. 538–552, Feb. 2014, doi: 10.4161/cc.27411.

[77] P. Gañán *et al.*, “The Evolution and Future Trends of Unsaturated Polyester Biocomposites: A Bibliometric Analysis,” Jul. 01, 2023, *Multidisciplinary Digital Publishing Institute (MDPI)*. doi: 10.3390/polym15132970.

[78] J. Ghosh *et al.*, “Development of UV protective and antimicrobial CVC fabric using colloidal zinc oxide solution with carrot and orange peel extract,” *SPE Polymers*, vol. 5, no. 4, pp. 576–589, Oct. 2024, doi: 10.1002/pls2.10144.

[79] Mortuza *et al.*, “commissioning dosimetry and in situ dose mapping of a semi industrial Co -60 gamma-irradiation facility using frickle and ceric-cerous dosimetry system and comparison with monte carlo simulation data,” *Radiation physics and chemistry*, pp. 256–264, Aug. 2017.

[80] “INTERNATIONAL STANDARD IS0 5084 Second edition Textiles-Determination of thickness of textiles and textile products.” [Online]. Available: https://standards.iteh.ai/catalog/standards/sist/a0159671-6586-4bb5-a840-

[81] M. H. S. Shohrawardy, M. K. Alam, M. F. Mina, and M. A. Khan, “Fabrication of strong and thermally more stable jute fabric/polypropylene composites by compression molding along with γ-ray irradiation,” *Polymer Bulletin*, vol. 71, no. 5, pp. 1219–1239, 2014, doi: 10.1007/s00289-014-1120-7.

[82] H. Naznin, A. K. Mallik, K. S. Hossain, M. Shahruzzaman, P. Haque, and M. M. Rahman, “Enhancement of thermal and mechanical properties of PMMA composites by incorporating mesoporous micro-silica and GO,” *Results in Materials*, vol. 11, Sep. 2021, doi: 10.1016/j.rinma.2021.100203.

[83] R. A. Masud *et al.*, "Preparation of novel chitosan/poly (ethylene glycol)/ZnO bionanocomposite for wound healing application: Effect of gentamicin loading," *Materialia (Oxf).*, vol. 12, Aug. 2020, doi: 10.1016/j.mtla.2020.100785.

[84] Erdem, yurudu, and N.O, "The evaluation of antibacterial activity of fabrics with Dimethyltetradecyl(3-(Trimethoxysilyl) Propyl) ammonium Chloride," pp. 115–122, 2008.

[85] S. C. Das, A. D. La Rosa, S. Goutianos, and S. Grammatikos, "Effect of accelerated weathering on the performance of natural fibre reinforced recyclable polymer composites and comparison with conventional composites," *Composites Part C: Open Access*, vol. 12, Oct. 2023, doi: 10.1016/j.jcomc.2023.100378.

[86] P. Cui *et al.*, "Investigation of biodegradable microparticle release and environmental accumulation in Poly(butylene succinate) degradation under UV and non-UV aging conditions," *Polym. Degrad. Stab.*, vol. 237, p. 111323, Jul. 2025, doi: 10.1016/J.POLYMDEGRADSTAB.2025.111323.

[87] V. K. Kaushik, A. Kumar, and S. Kalia, "Effect of Mercerization and Benzoyl Peroxide Treatment on Morphology, Thermal Stability and Crystallinity of Sisal Fibers," *International Journal of Textile Science*, vol. 1, no. 6, pp. 101–105, Jan. 2013, doi: 10.5923/j.textile.20120106.07.

[88] N. Akter, S. C. Das, M. M. Fahad, D. Islam, M. A. Khan, and S. M. Shamsuddin, "Tailoring the performance of cellulosic textiles by chemical treatment and ionizing radiation: Assessment of physical, mechanical, thermal, crystal and morphological properties," *Next Materials*, vol. 7, Apr. 2025, doi: 10.1016/j.nxmate.2024.100372.